

The Lost Lake Landslide;  
Evidence for an Earthquake-Triggered Landslide  
Vashon Island, Washington

Cole Jensen

A report prepared in partial fulfillment of  
the requirements for the degree of

Master of Science  
Earth and Space Sciences: Applied Geosciences

University of Washington

March 2020

Reading committee:

Kathy Troost  
Alison Duvall  
Mike Brown

MESSAGE Technical Report Number: [086]

©Copyright 2020

Cole Jensen

## **Abstract**

I address the large-scale stability and potential past and future triggers of the Lost Lake Landslide on Vashon Island, one of the largest mapped landslides in the Puget Lowland. I focus on three landslide triggers; groundwater fluctuation, the Seattle Fault Zone and the Tacoma Fault Zone and identify the most likely trigger. No previous work has analyzed the trigger, age, or stability of the slope. Using an end member approach, I calculate the factor of safety and seismic critical acceleration using a two-dimensional limit equilibrium model for three different Lost Lake Landslide scenarios. Two scenarios are a reconstruction of potential past failure and one scenario is a future failure of the modern slope. Using USGS ShakeMaps I compare modeled Seattle Fault Zone and Tacoma Fault Zone peak ground accelerations with calculated critical accelerations from this study. I find that significant groundwater fluctuations have a surprisingly low influence on large-scale slope stability. Additionally, shaking from either a Seattle Fault Zone or Tacoma Fault Zone earthquake could have triggered the Lost Lake landslide. A Tacoma Fault Zone earthquake is a more likely trigger due to its greater exceedance of the required critical acceleration to cause a slope failure. My results indicate that large magnitude crustal earthquakes can potentially trigger extremely large landslides in the Puget Lowland. As a first order assessment, factor of safety and critical acceleration analysis can potentially identify other large co-seismic landslides in the Puget Lowland.

## **TABLE OF CONTENTS**

<b>1.0 Introduction</b>	<b>1</b>
<b>2.0 Geologic History &amp; Setting</b>	<b>2</b>
<b>3.0 Background</b>	<b>3</b>
<b>4.0 Methods</b>	<b>6</b>
4.1 Subsurface Stratigraphy & Material Properties	6
4.2 Groundwater Determination	7
4.3 Bluff Reconstruction	8
4.4 Model Setup	8
4.5 Model Scenarios	10
<b>5.0 Assumptions</b>	<b>11</b>
<b>6.0 Results</b>	<b>11</b>
<b>7.0 Discussion</b>	<b>12</b>
<b>8.0 Limitations</b>	<b>14</b>
<b>9.0 Conclusion</b>	<b>15</b>
<b>10.0 Recommendations for Further Study</b>	<b>16</b>
<b>APPENDIX</b>	<b>55</b>
<b>LIST OF TABLES</b>	<b>73</b>
<b>LIST OF FIGURES</b>	<b>74</b>
<b>Acknowledgements</b>	<b>75</b>

## ***1.0 Introduction***

Landslides along coastal bluffs are a common and sometimes deadly hazard in the Puget Lowland (Schulz, 2007). Landslides can be generated by numerous causes both natural and anthropogenic. Historically, landslides occur during the wet season and coincide with increased winter precipitation (Tubbs, 1974). Development of regional co-seismic landslide models has also identified large magnitude crustal earthquakes as a future trigger for thousands of landslides (Allstadt et al., 2013; Grant, 2017). The combined effect of using historical evidence of landslides and predictive modeling of landslides develops a foundation for addressing future landslide triggers and risk. Landslide case studies that use slope stability analysis provide a more detailed look into local characteristics which address both the factor of safety (FS) and hillslope critical acceleration.

Slope stability analysis using the FS indicates that rapid changes in groundwater due to precipitation events can critically reduce the FS, causing slope failures in the Puget Lowland (Cool and Gordon, 2013). Stability analysis can also include seismic analysis, which identifies the required acceleration of the ground, known as the critical acceleration, to trigger a landslide. In the Puget Lowland, evidence for seismically triggered landslides is less abundant than groundwater-triggered landslides. This, however, does not reduce the importance of performing seismic analysis when addressing slope stability, especially when considering the likelihood of a future large magnitude crustal earthquake.

The Puget Lowland has experienced at least two large crustal earthquakes in the past 1200 years from the Seattle Fault Zone (SFZ) and Tacoma Fault Zone (TFZ) (Bucknam et al., 1992; Sherrod et al., 2004). The last major SFZ earthquake was a magnitude 7 or larger which occurred around 900 A.D., raising shorelines as much as 7 meters and generating a tsunami in Puget Sound (Bucknam et al., 1992; Atwater and Moore, 1992). The last major TFZ earthquake was between A.D. 770 and 1160 and was approximately a magnitude 7 (Sherrod et al., 2004). A landslide on Mercer Island was identified as a co-seismic landslide and is linked with the SFZ 900 A.D. event (Jacoby et al., 1992). This landslide exhibits 40 to 50 m high headscarps and bathymetric lobes which traveled 200 to 400m into Lake Washington with a total width from head scarp to toe of 500 to 750 m.

There are other potential co-seismic landslides in the Puget Lowland, which resemble the Mercer Island landslide in scale, geomorphic features and topographic/geologic setting. One such landslide is the Lost Lake landslide, located on an eastward facing slope on the southern tip of Vashon Island, Washington (Figures 1 and 2). Like the Mercer Island Landslide, the Lost Lake landslide has a bathymetric toe which displaced up to 750 m into quartermaster harbor. Both landslides also share similar topographic and geologic settings.

Slope stability analysis using two-dimensional limit equilibrium modeling presents an approach to calculate the FS and seismic critical acceleration. This can potentially isolate whether seismicity or groundwater fluctuation triggered a landslide. Seismic trigger scenarios can be examined by comparing the magnitude of critical acceleration ( $K_c$ ) of the slope with peak ground accelerations (PGA) from modeled earthquake scenarios.  $K_c$  is the required acceleration in percent gravity that will reduce the factor of safety to a value below 1.0, which theoretically triggers a failure.  $K_c$  is measured in the horizontal and downslope direction. PGA is a measurement (or model prediction) of the largest magnitude ground acceleration in percent gravity for a given location during a specific magnitude earthquake.

The goal of my study is to determine if historical earthquakes on the Seattle or Tacoma Fault could have triggered the Lost Lake landslide as either a first-time failure or reactivation of a preexisting failure. To make the determination I compare  $K_c$  and PGA in a slope stability analysis using a two-dimensional limit equilibrium model. Groundwater fluctuations are examined as a potential trigger by using distinct wet and dry season scenarios which affect pore pressure. Wet and dry seasons are also considered when calculating  $K_c$ , addressing the impact of an earthquake on slope stability in both wet and dry seasons. Using this approach, I make a first order assessment of groundwater fluctuations and/or seismic shaking as triggers for both past and future large-scale deep-seated failure of the Lost Lake landslide.

## ***2.0 Geologic History & Setting***

Vashon Island shares the same geologic history as the surrounding Puget Lowland and therefore a similar stratigraphy. During the Quaternary period numerous glacial and interglacial cycles occurred, leaving behind complex and highly variable packages of sediment. The deposits of interglacial and glacial origin which range from silts and clays to sands and gravels were subsequently covered by deposits from the most recent glaciation, the Vashon Stade. The most commonly exposed pre-Vashon deposits on Vashon Island are the Pre-Fraser interglacial coarse – and fine-grained units. The Pre-Fraser deposits include the Possession Drift and Pre-Olympia deposits (Booth, 1991; Booth et al., 2015).

The Vashon Stade of the Fraser glaciation deposited a relatively consistent package of glacial sediment associated with the advance and retreat of the glacier between 18,000 and 16,000 cal. yrs BP (Porter and Swanson, 1998). Around 18,000 cal. yrs BP the Vashon glacier began its advance into the Puget Lowland from British Columbia and divided into two lobes, the Puget Lobe and Juan de Fuca Lobe. As the glacier advanced south, the Juan de Fuca Lobe blocked the north drainage from the Puget Lowland. This process created a large proglacial lake in low lying topography that collected fine-grained deposits of silt and clay known as the Lawton Clay. As the glacier advanced south, proglacial deltas deposited thick layers of sand and gravel known as Vashon Advance Outwash over the Lawton Clay. The Advance Outwash deposits were

subsequently overridden by the advancing glacier and capped by sediment directly deposited subglacially known as the Vashon till.

The Puget Lowland's topography is also a product of glacial and glaciofluvial processes from numerous continental ice sheet advances and retreats during the Quaternary. These processes left behind the deep troughs now occupied by Puget Sound and many of the region's rivers. Subglacial scouring also created much of the steep topography across the landscape today (Troost and Booth, 2008).

In addition to its dynamic glacial history, the Puget Lowland is also subject to progressive deformation. South to north compression, produces east-west thrust faulting, including the SFZ and TFZ - two main crustal fault zones near Vashon Island (Figure 3). The SFZ is located 23km north of the Lost Lake Landslide (LLL) and is an east-west trending, north-verging reverse fault consisting of three strands (Blakely et al., 2002), although the exact fault geometry is still argued. The SFZ has produced large earthquakes, most recently a magnitude 7 or greater which occurred between 900-930 A.D (Bucknam et al., 1992). Vertical slip of the fault resulted in as much as 7 m of offset in Puget Sound (Bucknam et al., 1992). The earthquake generated a tsunami in Puget Sound and triggered landslides that left deposits in Lake Washington (Atwater and Moore, 1992; Jacoby et al., 1992). The TFZ is an active east-west trending south-verging reverse fault consisting of multiple fault strands which intersect Vashon Island and the LLL (Figure 3; Brocher et al., 2001). Uplift along the TFZ was either associated with the 900 A.D. SFZ uplift, or occurred as an unrelated event between A.D. 770-1160 (Sherrod et al., 2004). The TFZ can generate earthquakes of ~ magnitude 7 much like the SFZ (Sherrod et al., 2004).

Evidence for landslides triggered by seasonal fluctuations in groundwater is much more prevalent in the Puget Lowland than evidence for co-seismic landslides. Groundwater aquifer type and orientation must be carefully addressed in order to properly consider groundwater contributions to slope stability. Generally, groundwater in the Puget Lowland is split into two categories, shallow unconfined and deep confined aquifers. Shallow groundwater typically fluctuates 0.3 to 3.3 meters and responds quickly to seasonal fluctuation (Vaccaro et al., 1998). Previous regional scale co-seismic landslide modeling in the Puget Lowland used a wetness factor to quantify fluctuations in shallow groundwater between seasons (Grant, 2017). Deep groundwater typically fluctuates less than 1.2 meters and displays a seasonal lag of 1 to 3 months (Vaccaro et al., 1998). Both shallow unconfined and deep confined groundwater are considered for slope stability analysis.

### ***3.0 Background***

Vashon Island, Washington is in south Puget Sound, north of the city of Tacoma and south of the city of Seattle (Figure 1). Like surrounding areas of the Puget Lowland, Vashon Island hillslopes are susceptible to extensive landsliding due to primed steep bluffs with layers of high

permeability deposits (outwash) overlying layers of low permeability deposits (glaciolacustrine deposits and tills) and high mean annual precipitation throughout the region. Of the numerous landslides on the island one landslide stands out as the largest and most distinct feature. The Lost Lake landslide (LLL) is a roughly 1.1 km<sup>2</sup> landslide located near the southern tip of the island with bathymetric lobes that traveled 500 to 750 m into Quartermaster Harbor (Figure 2). The landslide is 2.5 km wide and extends between 250 and 500 meters back from the beach. The slope above the head scarp is approximately 110 meters above the beach with an average slope of 11 degrees across the landslide deposit and local slopes as steep as 36 degrees. The head scarp has an average height of around 50 m. The landslide is split into a north and a south section by an intact lobe protruding from the center of the head scarp. Adjacent and south of the intact lobe is a deep ravine carved by Chen Creek. The northern portion of the landslide contains one sag pond named Lost lake while the southern portion of the landslide contains two unnamed sag ponds (Figure 1). The surface features of the LLL, including a substantial head scarp, series of back tilted benches, and extreme width of failure, indicate a deep-seated rotational failure (Figures 2 and 4). Rotational failures are most easily identified by their prominent head scarps and back tilted topographic benches (Hungr et al., 2014). Deep rotational failures are typically driven by groundwater conditions influenced by extensive wet periods (Baum et al., 2005).

Several large landslides and landslide complexes around the Puget Lowland share similar geology and geomorphic features as the LLL. Most recently, in 2013 the Ledgewood landslide on Whidbey Island initiated as a reactivation within a much larger rotational landslide complex and displaced 75 m into Puget Sound. The entire complex is ~2.4 km in length and similar in length to the LLL however, the widest portion of the failure is ~190 m which is approximately half the width of LLL (Figure 5). The cause of the most recent reactivation of the Ledgewood slide was a combination of over steepening from wave erosion at the toe and unfavorable groundwater conditions (Cool and Gordon, 2013). Failures of this type primarily respond to groundwater and as such, the slope of the Ledgewood slide will continue to be unstable. The original trigger of the larger Ledgewood complex is unknown and may have begun as a coseismic landslide. Many other landslides in the Puget Lowland resemble the Ledgewood landslide style of failure. The Southeastern Mercer Island landslide (SMIL) is a larger landslide than the Ledgewood Landslide and similar in scale to the LLL, with a length of ~1.5 km and ~330 m wide (Figure 6). The SMIL represents a one-time large-scale failure that responded to seismicity. This landslide is one of the few in the Puget Lowland which is considered direct evidence for a coseismic landslide triggered by the 900 A.D. Seattle Fault earthquake (Jacoby et al., 1992). Both the Ledgewood landslide and SMIL share similar geologic, geomorphic and topographic conditions to the LLL indicating that these features alone cannot distinguish a trigger for the LLL.

The Woodway landslide is another deep seated rotational failure which was likely triggered by increases in pore water pressure in January, 1997 (Savage, 2000). The landslide was

approximately 180 m wide with a toe that extended 220 m from the head scarp and occurred after a period of increased precipitation (Savage, 2000). The Woodway landslide is significantly smaller than the LLL but still caused significant damage by derailing 5 freight train cars, pushing them into Puget Sound. Finite element modeling predicted that the landslide would have required a pore pressure head of 5 m above the Lawton Clay to fail (Savage, 2000). Prior limit equilibrium modeling of failure also predicted a pore pressure head of 5 m above the Lawton Clay (Arndt, 1999). Pore-pressure transducers installed post-failure show that perched groundwater above the Lawton clay fluctuates seasonally by approximately 0.5 m and is approximately 2.4m thick (Savage, 2000). While prior studies indicate that the landslide was most likely triggered from increased pore pressure it is difficult to say if these groundwater conditions existed at the time of failure (Savage, 2000).

The Puget Lowland is one of many geologic settings which has the potential for widespread landslide damage from earthquake shaking. Vashon Island specifically is susceptible to progressive deformation and active faulting because of its proximity to the SFZ and TFZ. While the Puget Lowland lacks recent evidence of co-seismic landslide potential, other regions in North America have experienced recent widespread co-seismic landsliding from shallow crustal fault earthquakes. These events have contributed to our overall understanding of co-seismic landslides. The 1994 Northridge, California Earthquake was a magnitude 6.7 generated from an unknown blind thrust fault. The event triggered more than 11,000 landslides, with tens to hundreds of deep-seated failures thicker than 5 m (Harp and Jibson, 1996). A few of the deep-seated landslides reached volumes in the several millions of meters. Most of these deep-seated failures were reactivations of existing landslide complexes. Landslides triggered by the Northridge Earthquake were in mostly topographically steep and undeveloped regions, causing minor damage to infrastructure in cities like Los Angeles. As shallow crustal fault sources, both the TFZ and SFZ are similar to the Northridge thrust fault and can generate even larger magnitude earthquakes. While the co-seismic landslide hazard of Seattle is analogous to the Northridge Earthquake, the risk of damaging densely populated communities is much higher due to the steeper topography in populated areas. Allstadt et al., (2013) predicted that a M 7.0 SFZ earthquake could generate between 4977 and 30,000 shallow co-seismic landslides across Seattle and did not take deep seated landslides into account. Using ground motions from Allstadt et. al., (2013), Grant, (2017) determined that a magnitude 7.0 SFZ earthquake is severe enough to cause widespread deep rotational and shallow translational landslides in dry conditions and much more severe landslides in wet conditions.

Recent retroactive study on seismically induced landslides, and model development has refined our understanding of co-seismic landslides and revealed that landslide hazards can often be underpredicted (Villeneuve et al., 2017). Past regional scale co-seismic landslide hazard models often only considered PGA, under the assumption that co-seismic landslides and PGA are spatially coincident. However, other factors should be considered, such as proximity to the fault

rupture, topographic amplification, rupture characteristics, earthquake source characteristics, geology, vegetation and aftershocks (e.g., Massey et al., 2018; Gorum and Yildirim, 2017; Roback et al., 2018; Villeneuve et al., 2017). These retroactive studies suggest that factors other than PGA can potentially have a larger impact on slope stability.

## ***4.0 Methods***

Slope stability modeling and analysis calculates the FS to quantify a slope as either stable or unstable. The FS is a ratio of the shear stress to the shear strength. In theory if the shear stress is greater than the shear strength the  $FS < 1$  and the slope is considered unstable and if the shear strength is greater than the shear stress the  $FS > 1$  and the slope is considered stable. In geotechnical practice, the FS must be considerably greater than one to be considered stable. Seismic analysis can be used with the FS to assess the seismic acceleration required to reduce the FS below 1 if a slope is already stable. To address the shear stress the FS calculates the component of stress that operates in the down-slope direction using soil unit weight, soil thickness and slope angle. To address shear strength the FS calculates the variables that resist shear stress, i.e. cohesion, angle of internal friction and the normal force.

To determine whether seismic shaking could have or will in the future trigger mass wasting at the LLL, I developed three model scenarios which address potential past configurations (scenarios 1 and 2) and future failure (scenario 3). I used a collection of new field mapping, unpublished geologic maps, surface topography analysis in GIS and existing subsurface data to build a representation of the LLL. For the elevation profile, I selected a cross section which is located on the southern half of the landslide (Figure 1) due to its strong geomorphic characteristics (Figure 2 & 4) and proximity to available subsurface data (Appendix).

### ***4.1 Subsurface Stratigraphy & Material Properties***

To calculate the FS of the LLL I had to establish the subsurface stratigraphy and assign material properties to each soil unit. The subsurface stratigraphy is depicted in a conceptual geologic model which designates material properties and provides a short summary of each unit (Figure 7). I determined the stratigraphy for the model using field verification of soils where possible, an unpublished geologic map and cross section (Figure 8 and 9; Troost and Booth 2004), publicly available well logs and geotechnical boring logs (see Appendix for all logs). Through field mapping I was able to identify the upper ~50 m of stratigraphy as Vashon till at the top of the head scarp which occasionally had a thin cap of recessional outwash. Vashon advance outwash underlies the Vashon till and is exposed in a road cut through the head scarp. Below the Advance Outwash and exposed in both a road cut and the Chen Creek Ravine is a Pre-Fraser fine-grained unit. Both the unpublished geologic map (Figure 8) and boring logs within the upper ~50 m of the slope were consistent with my field mapping. Stratigraphy of the lower ~60 m of the slope was not exposed so I constrained it by comparing 13 boring logs. The information in the boring

logs below the upper ~50 m of the slope became inconsistent and often difficult to interpret. However, the geologic map (Figure 8) and the typical glacial sequencing of Vashon Island (Figure 9) provided context to the logs and helped constrain the lower stratigraphy. I assigned Mohr-Coulomb material properties to each layer for unit weight, saturated unit weight, cohesion ( $c$ ) and friction angle ( $\phi$ ). Geologic material properties are from a study in the Puget Lowland (Troost et al., 2017).

## *4.2 Groundwater Determination*

Groundwater generally falls into two categories on Vashon Island, shallow unconfined groundwater (~ 60-70 m elevation) within the advance outwash unit, and deep confined groundwater in the Pre-Fraser deposits (33 m elevation). These separate groundwater systems are represented by a water table (shallow groundwater) and a piezometric line (deep groundwater) and generate pore pressures within the model. I used a combination of well monitoring data near the LLL (Figure 10) and general wetness index values for the Puget Lowland to determine the groundwater for both the dry and wet seasons in the shallow aquifer. The wetness index is a ratio of the saturated thickness of a layer to its total thickness. Typical wetness index values for dry season fall within 0.0 to 0.2 and between 0.4 to 0.6 for the wet season (Smith et al., 2017). I used a wetness value of 0.2 for the dry season which was consistent with a nearby dry season well reading (see 11056 in the Appendix), and a wetness value of 0.4 for the wet season. This corresponds to a total fluctuation in groundwater between wet and dry season of 7.6 m (~25 feet). This fluctuation generally agrees with the fluctuation observed in a monitoring well over three years of monitoring (Figure 10) but is significantly more than other monitored groundwater fluctuation near bluff landslides (Savage, 2000). To determine the piezometric line for the deep aquifer I used two wells close to the LLL which were screened near sea level (see 12057 & 12156 in the Appendix), a commonly observed depth of the Pre-Fraser confined aquifer. The average elevation of the piezometric line from the two well logs was 33 m elevation. Since the deep confined groundwater on Vashon Island does not significantly fluctuate between wet and dry seasons (Bilir, 2013) I used a static level of 33 m for all scenarios.

For Scenarios 2 and 3 that include landslide deposits, quantifying groundwater within the landslide unit was complicated because of a lack of data on water level and seasonal variations in water level. Water levels within landslide deposits can be highly variable and unpredictable, making groundwater determination difficult. Sag ponds within the landslide and one geotechnical boring (see B-1 in the Appendix) provided some context on where the water table is located but lack enough information to advise the entire model. For these scenarios I used sag ponds as guidance for the groundwater table shape in wet and dry seasons. Fluctuation in groundwater between wet and dry seasons was ~6 m at each topographic peak within the landslide debris. This is a high degree of fluctuation in groundwater between wet and dry seasons when compared to typical fluctuation ranges seen in shallow groundwater (Vaccaro et al., 1998).

### 4.3 Bluff Reconstruction

To perform analysis on the pre-failure conditions of the LLL, I created an intact idealized bluff (Scenario 1) using existing intact bluffs as analogs. I collected four profiles of intact bluffs on Vashon and Maury Islands surrounding the LLL (Figure 11). Modern intact bluffs on Vashon and Maury Islands share similar geology and setting and are the most accurate representation of an intact bluff at the LLL location. The average slope of the selected bluffs is 35 degrees (Table 1). I used this slope value for Scenario 1. Bluff profiles 1 through 4 are found in the Appendix.

### 4.4 Model Setup

I used a two-dimensional limit equilibrium slope stability model to calculate the FS of a circular slide plane within the bluff subsurface. Generally, limit equilibrium models use statics to solve for vertical forces, horizontal forces and moments acting between thin vertical slices which are discretized by the model across the slide mass (GEO-SLOPE, 2012; Figure 12). These forces/moments are also known as interslice forces and moments. The model uses the sum of the interslice forces (Equation 1) and/or moments (Equation 2) across the entire slide mass to calculate an overall FS. In order to solve the FS, different limit equilibrium methods make different assumptions about the interslice shear and normal forces and their resultant angles. Some methods only satisfy force equilibrium between slices and others only moment equilibrium. Rigorous methods satisfy both force and moment equilibrium using a function to define interslice relations and require computer algorithms to solve.

$$F_m = \frac{\sum[c'l + (N - ul)\tan\phi']}{\sum W\sin\alpha} \quad (1)$$

$$F_f = \frac{\sum[c'l\cos\alpha + (N - ul)\tan\phi'\cos\alpha]}{\sum N\sin\alpha} \quad (2)$$

The terms in the equations are:

$F_m$  = moment factor of safety

$F_f$  = force factor of safety

$c'$  = effective cohesion

$\phi'$  = effective angle of frictions

$u$  = pore pressure  
 $l$  = geometric parameter  
 $N$  = slice base normal force  
 $W$  = slice weight  
 $\alpha$  = inclination of slice base

Circular failure planes are generated based from a grid point above the slope surface. The grid point is a part of a collection of other grid points which are placed at regular intervals inside a grid box above the slope. The failure dimensions and geometry are defined by the radius of the failure (i.e., the radius of the circle used to define the slip plane) and the location of the grid point above the slope (i.e., the point within the grid box from which the radius of failure is generated). After the slide plane is created, vertical slices are discretized, and the limit equilibrium method is performed. I used the General Limit Equilibrium / Morgenstern Price method within Slide for all LLL analyses. This method is a rigorous method that satisfies both force and moment equilibrium.

For every grid point, the model generated rotational slide planes (using different radii selected by the model) which were within the bounds of the designated initiation zone and exit zone. This means that only specific combinations of failure grid point locations and radii (essentially the failure depth) were within the bounds of my analysis. I forced the model to create deep-seated failures at locations and depths of interest. Without this designation the model tended to generate shallow slide planes that were not applicable to the large-scale failure approach of this study. I averaged the minimum FS values for each grid point within the bounds of the analysis to estimate the FS of a failure resembling the LLL. Averaging FS values from a range of constrained model generated failure geometries reduces potential bias from assuming a single failure geometry.

The model can also determine  $K_c$  by calculating the required ground acceleration for failure (FS=1). The model performs the analysis for different failure planes by using the same grid point method as for FS calculation. Slide uses Newmark analysis in order to calculate the required  $K_c$  in the horizontal downslope direction. I used the same averaging technique for evaluating the value of  $K_c$  along multiple constrained failure geometries for each scenario.

To put the  $K_c$  into perspective with realistic earthquake scenarios I used ShakeMap PGA's developed by the United States Geological Survey (USGS) for two different scenarios; a magnitude 7.2 SFZ scenario (Figure 13; USGS Seattle, 2017) and 6.9 TFZ scenario (Figure 14; USGS Tacoma, 2017). ShakeMaps are a realization of a potential earthquake assuming a magnitude, location and fault rupture geometry (Wald et al., 2006). I compared the predicted PGA from ShakeMaps with the  $K_c$  output from each scenario to determine in which scenarios  $K_c$  was exceeded and by how much. Implementing factors other than PGA into coseismic landslide

hazard models requires more detailed earthquake modeling data for the Puget Lowland. This data will develop and become available over time and in response to future earthquake data. Meanwhile, PGA alone provides a good first order estimation of regional and local scale coseismic landslide hazards.

#### *4.5 Model Scenarios*

I developed multiple model scenarios and calculated FS for both wet and dry season groundwater. If the FS for a scenario was greater than 1 and therefore already theoretically stable, I calculated the critical seismic acceleration ( $K_c$ ) required to bring the FS to 1. I performed this analysis for three different scenarios, two reconstructions of a potential paleo-bluff and a future scenario using the existing bluff configuration. I split the past scenarios into a reconstruction that assumed a single large failure occurring on an intact bluff (Scenario 1) and another reconstruction which assumed an iterative style of failure of a previously bluff (Scenario 2). For the future failure scenario (Scenario 3) I used an elevation profile from a LiDAR-derived elevation dataset (Figure 2). I assumed the future failure would be a new large-scale failure initiating behind the current head scarp. Scenario 1, 2 and 3 have average slopes of 35, 16 and 11 degrees respectively.

For both Scenario 1 and 2, I constrained the boundaries for where the failure plane was initiated and where it exited. For Scenario 1, I set the initiation zone between 470 m and 500 m back from the base of the intact bluff (Figure 15a & 15b). For this scenario, I assumed the base of the reconstructed paleo-bluff was located at the current beach location and that the failure initiated behind the paleo-bluff face at the current head scarp location. For Scenario 2, I created a pre-LLL failure complex by taking the upper back tilted bench of the current profile (Figure 4) and shifting it upslope back into place (Figure 16). Scenario 2 models bluff failure assuming progressive failure, similar to the style of failure seen at the Ledgewood landslide complex. I set the initiation zone for Scenario 2 between 470 m and 500 m behind the base of the modern beach/slope interface (Figure 17a & 17b), a distance in which a reactivated failure resembles the modern head scarp location. For Scenario 3, I set the initiation zone between 0 m to 50 m behind the current head scarp to resemble a future deep-seated failure initiating behind the current head scarp (Figure 18a & 18b). For all scenarios, I designated the slide plane exit zone as 0 m to 200 m beyond the base of the bluff or slope. I used a large range in exit zone distance to account for the lack of information on the location of the slide plane at the toe.

Each scenario has an external boundary, which defines the total area of the analysis. Failure planes are not allowed to exit the external boundary and then re-enter. In other words, all generated failure plains must be contained within the external boundaries. In this regard, the bottom external boundary acts as a limit on the total depth of each failure plain. I defined the elevation of the bottom external boundary as 40 m below sea level. This allows the model to

generate a collection of different failure geometries but confines it from creating failures which are unrealistically deep.

## ***5.0 Assumptions***

Slope stability modeling inherently relies on the information available to the user. Given the generally limited information, it is impossible to conclude definitively the characteristics of the LLL such as failure history and failure depth. However, the modeling is meant to analyze potential end members of failure and place bounds on likely triggers.

Given the available information, I had to make several assumptions:

- I constrained the lower half of the stratigraphy (Qpff and Qpf units) to the best of my ability considering well logs were vague and field verification of the soils was not possible because of the extent of cover by blocky landslide debris. I made informed assumptions of the lower stratigraphy based on regional cross-sectional data for Vashon Island (Troost and Booth, 2004) and typical Vashon Island stratigraphy (Booth et al., 2015; Figure 9). This provided context to develop the most likely lower subsurface configuration. Since, the deposits in the lower half of the bluff are known to be interbedded fine and coarse grained, I used average values.
- For both Scenario 1 and 2 (pre-failure intact bluff and reactivation) I assumed that the base of the paleo-bluff was at the location of the modern beach/bluff interface (Figure 19). The current beach/bluff interface is likely a reasonable representation of a historical shoreline that existed pre-failure or in between failures. I also assumed for both scenarios that the most recent sliding initiated near the current location of the head scarp.
- Groundwater data within the landslide debris was limited to only one boring which provided limited information. For Scenarios 2 & 3 that included landslide debris I estimated the groundwater level and amount of fluctuation within the portion of the slope that included landslide deposits. I assumed that during the dry season the sag ponds were less deep and generally discharging into the groundwater and during the wet season were deeper and recharging from groundwater. I also assumed that groundwater fluctuation between wet and dry seasons was ~6 m at the peaks of groundwater elevation. This groundwater variability is less than the variability used in the intact materials (7 m) to account for the bluff face as a discharge point. Furthermore, given the interbedded nature of the deposits in the lower half of the bluff, additional groundwater layers are likely present.

## ***6.0 Results***

The results for the FS and  $K_c$  are split into the 3 scenarios and into wet and dry seasons for each scenario. Scenario 1 had a dry and wet FS of 2.49 and 2.46 and a  $K_c$  0.28 g and 0.28 g respectively. Scenario 2 had a dry and wet FS of 2.53 and 2.48 and a  $K_c$  0.29 g and 0.29 g

respectively. Scenario 3 had a dry and wet FS of 3.65 and 3.58 and a  $K_c$  0.34 g and 0.33 g respectively. These data show that all scenarios were stable in both dry and wet seasons and have minimal sensitivity to changing groundwater. Scenario 1 has a slightly lower FS than Scenario 2 but not enough to observe a difference in the  $K_c$ . Scenario 3 has a significantly higher FS and  $K_c$  which indicates the slope is in a more stable configuration today than in the past. FS and  $K_c$  results for each scenario are presented in Table 2 and displayed in Figures 20 to 31.

PGAs for the M 7.2 SFZ earthquake vary from 0.32 to 0.36 across the LLL and vary from 0.52 to 0.56 for the M 6.9 TFZ earthquake (Figures 13 and 14). PGAs decrease from north to south across the LLL for both earthquake scenarios. For the slope stability, seismic analysis results are presented as a  $K_c$  exceedance magnitude. This value represents the amount by which  $K_c$  for each scenario was exceeded by the PGA in percent gravity (%g) for either the SFZ or TFZ.  $K_c$  exceedance magnitudes are represented as a range because of variability in PGAs across the LLL and are presented in Table 3. Scenarios 1 and 2 with a TFZ source had the largest magnitudes of  $K_c$  exceedance and Scenario 3 with a SFZ source had the smallest magnitude of  $K_c$  exceedance. The variability in  $K_c$  exceedance from fluctuating groundwater was minimal due to the low sensitivity of the FS to groundwater fluctuations.

## ***7.0 Discussion***

Slope stability analysis using 2-D limit equilibrium modeling presents an approach to calculate the FS and seismic  $K_c$ . Referencing these values with ShakeMaps can isolate whether seismicity or groundwater fluctuation triggered the LLL. Generally, all scenarios show a surprisingly low sensitivity to seasonal changes in groundwater. The most sensitive scenario to groundwater was Scenario 3 with a decrease of 0.06 in FS and .01 g in  $K_c$  in the wet season, while Scenarios 1 and 2 show virtually no sensitivity to groundwater fluctuations. This low sensitivity indicates that for both past and future large-scale failures, changes in pore pressure of shallow groundwater had little to no role in the failure. If fluctuations in groundwater are influencing slope stability it is likely that they contribute more heavily to shallow failures along steep localized sections of the slope. It is possible that a groundwater driven shallow failure on the landslide toe of Scenario 2 or 3 could de-buttress the landslide upslope and lead to a larger failure. If groundwater has contributed to large-scale stability across the whole landslide it has likely contributed in this manner, rather than directly initiating a singular large failure event. These types of progressive failures are common in the Puget Lowland.

The 2013 Ledgewood landslide began as block movement within the toe of the complex days before the final larger event. The block movement caused progressive failure up the slope leading to approximately 30 m of material being removed from the head scarp (Cool and Gordon, 2013). Past failures were typically observed between February and March and the 2013 failure displayed significant seepage from the head scarp post failure. Both are indicators that seasonally perched groundwater above or within the colluvium is responsible.

If I had not constrained the model to only generate deep-seated failures it would have identified numerous shallow low FS slip surfaces on localized steep slopes. My results do not address the importance of groundwater fluctuation on these types of low FS shallow landslides which are likely more sensitive to changes in shallow groundwater. My results are also not meant to undervalue the importance of groundwater fluctuation on deep-seated landslides but does highlight that in certain cases groundwater alone may not explain large deep-seated failures.

Changes in groundwater level had little impact on large-scale failure at the LLL, earthquakes from the SFZ and TFZ produce ground accelerations capable of triggering large-scale movement. This is surprising considering that previous studies from Arndt et al., (1999), Savage et al., (2000), Cool and Gordon, (2013) suggest that the stability of other deep seated landslides in the Puget Lowland are highly sensitive to and likely triggered by groundwater. However, my results suggest that larger failures like the LLL are not as sensitive to groundwater and have FS that are double or event triple that of landslides like the Ledgewood and Woodway landslide. In these situations, it may be unreasonable to assume that changes in groundwater can reduce the FS enough to reach a critical level and trigger a large failure. This is substantiated by the SMIL which is a similar scale failure as the LLL and was not triggered by groundwater but rather by the 900 A.D SFZ earthquake.

In all scenarios either a 7.2 M SFZ or 6.9 M TFZ could have exceeded the  $K_c$  of a new large slip plane starting behind the existing head scarp. Scenario 3 is an exception in that for a 7.2 M SFZ earthquake,  $K_c$  is not exceeded by the lower range of PGA (0.32 g) but is exceeded by the upper range (0.36 g). For both Scenarios 1 and 2  $K_c$  exceedance indicates that either a SFZ or TFZ earthquake could have triggered the LLL in the past but that the TFZ is a much more convincing source. PGAs for the TFZ scenario are significantly higher than PGAs for the SFZ scenario at the LLL. This is a result of the proximity of the TFZ to the LLL (Figure 3) and results in PGAs which more confidently exceed the required  $K_c$  than the SFZ PGAs.  $K_c$  exceedance alone cannot dictate which fault is more likely to have triggered the LLL, however, scenarios where PGA exceeds  $K_c$  by a larger magnitude portrays a higher confidence that shaking would overcome  $K_c$  in a real-world situation. Recent evidence also suggests that proximity to the deepest section of fault rupture can play a major role in co-seismic landslide hazards (Roback et al., 2018).

$K_c$  exceedance magnitudes suggest that both Scenarios 1 and 2 could have been in response to either a SFZ or TFZ earthquake. Scenario 1 and 2 require almost identical  $K_c$  for both seasons (within 0.01 g) and have FS that are within 0.02 to 0.04 of each other. Scenario 1 is the slightly less stable configuration with a lower FS and  $K_c$ . The slight decrease in FS and  $K_c$  may be attributed to the increase in average steepness of the slope, from 35 degrees in Scenario 1 to 16 degrees in Scenario 2. This means that if the slope had failed previously, that it may have failed into a slightly more stable position in regards to large scale failures. The slight decrease in FS

and  $K_c$  suggests that Scenario 1 would have been slightly easier to trigger from seismic acceleration. Ultimately, the difference in FS and  $K_c$  is insignificant and makes determining the more likely scenario difficult.

Interpreting future failure of the LLL is as, if not more important than reconstructing past failures. Analysis of modern conditions and future large failure in Scenario 3 show more intriguing results than Scenarios 1 and 2. The FS for a future large failure was higher than that of a past failure, ranging from 3.58 in wet to 3.65 in dry. This indicates that the current slope is much less likely to fail as a new large failure than in Scenario 1 and 2. Scenario 3 shows the most variability in FS due to groundwater, although still not significant enough to affect overall stability. This variability could result from the larger mass of colluvium which has undulating topography. These conditions may allow for water to more readily collect on and within the slope and reduce efficiency of water seepage to the Sound. Colluvium is often highly variable in consistency and tilted blocks of silt and clay can effectively “dam” groundwater and increase pore pressures. This type of “damming” effect on groundwater was attributed to having influenced the 2013 Ledgewood landslide (Cool and Gordon, 2013).

Due to the higher FS, the  $K_c$  are 0.04 to 0.06 g higher (0.33 g for wet to 0.34 g for dry) than both past scenarios. This increase in  $K_c$  is significant, raising the  $K_c$  to a value that straddles above and below the SFZ PGAs. Meaning in certain situations SFZ PGAs exceed  $K_c$  while in others they do not. SFZ PGAs range from 0.32 to 0.36 g across the LLL with most of the study area within the lower 0.32 g zone (Figure 13). The overlap of  $K_c$  and PGA values suggests that a future M 7.2 SFZ scenario would be at the theoretical cusp of triggering a new large failure at the LLL. This means that a future M 7.2 SFZ earthquake would potentially not reach the required acceleration and would require greater PGA. In this configuration small changes in groundwater could theoretically reduce the FS by just enough to prime the slope for a co-seismic landslide. More likely, the SFZ would cause localized failures within the LLL complex, potentially leading to reactivation style failures like the 2013 Ledgewood landslide. Whilst a future M 7.2 SFZ scenario is at the cusp of triggering a new large failure of the current slope, a M 6.9 TFZ scenario could still easily trigger the same scale failure in Scenario 3. The magnitude of  $K_c$  exceedance by the TFZ PGA is still much greater than the required acceleration for future global movement, exceeding  $K_c$  by 0.18 g to 0.23 g. This reasoning does not rule out the SFZ as a trigger but highlights that the TFZ has a greater likelihood and potential to generate the required accelerations for future large failure initiating behind the existing head scarp.

## ***8.0 Limitations***

The aim of this study was to analyze potential end members of past and future failure and to constrain potential triggers given available information. The conclusions of this study are based on the limited information I have and educated assumptions I made to the best of my ability. Using a slope stability model with limited information to constrain a landslide trigger is an

inherently disadvantaged method compared to other methods such as radiocarbon age matching of landslide age and fault rupture. The FS,  $K_c$  values, and groundwater sensitivity are highly dependent on characteristics of the landslide that are only loosely constrained, such as the failure plane geometry, deep subsurface, and groundwater depth/variability. However, given the model configuration is roughly representative of actual conditions, it is a reasonable first order approximation of which landslide triggers and scenarios are more likely.

## ***9.0 Conclusion***

2-D limit equilibrium slope stability modeling of global failure revealed that all scenarios, past and future have a low sensitivity to groundwater and have  $K_c$  values which are exceeded by both the TFZ and SFZ PGA. My results suggest it is unlikely that seasonal fluctuations of groundwater alone were responsible for past large-scale failures at the LLL. Analysis also indicates that a future large-scale failure behind the current head scarp would not be initiated by fluctuations in groundwater. This analysis does not recognize the influence of groundwater fluctuations on localized failures which could lead to larger failures. While this is a potential scenario it is beyond the scope of this study. My modeling indicates that potential past slope configurations and the current slope configuration of the LLL are unstable during seismic shaking. Both the SFZ and TFZ earthquakes could theoretically have caused the LLL in both Scenario 1 and 2. Due to potential inaccuracies in the model, from limited groundwater and deep subsurface information, I have more confidence that movement on the TFZ triggered the LLL than the SFZ. The TFZ consistently exceeds the  $K_c$  by tenths of a g while the SFZ only ever exceeds  $K_c$  by hundredths of a g. Modeling of a future failure (scenario 3) shows that a M 7.2 SFZ earthquake may not exceed  $K_c$  while a M 6.9 TFZ earthquake would significantly exceed  $K_c$ . It is important to note that the magnitude of  $K_c$  exceedance is not a direct indicator of which seismic source is a more probable trigger. For a landslide to occur it only requires that the shaking source reach the critical acceleration not that it exceed it. However, given the potential model inaccuracies, the magnitude by which each source exceeds the  $K_c$  provides confidence that during an actual earthquake a landslide would be triggered.

Understanding the scale of potential co-seismic landslides is an important aspect in understanding future potential landslide hazards. My study supports that large deep-seated landslides like the LLL are potentially coseismic and can be triggered from an earthquake on the SFZ or TFZ. Although modeling results suggest that it is reasonable that the LLL failed as one large mass it is also could have failed as three smaller rotational failures in sequence which would have required less energy to generate. This style of failure would only require a relatively small initial rotational failure at the bluff face which would then de-buttress the newly exposed slope and cause further failures into the slope. Regardless of the failure style, my modeling suggests that it is possible that the LLL and other landslides similar in scale could respond as a singular event during earthquake shaking from the TFZ or SFZ. Slope stability analysis using FS

and  $K_c$  could prove a useful and relatively quick first order tool in identifying other co-seismic landslides in the Puget Lowland.

### ***10.0 Recommendations for Further Study***

More detailed modeling in the future could reveal unknown characteristics of the LLL and influence our overall understanding of the failure. However, this would require better constraint on key characteristics such as slide plane(s) depth(s) and geometry (s), groundwater depth and fluctuation and deep stratigraphy type/thickness. Geotechnical drilling and installing monitoring wells and slope inclinometers within the LLL and behind the head scarp would help to constrain key characteristics and quantify ongoing movement. The LLL also has a significant amount of landslide debris covered by water in Quartermaster Harbor (Figure 2). This material could contain tree stumps and presents an opportunity for future radiocarbon dating of wood much like the SMIL. The sag ponds also present an opportunity for radiocarbon dating of either wood or bulk sediment obtained through coring of the bottom of the sag pond sediment. Radiocarbon studies could directly link the failure age to a past SFZ or TFZ earthquake.

### **References**

- Allstadt, K., Vidale, J.E., and Frankel, A.D., 2013, A Scenario Study of Seismically Induced Landsliding in Seattle Using Broadband Synthetic Seismograms: Bulletin of the Seismological Society of America, v. 103, p. 2971–2992, doi:[10.1785/0120130051](https://doi.org/10.1785/0120130051).
- Arndt, B.P., 1999, Determination of the conditions necessary for slope failure of a deep-seated landslide at Woodway, Washington: Golden, Colorado, Colorado School of Mines unpub. M.S. thesis, 102 p.
- Savage, W.Z., Baum, R.L., Morrissey, M.M., and Arndt, B.P., 2000, Finite-element analysis of the Woodway landslide, Washington: US Geological Survey, Bulletin 2180
- Atwater, B.F., and Moore, A.L., 1992, A Tsunami About 1000 Years Ago in Puget Sound, Washington: Science, v. 258, p. 1614, doi:[10.1126/science.258.5088.1614](https://doi.org/10.1126/science.258.5088.1614).
- Baum, R.L. et al., 2005, Regional landslide-hazard assessment for Seattle, Washington, USA: Landslides, v. 2, p. 266–279, doi:10.1007/s10346-005-0023-y.
- Bilir, S., Ferguson, E., and DeGasperi, C., 2013, Vashon-Maury Island Water Resources - A Retrospective of Contributions & Highlights: King County, 169 p.

- Blakely, R.J., Wells, R.E., Weaver, C.S., and Johnson, S.Y., 2002, Location, structure, and seismicity of the Seattle fault zone, Washington: Evidence from aeromagnetic anomalies, geologic mapping, and seismic-reflection data: *GSA Bulletin*, v. 114, p. 169–177, doi:[10.1130/0016-7606\(2002\)114<0169:LSASOT>2.0.CO;2](https://doi.org/10.1130/0016-7606(2002)114<0169:LSASOT>2.0.CO;2).
- Booth, D.B., 1991, Geologic map of Vashon and Maury Islands, King County, Washington: Miscellaneous Field Studies Map Report 2161, doi:[10.3133/mf2161](https://doi.org/10.3133/mf2161).
- Booth, D.B., Troost, K.G., and Tabor, R.W., 2015, Geologic map of the Vashon 7.5' quadrangle and selected areas, King County, Washington: U.S. Geological Survey Scientific Investigations Map 3328, scale 1:24,000.
- Brocher, T.M., Parsons, T., Blakely, R.J., Christensen, N.I., Fisher, M.A., and Wells, R.E., 2001, Upper crustal structure in Puget Lowland, Washington: Results from the 1998 Seismic Hazards Investigation in Puget Sound: *Journal of Geophysical Research: Solid Earth*, v. 106, p. 13541–13564, doi:[10.1029/2001JB000154](https://doi.org/10.1029/2001JB000154).
- Bucknam, R.C., Hemphill-Haley, E., and Leopold, E.B., 1992, Abrupt Uplift Within the Past 1700 Years at Southern Puget Sound, Washington: *Science*, v. 258, p. 1611, doi:[10.1126/science.258.5088.1611](https://doi.org/10.1126/science.258.5088.1611).
- Cool, S.W., and Gordon, R.J., 2013, Ledgewood Landslide Evaluation Coupeville, Washington: Geotechnical Engineering Services, No. 0422-097–00.
- Ferguson, E., 2009, Vashon-Maury Island 2009 Water Resources Data Report: King County, 101 p.
- GEO-SLOPE International Ltd, 2012, Stability Modeling With Slope/W: GEO-SLOPE International Ltd Techniques and Methods.
- Gorum, T., and Yildirim, C., 2017, Preliminary results on landslides triggered by the Mw 7.8 Kaikoura earthquake of 14 November 2016 in northeast South Island, New Zealand: *EGUGA*, p. 3545.
- Grant, A., 2017, Regional-Scale Coseismic Landslide Hazard Modeling and Consequence Analysis: University of Washington, 275 p., <https://digital.lib.washington.edu/researchworks/handle/1773/40863>.
- Harp, E.L., and Jibson, R.W., 1996, Landslides triggered by the 1994 Northridge, California, earthquake: *Bulletin of the Seismological Society of America*, v. 86, p. S319–S332.

- Hungr, O., Leroueil, S., and Picarelli, L., 2014, The Varnes Classification of Landslide Types, an Update: *Landslides*, v. 11, p.167-194, doi:[10.1007/s10346-013-0436-y](https://doi.org/10.1007/s10346-013-0436-y).
- Jacoby, G.C., Williams, P.L., and Buckley, B.M., 1992, Tree Ring Correlation Between Prehistoric Landslides and Abrupt Tectonic Events in Seattle, Washington: *Science*, v. 258, p. 1621–1623.
- Porter, S.C., and Swanson, T.W., 1998, Radiocarbon Age Constraints on Rates of Advance and Retreat of the Puget Lobe of the Cordilleran Ice Sheet during the Last Glaciation: *Quaternary Research*, v. 50, p. 205–213, doi:[10.1006/qres.1998.2004](https://doi.org/10.1006/qres.1998.2004).
- Roback, K., Clark, M.K., West, A.J., Zekkos, D., Li, G., Gallen, S.F., Chamlagain, D., and Godt, J.W., 2018, The size, distribution, and mobility of landslides caused by the 2015 Mw7.8 Gorkha earthquake, Nepal: *Geomorphology*, v. 301, p. 121–138, doi:[10.1016/j.geomorph.2017.01.030](https://doi.org/10.1016/j.geomorph.2017.01.030).
- Schulz, W.H., 2007, Landslide susceptibility revealed by LIDAR imagery and historical records, Seattle, Washington: *Engineering Geology*, v. 89, p. 67–87, doi:[10.1016/j.enggeo.2006.09.019](https://doi.org/10.1016/j.enggeo.2006.09.019).
- Sherrod, B.L., Brocher, T.M., Weaver, C.S., Bucknam, R.C., Blakely, R.J., Kelsey, H.M., Nelson, A.R., and Haugerud, R., 2004, Holocene fault scarps near Tacoma, Washington, USA: *Geology*, v. 32, p. 9–12, doi:[10.1130/G19914.1](https://doi.org/10.1130/G19914.1).
- Smith, J.B., Baum, R.L., Mirus, B.B., Michel, A.R., and Stark, B., 2017, Results of hydrologic monitoring on landslide-prone coastal bluffs near Mukilteo, Washington: Open-File Report Report 2017–1095, 60 p., doi:[10.3133/ofr20171095](https://doi.org/10.3133/ofr20171095).
- Troost, K. G., and Booth D. B., 2008, *Geology of Seattle and the Seattle Area*, Washington: Geological Society of America Reviews in Engineering geology XX, p. 1 – 35.
- Troost, K.G., and Booth, D.B., 2004, *Geologic map of Vashon and Maury Islands*, King County, Washington: GeoMapNW, scale 1:12,000.
- Troost, Kathy Goetz, Brooks, Justin L., Kohn, James A., Teague, Katherine, Wisher, Aaron P., Thompson, Lauren K., and Porter, Matthew, 2017, *Kirkland Geology and Geological Hazards Maps and Products*, GeoMapNW, Department of Earth and Space Sciences, University of Washington, Seattle WA.

- U.S. Geological Survey, 2017, Magnitude 7.2 Scenario Earthquake – Seattle Fault Zone – northern Peak Ground Acceleration:  
[https://earthquake.usgs.gov/scenarios/eventpage/bssc2014570n\\_m7p23\\_se/shakemap/pga](https://earthquake.usgs.gov/scenarios/eventpage/bssc2014570n_m7p23_se/shakemap/pga)  
(accessed November 2019).
- U.S. Geological Survey, 2017, Magnitude 6.9 Scenario Earthquake – Tacoma Fault Zone – Peak Ground Acceleration:  
[https://earthquake.usgs.gov/scenarios/eventpage/bssc2014570n\\_m7p23\\_se/shakemap/pga](https://earthquake.usgs.gov/scenarios/eventpage/bssc2014570n_m7p23_se/shakemap/pga)  
(accessed November 2019).
- Tubbs, D.W., 1974, Landslides in Seattle: State of Washington Department of Natural Resources Division of Geology and Earth Sciences: Olympia, Washington, p. 26.
- Vaccaro, J.J., Hansen, A.J., and Jones, M.A., 1998, Hydrogeologic Framework of the Puget Sound Aquifer System, Washington and British Columbia: U.S. Geological Survey, 92 p.
- Villeneuve, M., Dellow, S., Massey, C., McColl, S., and Townsend, D., 2017, Landslides caused by the 14 November 2016 Kaikoura earthquake, South Island, New Zealand: Proceedings of 20th NZGS Symposium, p. 8.
- Wald, D.J., Worden, B.C., Quidoriano, V., and Pankow, K.L., 2006, ShakeMap Manual: technical manual, user's guide, and software guide: United States Geological Survey Techniques and Methods.
- Washington State Department of Natural Resources, 2019, Seismogenic Features (Faults and Earthquakes) Geodatabase:  
<https://www.dnr.wa.gov/programs-and-services/geology/publications-and-data/gis-data-and-databases> (accessed January 2020).

## TABLES

Bluff	Slope (Degrees)
1	35
2	34.2
3	37.5
4	34.5
Average	35.3

**Table 1:** Average slope of intact bluffs used for Scenario 1 model. Location of bluff profiles are found on Figure 10.

	Intact Bluff (Scenario 1)		Reactivation (Scenario 2)		Future (Scenario 3)	
	FS	K <sub>c</sub> (%g)	FS	K <sub>c</sub> (%g)	FS	K <sub>c</sub> (%g)
Dry	2.49	0.28	2.53	0.29	3.65	0.34
Wet	2.46	0.28	2.48	0.29	3.58	0.33
Average Slope (Deg.)	35		16		11	

**Table 2:** Factor of Safety and critical acceleration results for all model scenarios in wet and dry seasons.

	Intact Bluff (Scenario 1)		Reactivation (Scenario 2)		Future (Scenario 3)	
	SFZ	TFZ	SFZ	TFZ	SFZ	TFZ
Dry K <sub>c</sub> Exceedance (%g)	0.04-0.08	0.24-0.28	0.03-0.07	0.23-0.27	-0.02-0.02	0.18-0.22
Wet K <sub>c</sub> Exceedance (%g)	0.04-0.08	0.24-0.28	0.03-0.07	0.23-0.27	-0.01-0.03	0.19-0.23
Average Slope (Deg.)	35		16		11	

**Table 3:** Magnitude of K<sub>c</sub> exceedance for all model scenarios in wet and dry seasons. Values are presented as a range, resulting from variation in ShakeMap PGAs across the LLL (Figures 12 and 13). Negative values represent scenarios where the K<sub>c</sub> is not exceeded.

# FIGURES

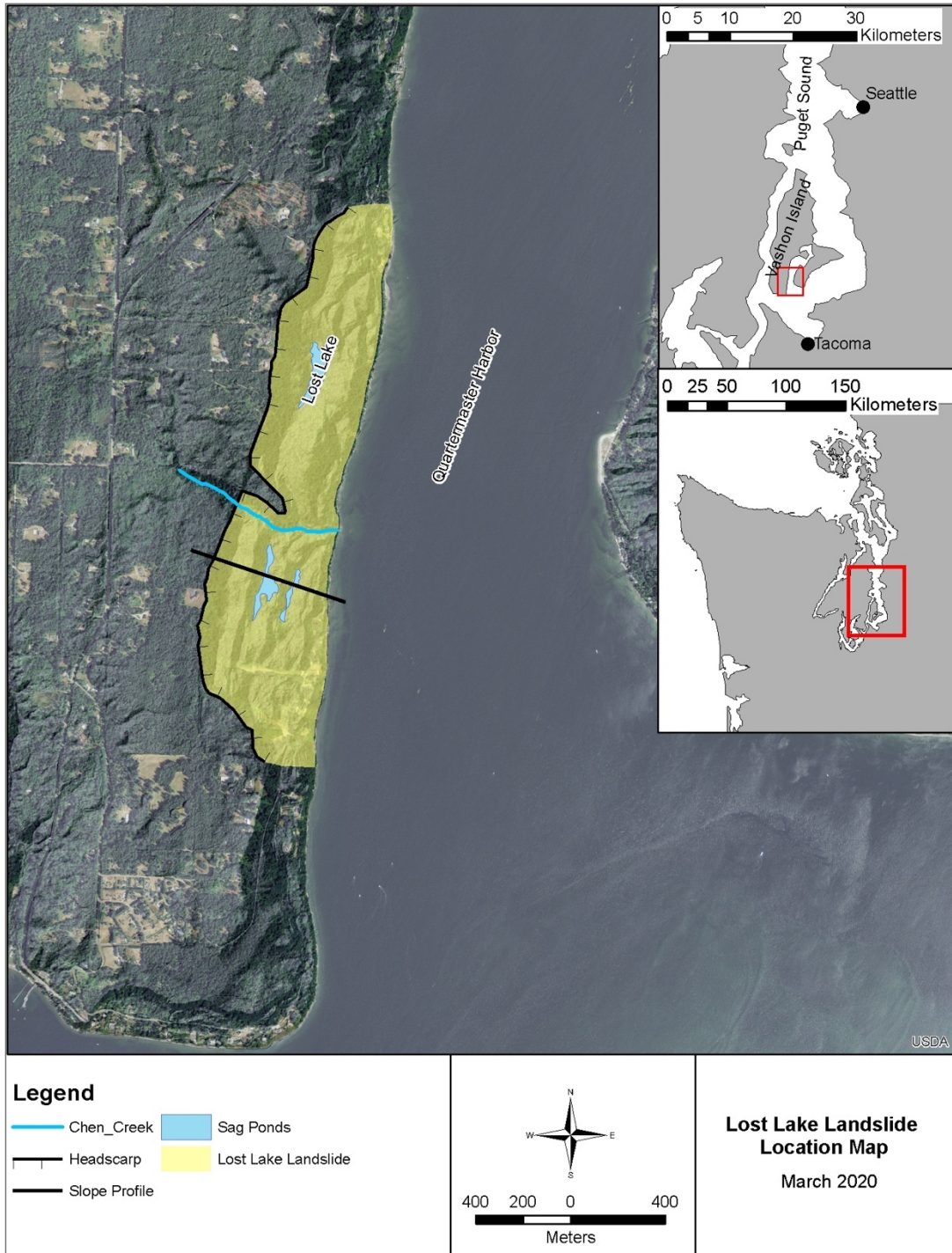


Figure 1: Location Map of the Lost Lake Landslide located on the southern end of Vashon Island, Washington. Aerial imagery of Vashon Island is displayed as aerial imagery over a DEM hill shade.

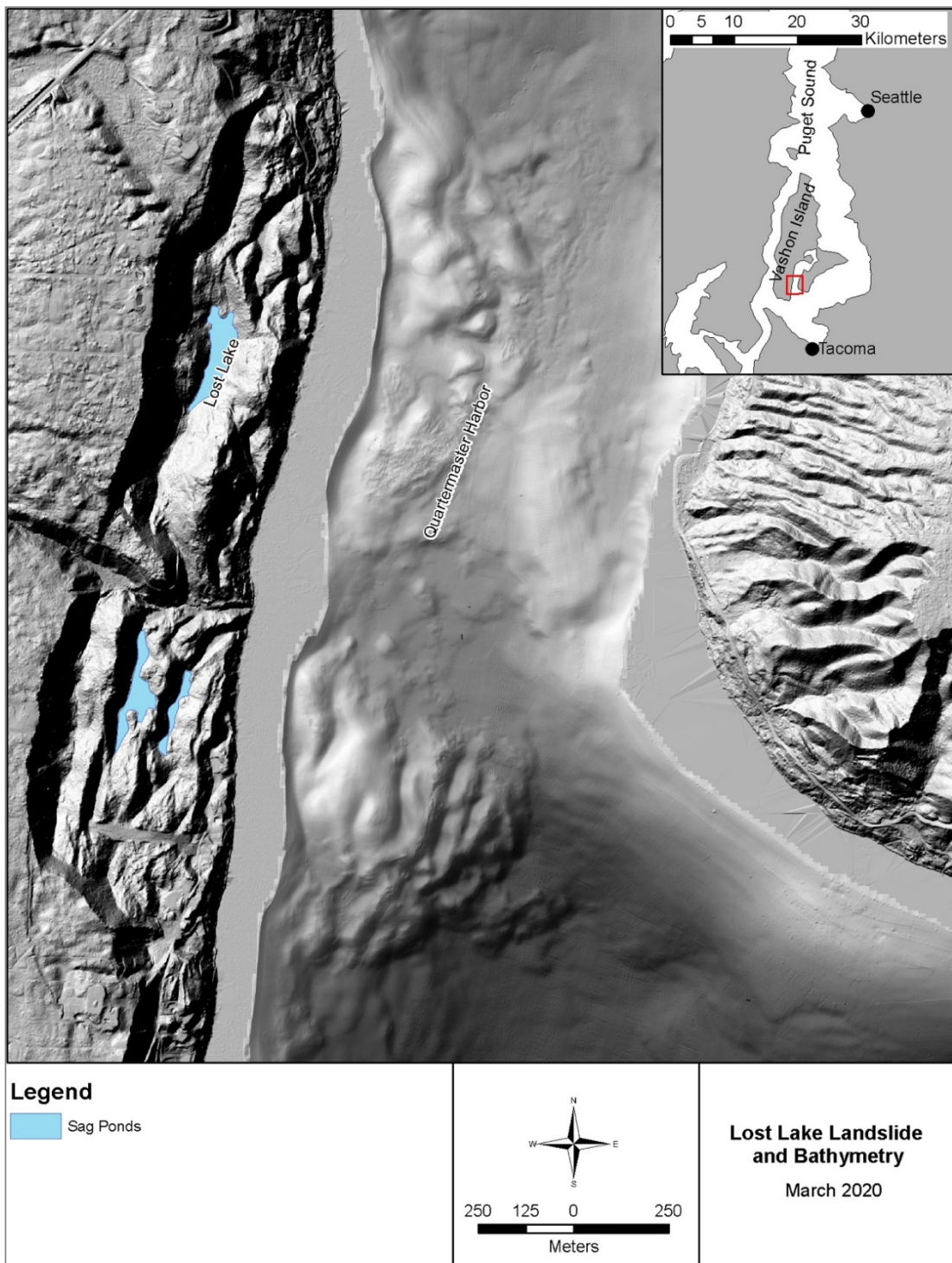


Figure 2: The terrestrial portion of the LLL in LiDAR and the bathymetry of the toe in Quartermaster Harbor. LiDAR acquired from the Washington State DNR LiDAR Portal and bathymetry acquired from NOAA bathymetric data viewer. Note the large landslide on the south end of Maury Island on the right side of figure. Another large landslide exists on Maury Island below the index map.

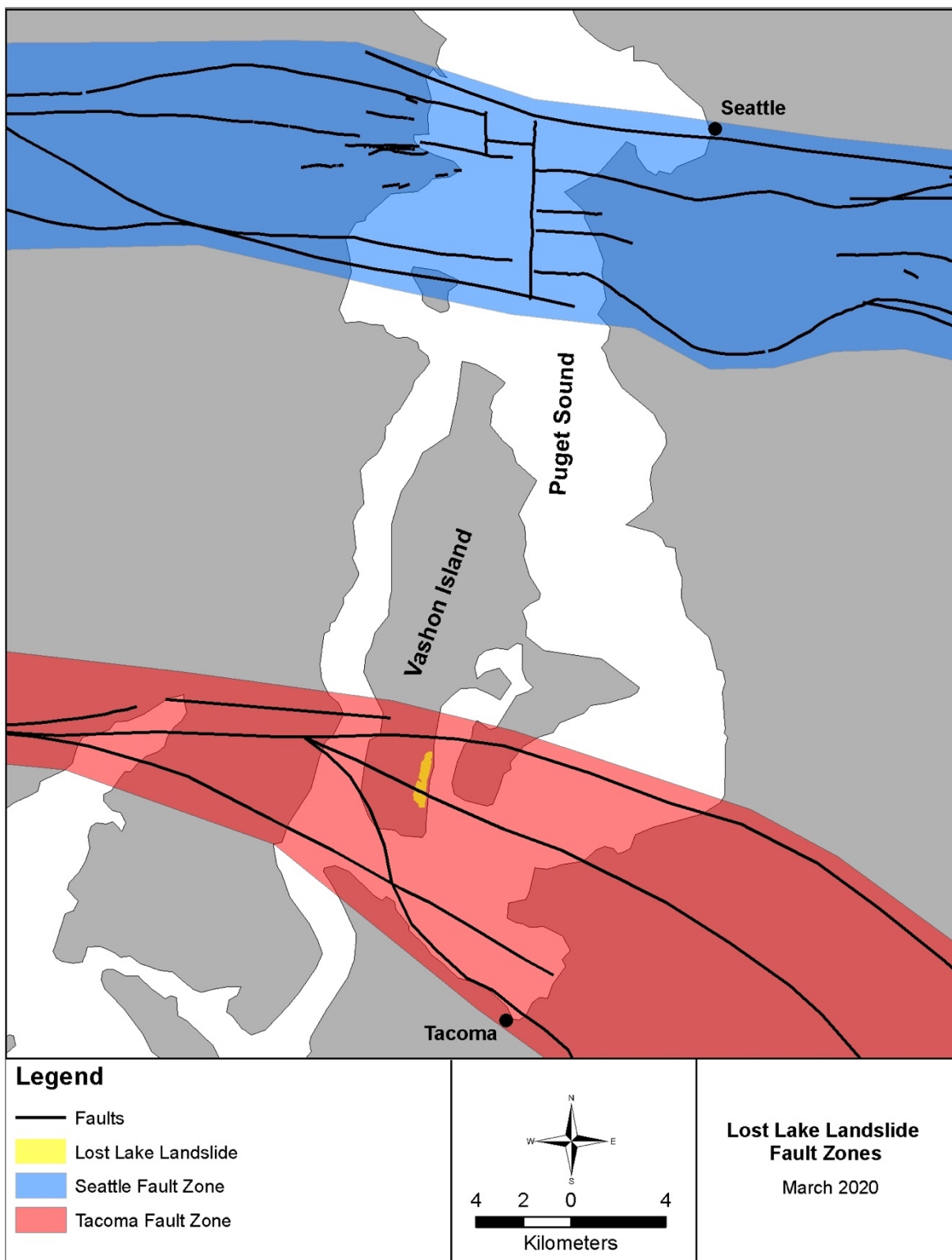


Figure 3: The Seattle Fault Zone (Blue) and Tacoma Fault Zone (Red) within Puget Sound. The Lost Lake Landslide falls within the Tacoma Fault Zone. Fault data acquired from Washington State DNR Geology Portal (Washington, 2019)

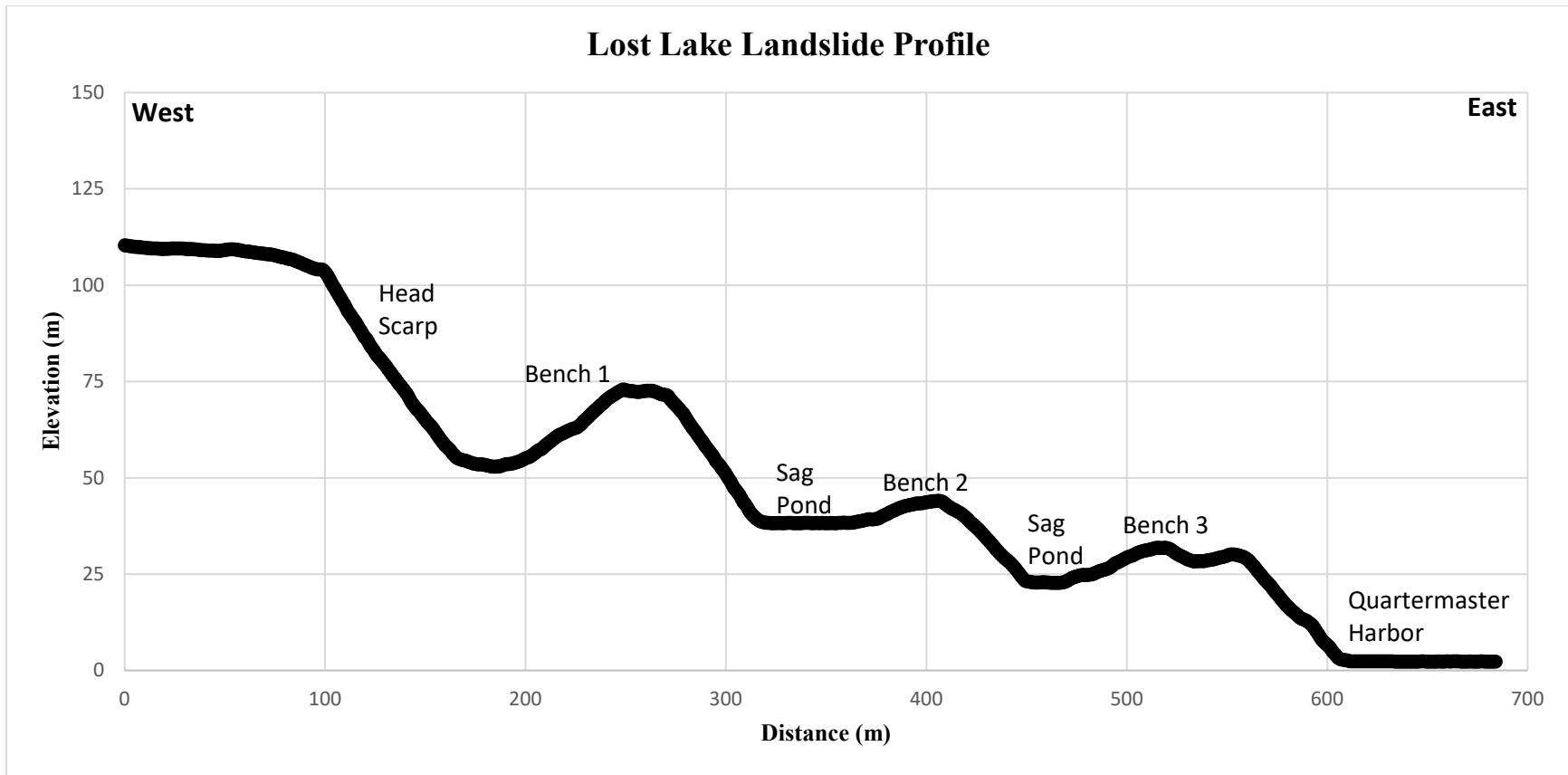


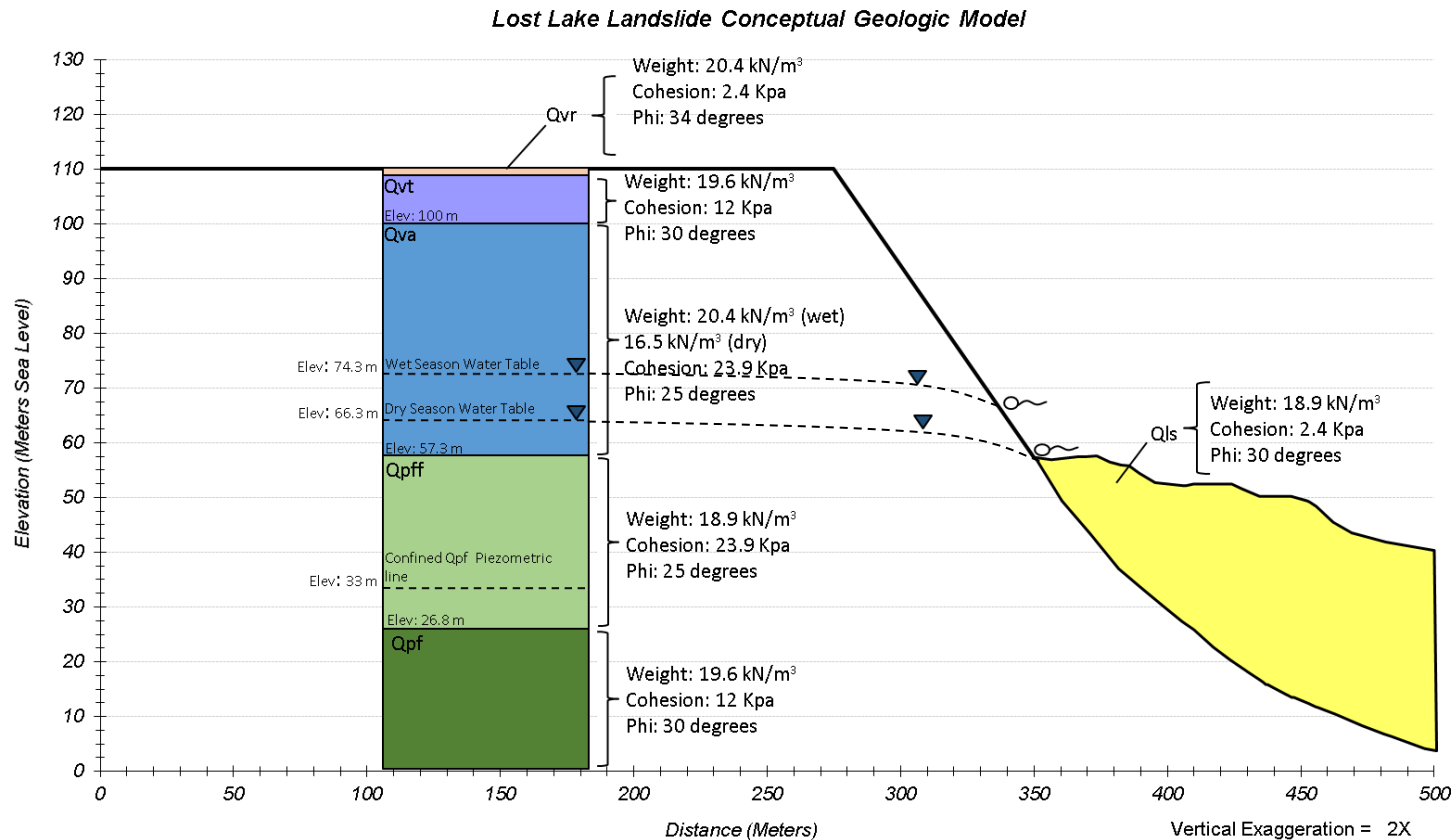
Figure 4: Modern profile of the Lost Lake Landslide. Vertical exaggeration is approximately 2x. See Figure 1 for profile location.



Figure 5: Ledgewood Landslide, on Whidbey Island. Landslide complex highlighted in yellow.



Figure 6: Southeastern Mercer Island Landslide highlighted in yellow.



Unit	Description
Qvr	<b>Recessional Outwash Deposits:</b> Loose to dense, grayish brown, sand and gravel, horizontally to cross bedded, well graded. Locally 0 to 1.5 m thick.
Qvt	<b>Vashon Till:</b> Highly varied deposits of very dense, brown to grey, silt, sand and gravel. Often contains sand lenses, cobbles and sometimes boulders. Matrix supported with subrounded to well-rounded grains. Locally 7.5 m thick.
Qva	<b>Advance Outwash Deposits:</b> Dense to very dense, brownish grey, interbedded sand and gravel with low plasticity silt lenses common in upper and lower portions of the deposit, predominantly medium grained sand, horizontally to cross bedded. Locally 43 m thick.
Qpff	<b>Pre-Fraser Fine Grained Deposits:</b> Hard, grey, low plasticity silt and clay with occasional fine sand partings, laminated to massive, localized iron-oxide cemented layers. Locally 30.5 m thick.
Qpf	<b>Deposits of Pre-Fraser Glaciation Age:</b> Very dense to hard sand, gravel, silt and diamicts, interbedded.
Qls	<b>Landslide Deposits:</b> Very loose to very dense or soft to hard diamict transported by downslope movement. Mixed fine and coarse grain deposits. Blocks of intact material are common and often display fracturing, rotated bedding, or slickensided surfaces. Variable thickness.

Figure 7: Conceptual geologic model of the Lost Lake Landslide location. Indicates orientation and thickness of subsurface layers and also Mohr-Coulomb properties used for each.

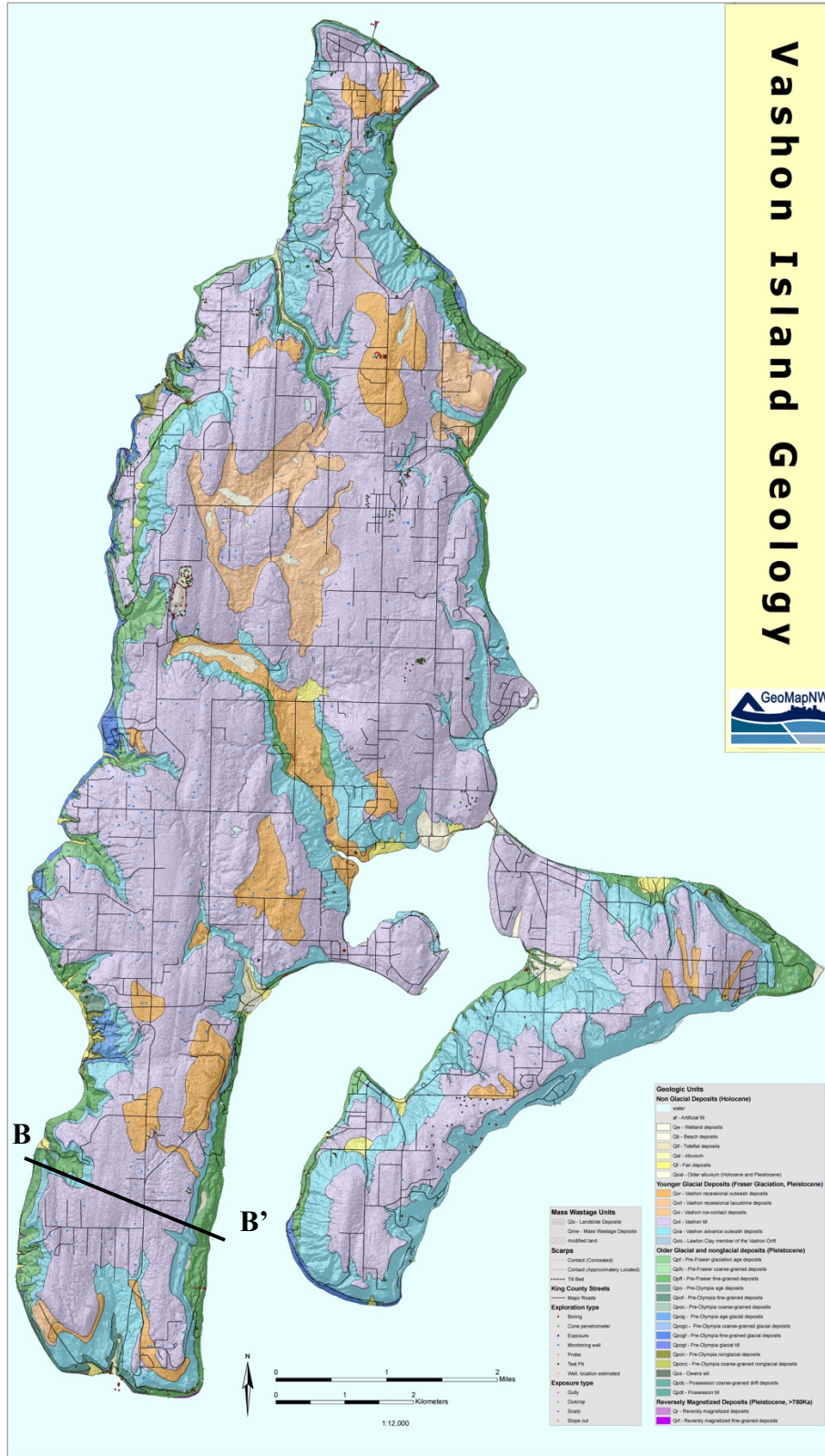


Figure 8: Geologic Map of Vashon Island, Washington. The profile B to B' is shown in Figure 9 (Troost and Booth, 2004).



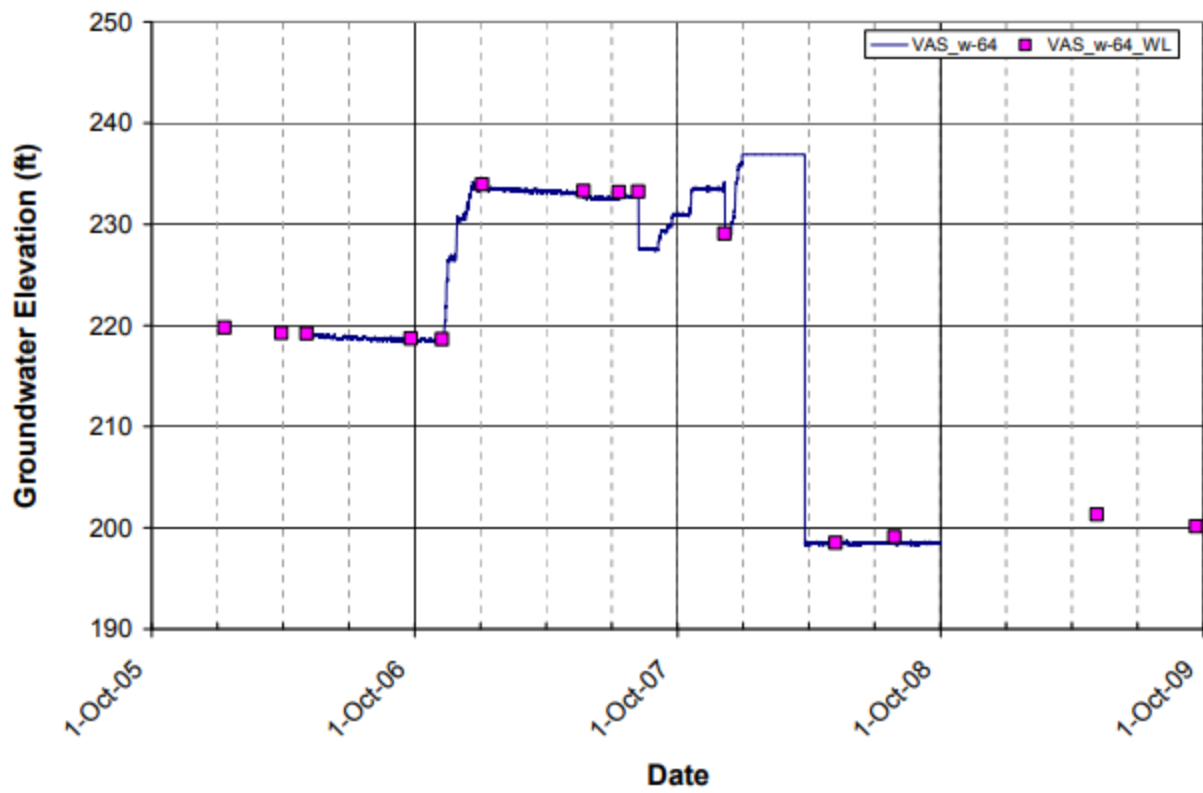


Figure 10: Well monitoring data from well VAS-W-64 used for groundwater fluctuation determination (Ferguson, 2009).

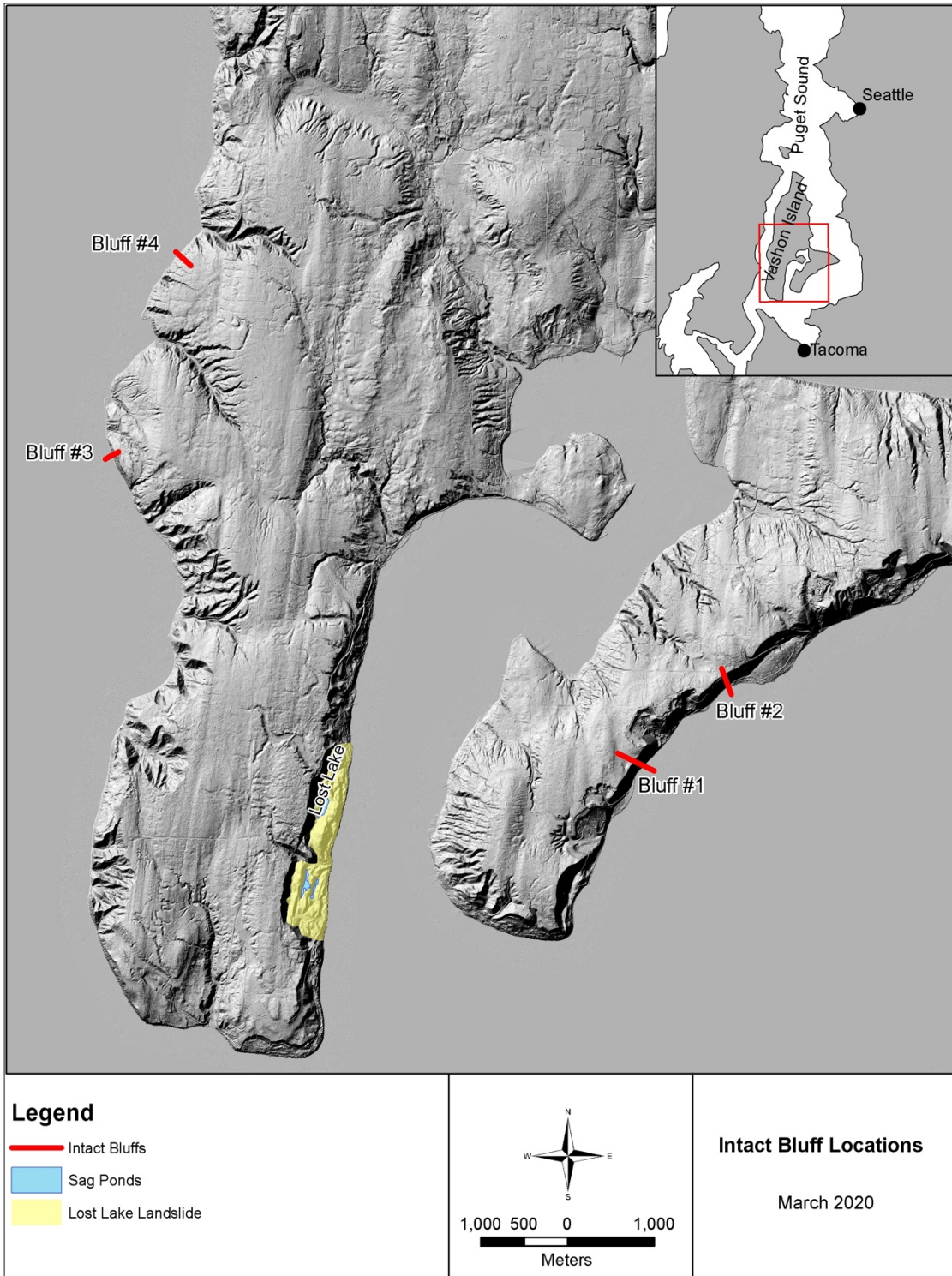


Figure 11: Location of intact bluffs around Vashon and Maury Island selected for comparison. Profiles from these locations were used to determine an average slope for the reconstructed bluff in Scenario 1. See Table 1 for slope values and the Appendix for bluff profiles.

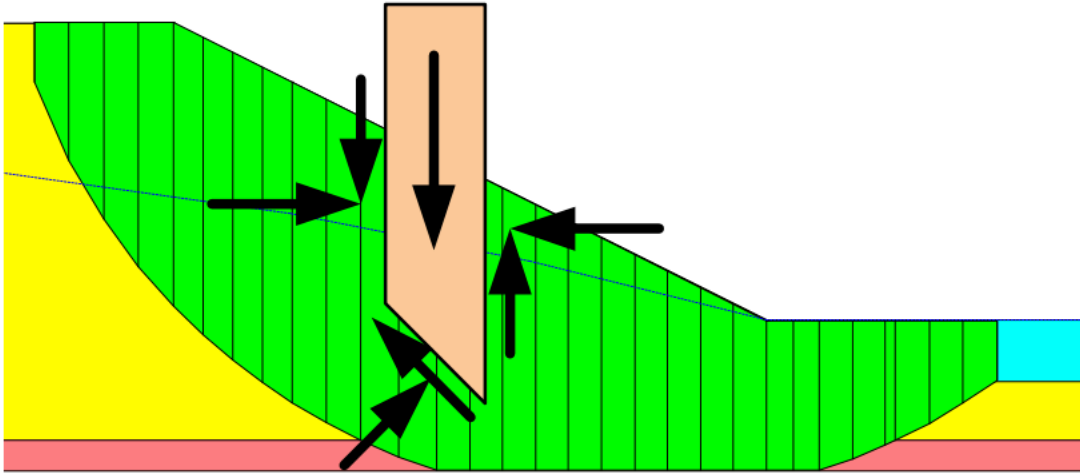


Figure 12: Division of slide mass into vertical slices and discretization of shear and normal forces acting on a slice. Rotational slide mass is shown in green. (GEO-SLOPE, 2012).

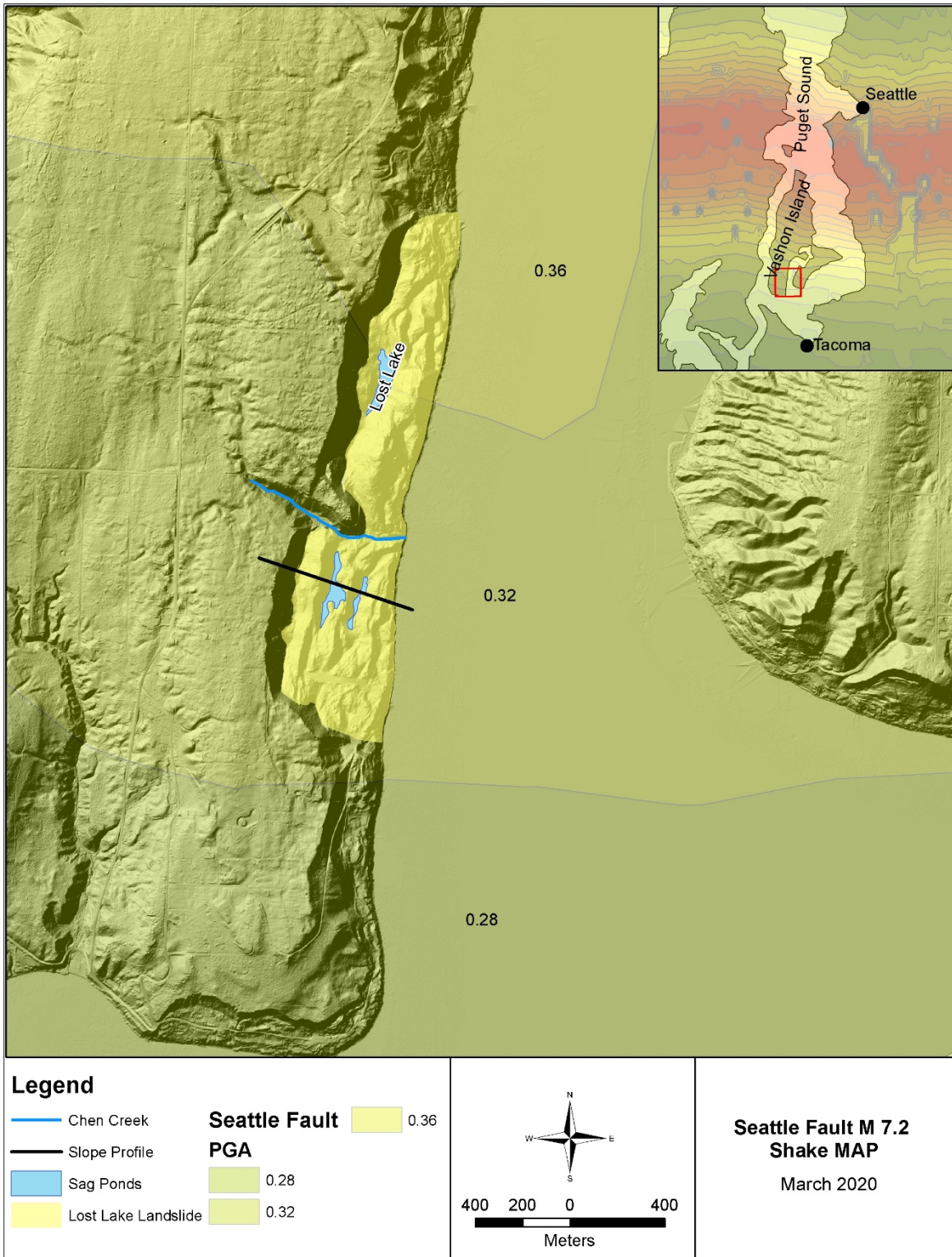


Figure 13: Peak ground acceleration contours for a magnitude 7.2 Seattle Fault Zone earthquake. Peak ground acceleration data was acquired from a M 7.2 USGS ShakeMap model scenario (USGS Seattle, 2017).

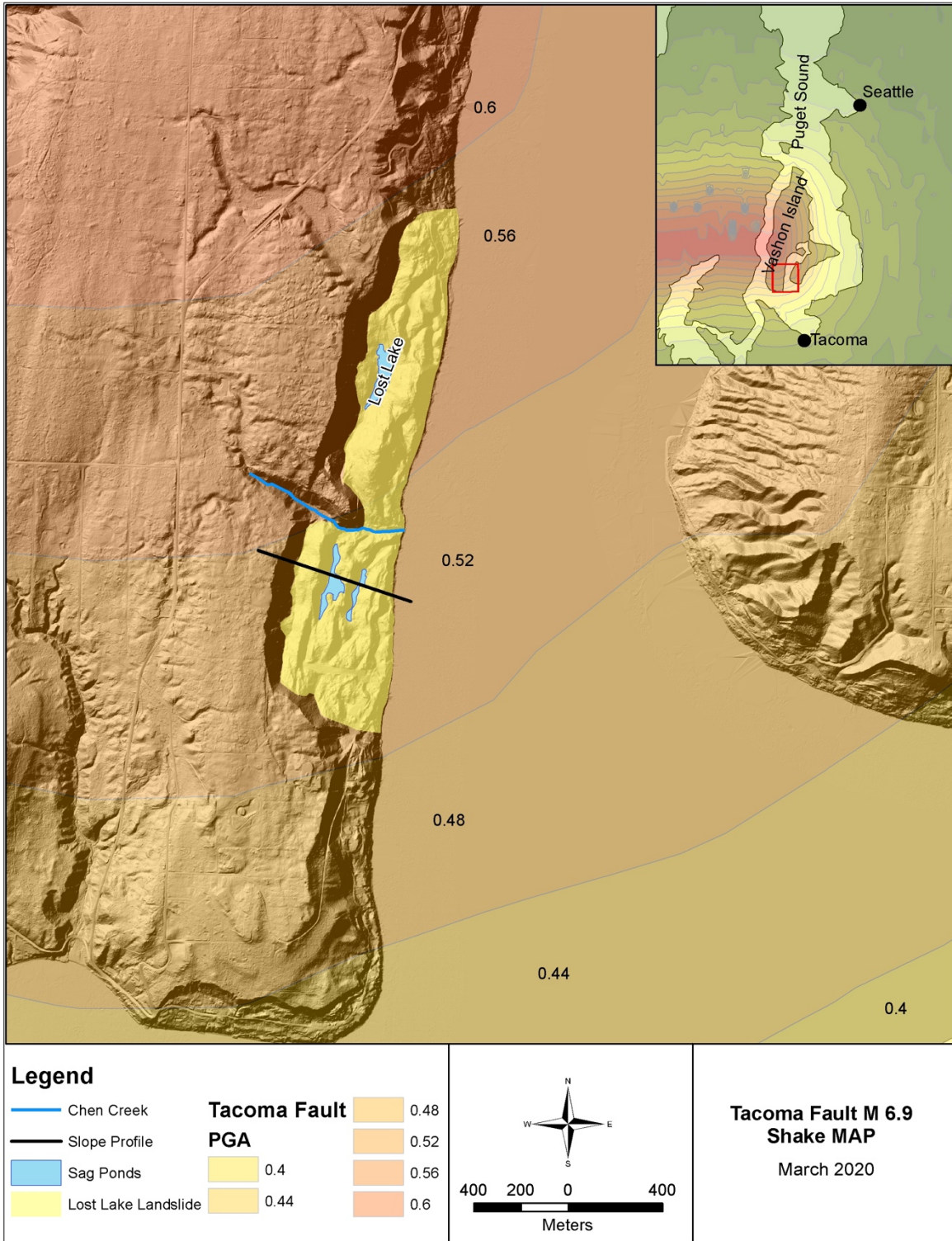


Figure 14: Peak ground acceleration contours for a magnitude 6.9 Tacoma Fault Zone earthquake. Peak ground acceleration data was acquired from a M 6.9 USGS ShakeMap model scenario (USGS Tacoma, 2017).

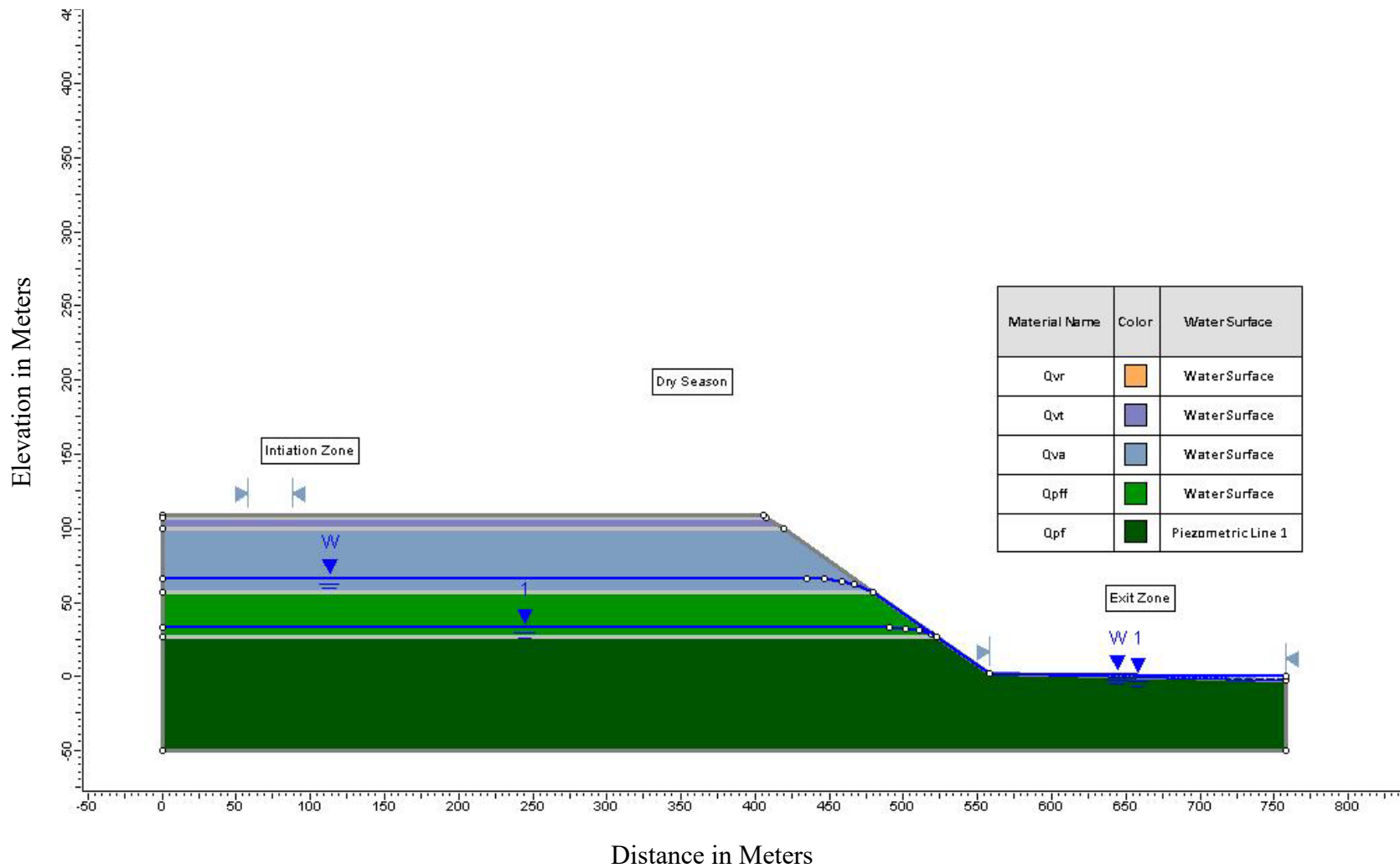


Figure 15a: Model Scenario 1 during dry season. The water surface column describes which groundwater surface defines the pore pressure for the corresponding units. The water surface is the upper blue line labeled W and the piezometric line is the lower blue line labeled 1.

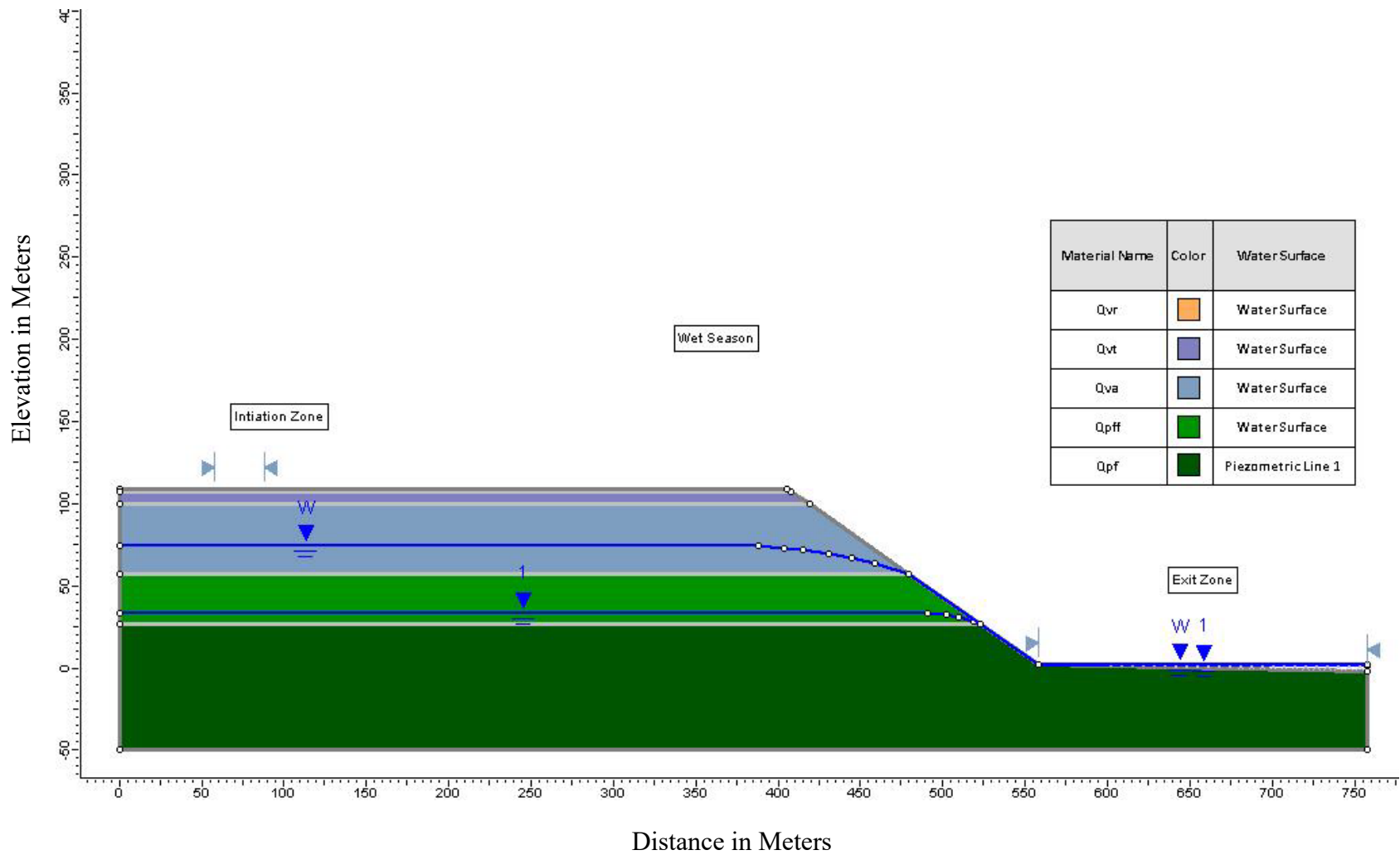


Figure 15b: Model Scenario 1 during wet season.

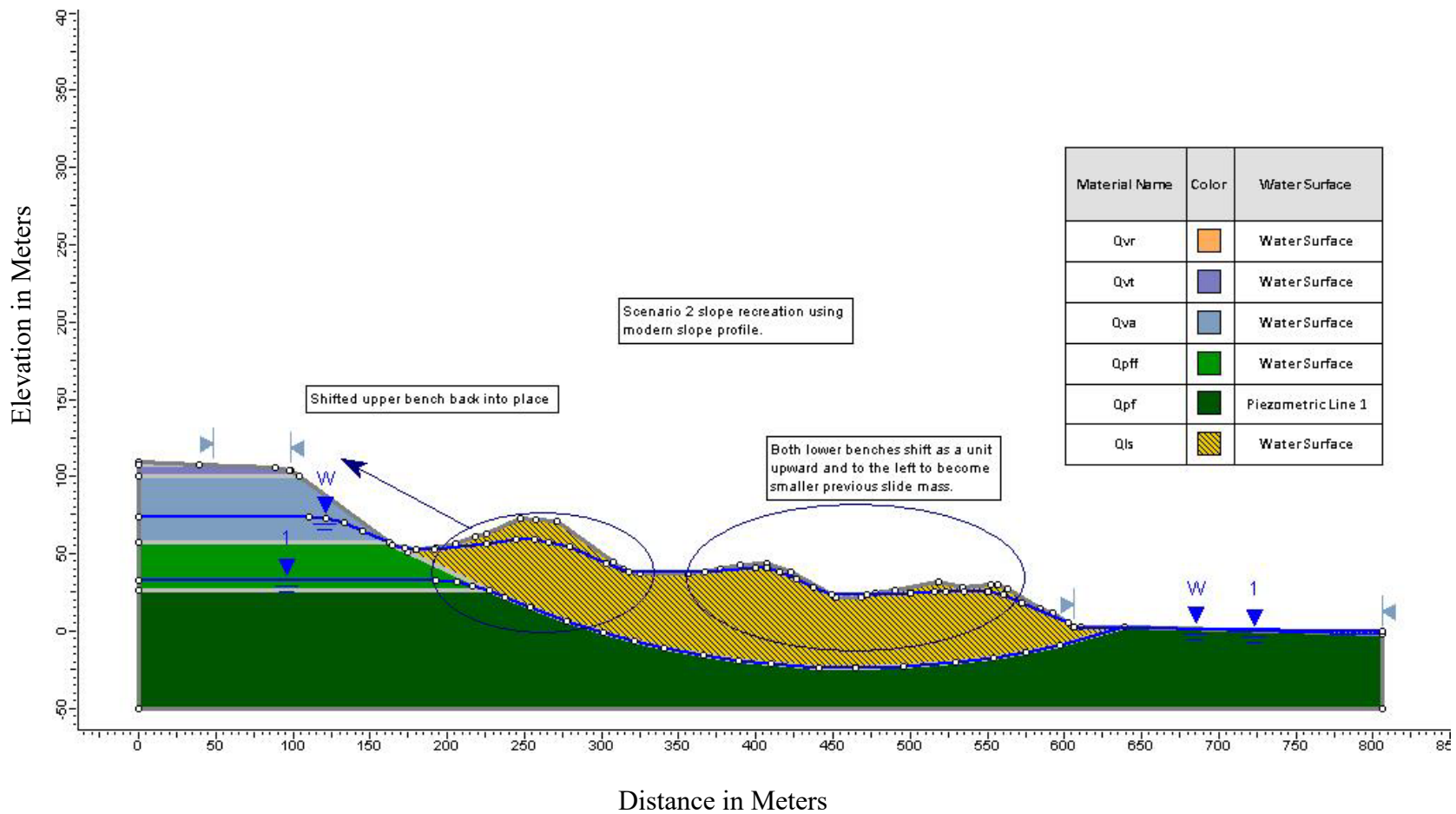


Figure 16: Set up of model Scenario 2. Shows how the uppermost back-tilted block was shifted upslope and into place to re-create a potential previous iteration of failure. This is not model Scenario 2, only a depiction of how it was set up. Scenario 2 is shown in Figures 17a and 17b.

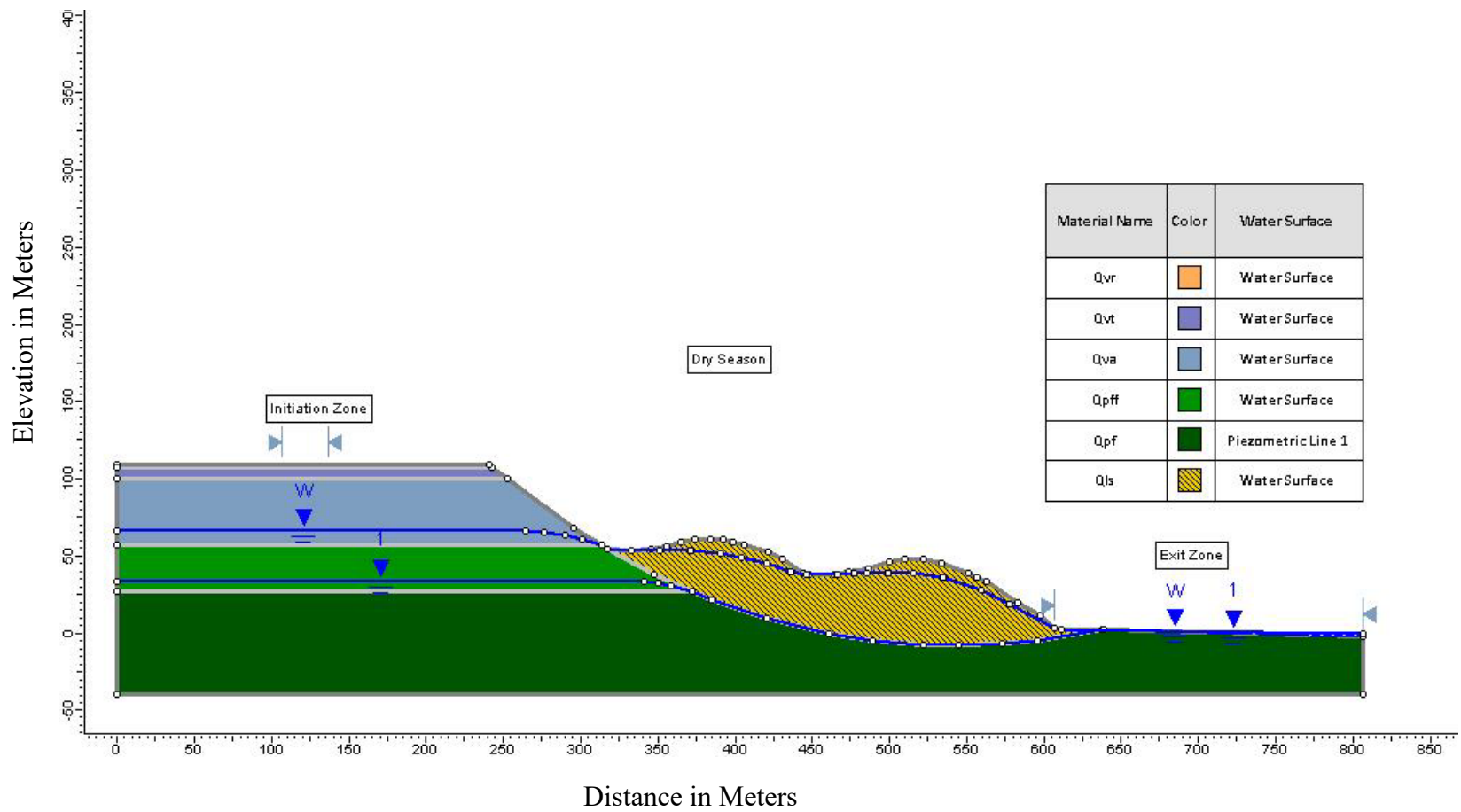


Figure 17a: Model Scenario 2 during dry season.

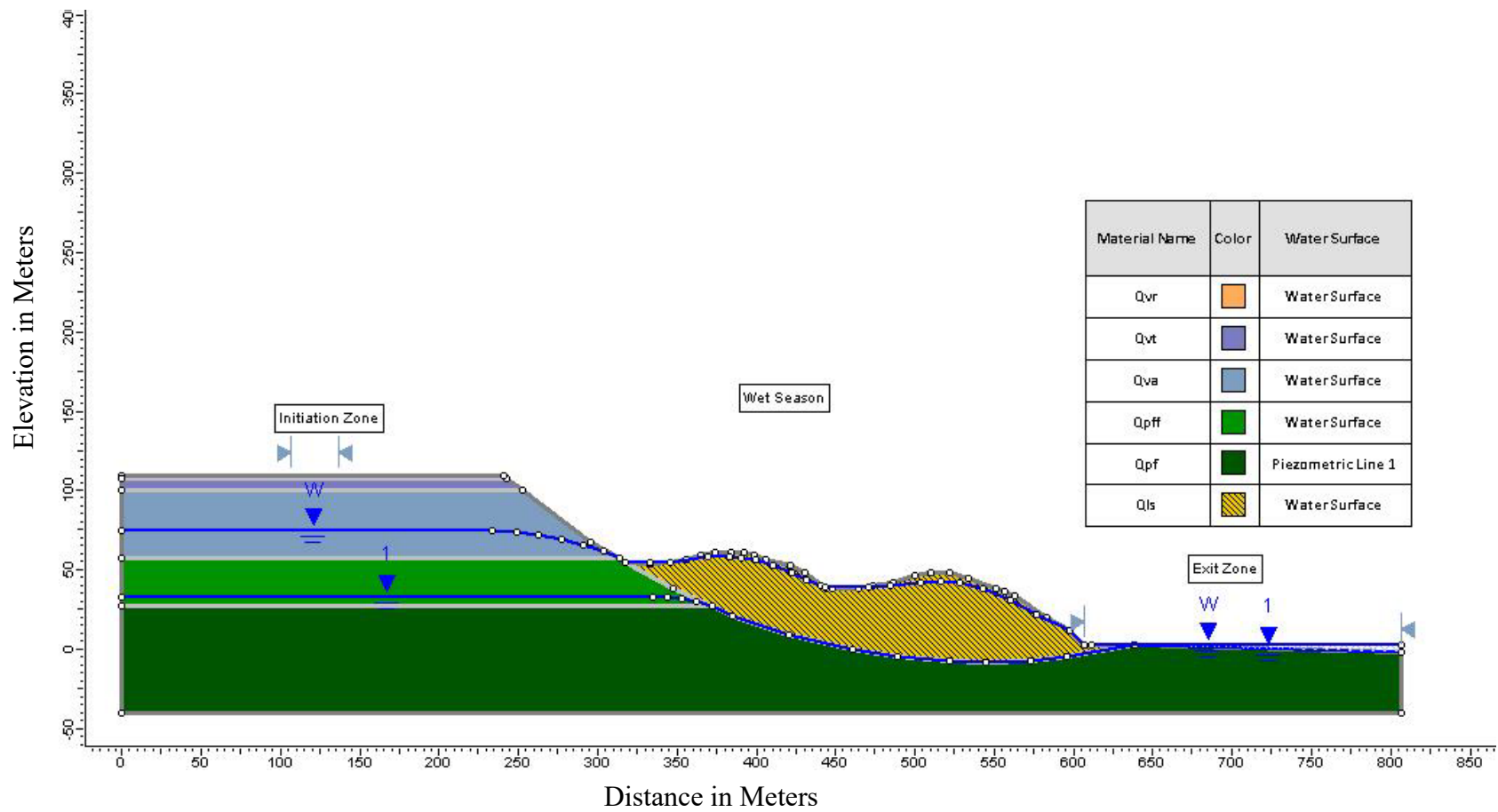


Figure 17b: Model Scenario 2 during wet season.

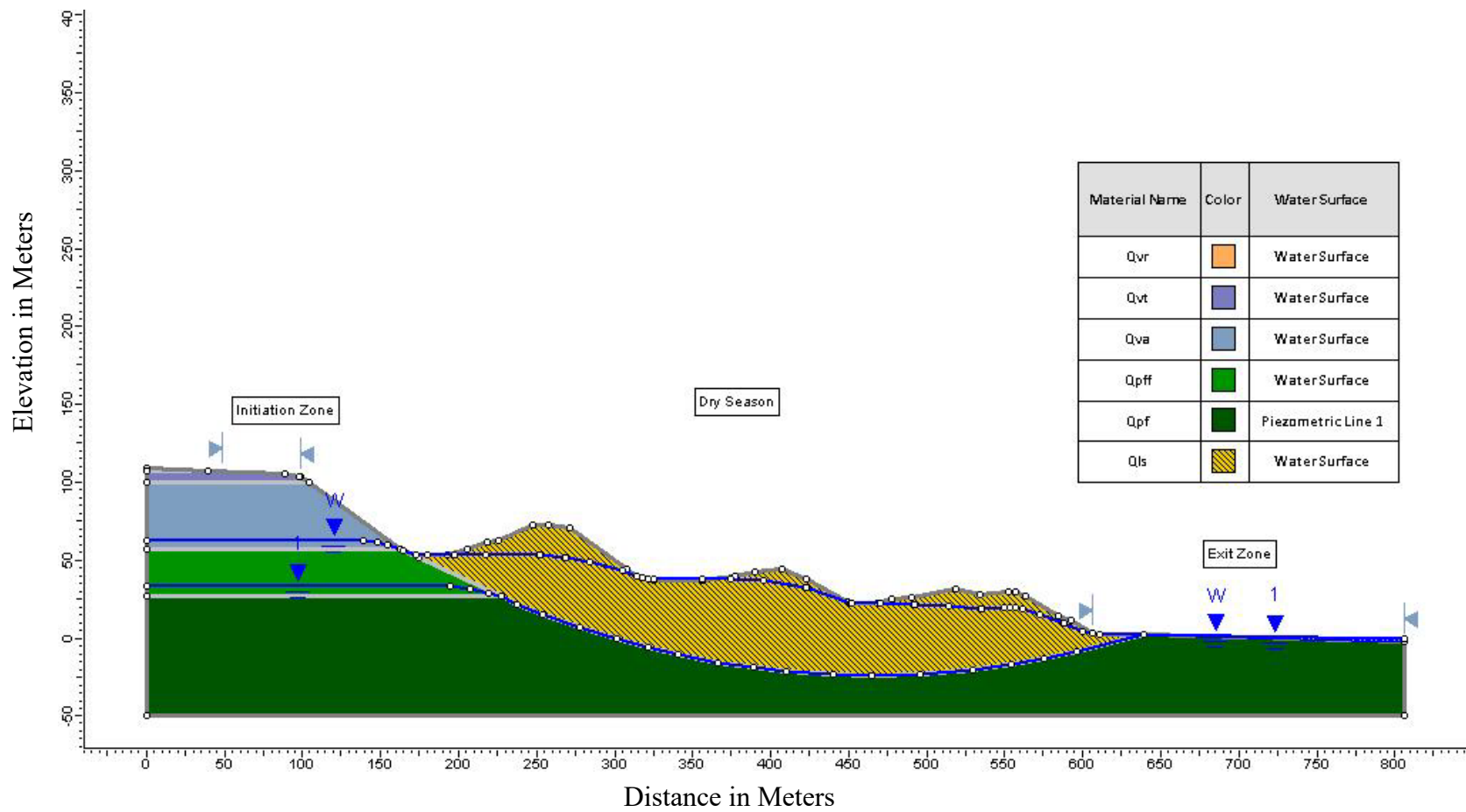


Figure 18a: Model Scenario 3 during dry season.

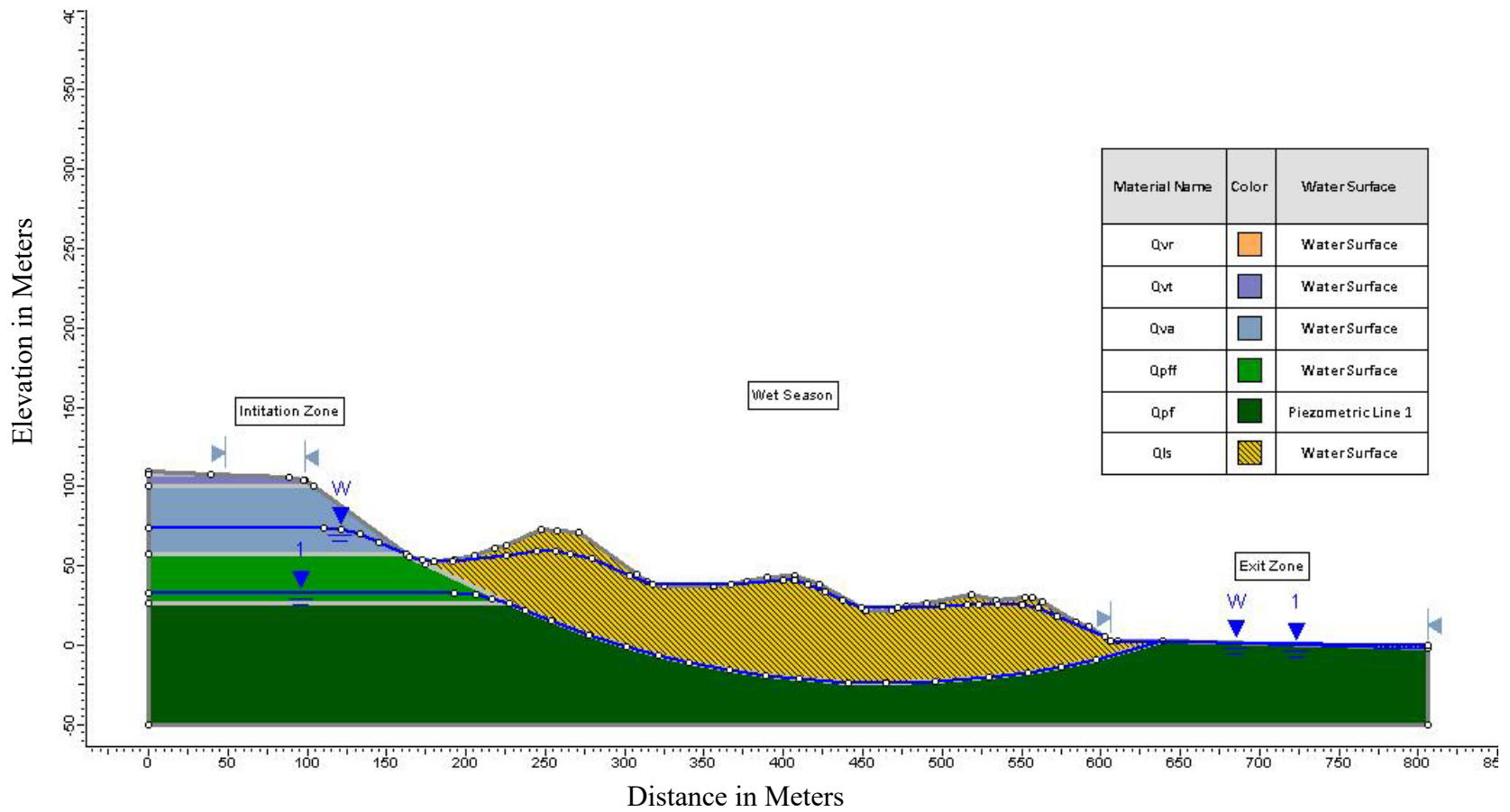


Figure 18b: Model Scenario 3 during wet season.

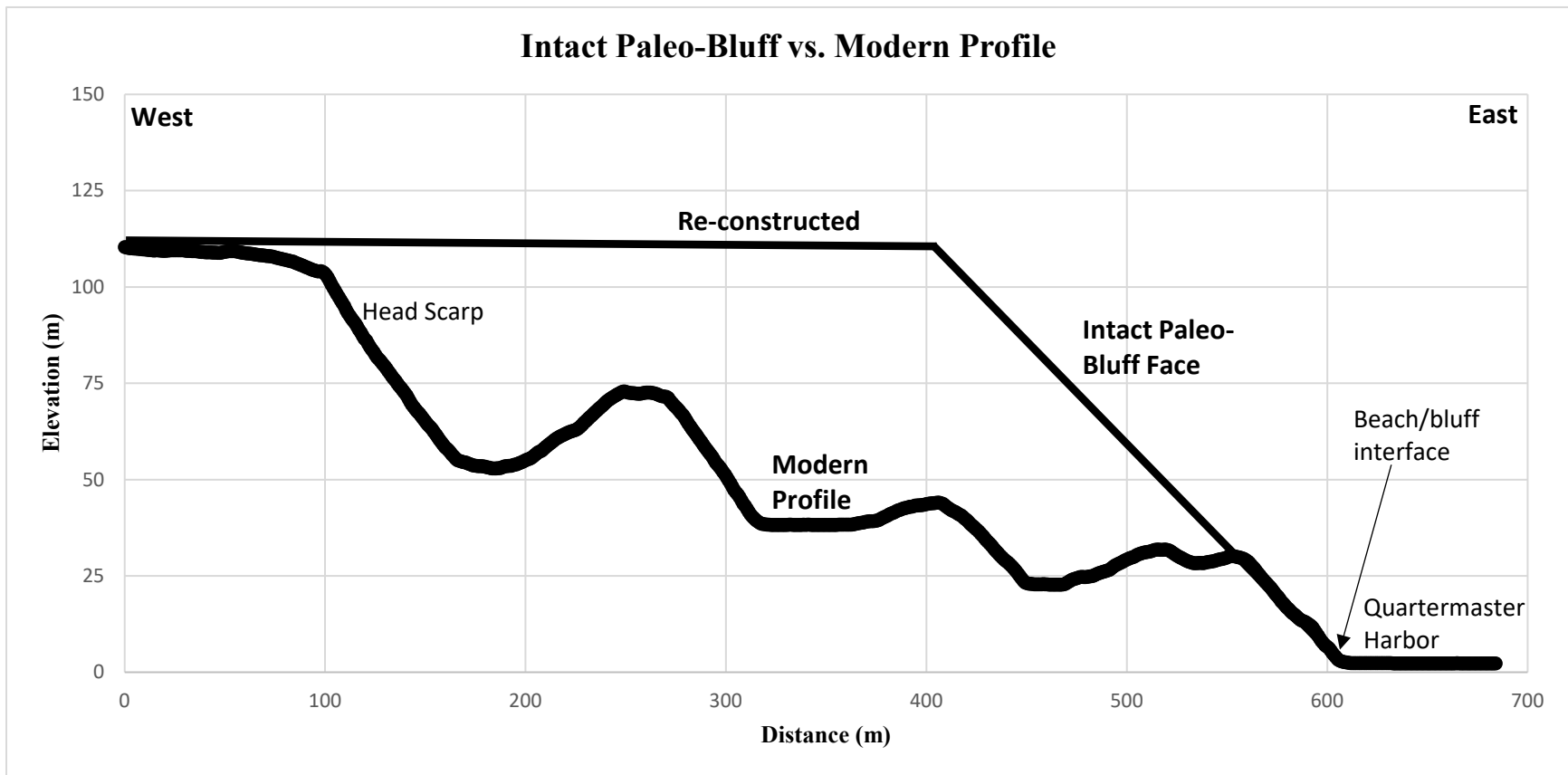


Figure 19: Reconstruction of the paleo-bluff based on the current head scarp and beach/bluff interface.

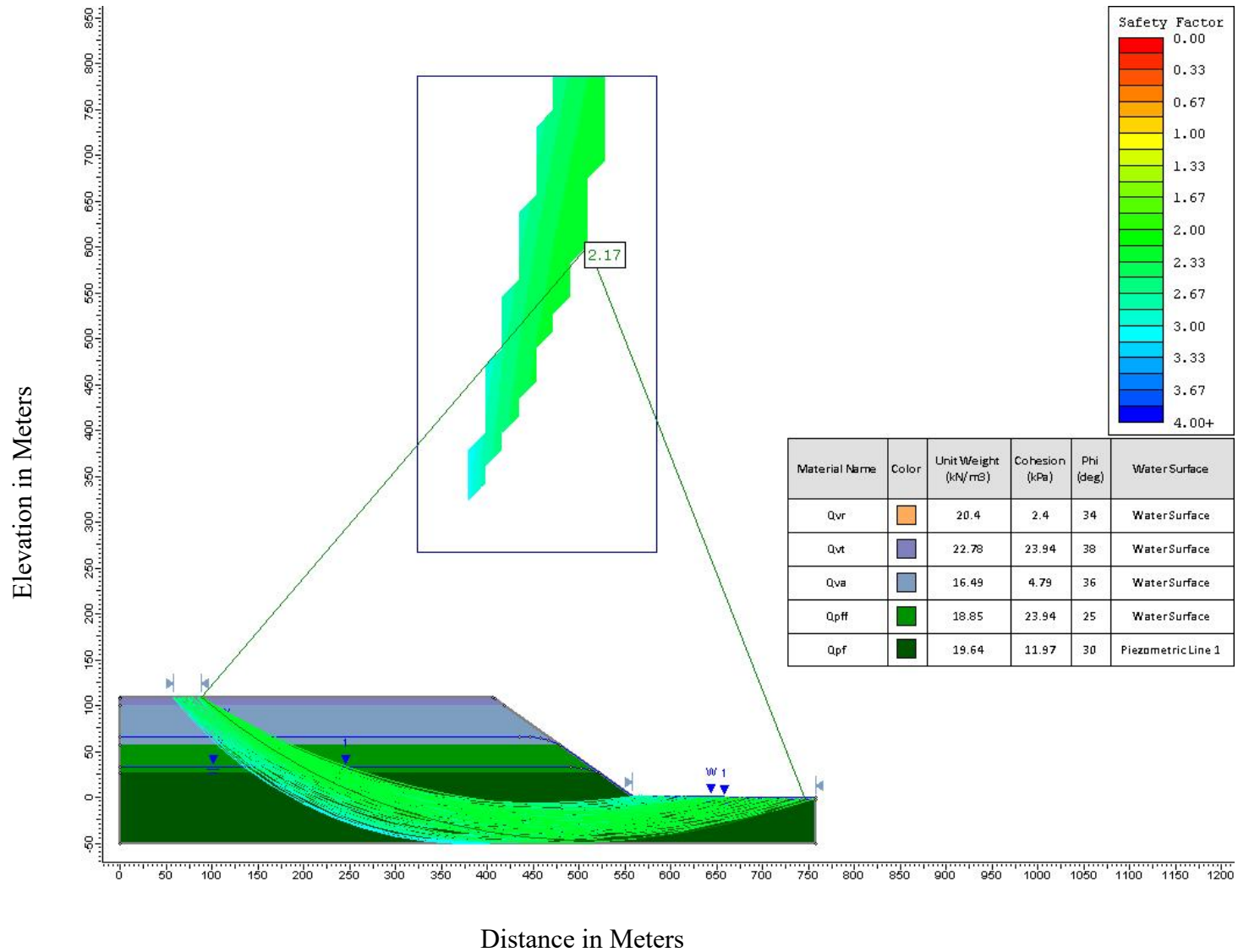


Figure 20: Scenario 1 dry season model results for factor of safety. The average of all slip surfaces was used to assign a general factor of safety to this scenario. The factor of safety value shown in green is the global minimum slip surface. Note the grid box above the slope which constrains where failure grid points are generated.

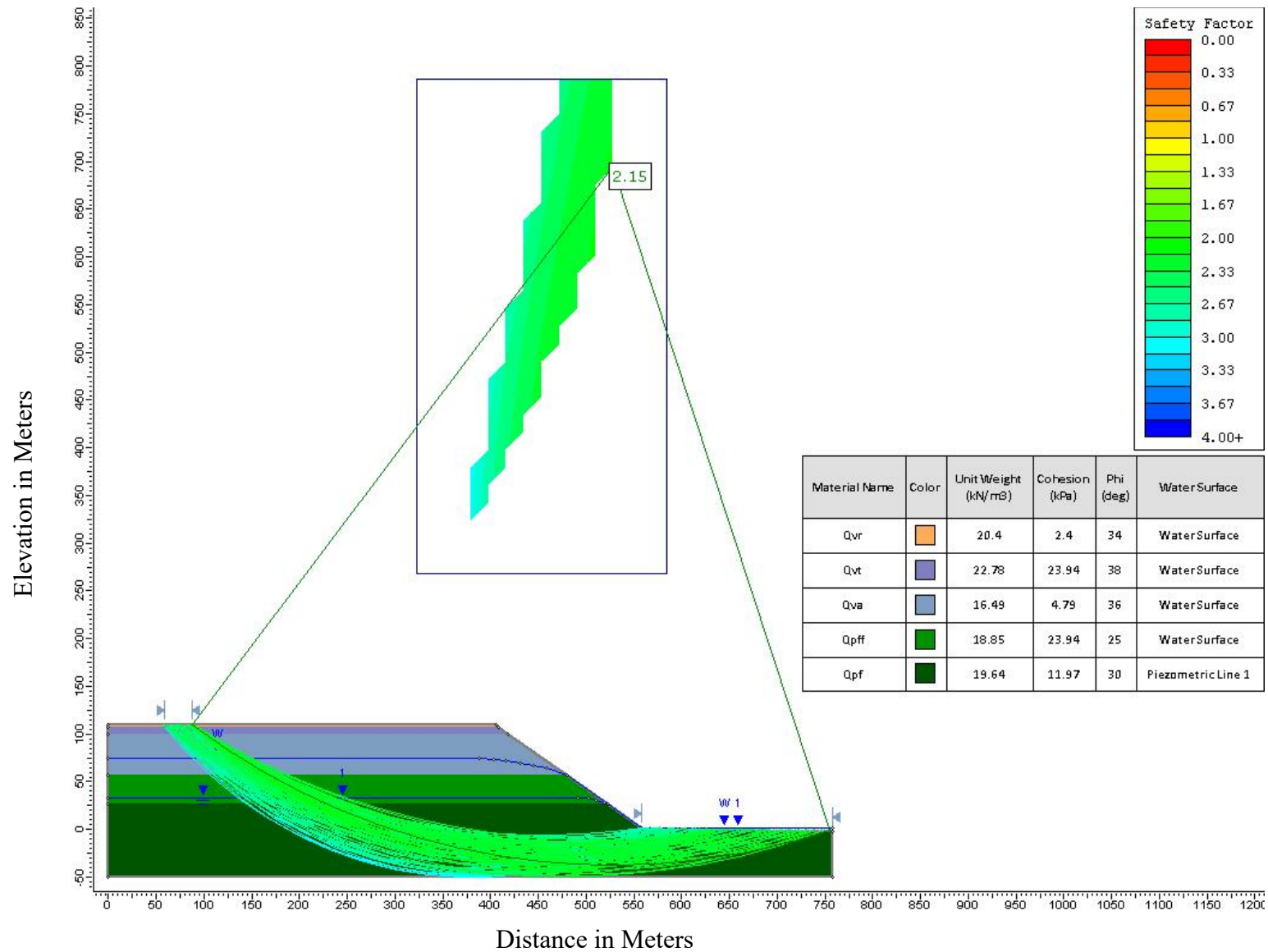


Figure 21: Scenario 1 wet season model results for factor of safety. The average of all slip surfaces was used to assign a general factor of safety to this scenario. The factor of safety value shown in green is the global minimum slip surface.

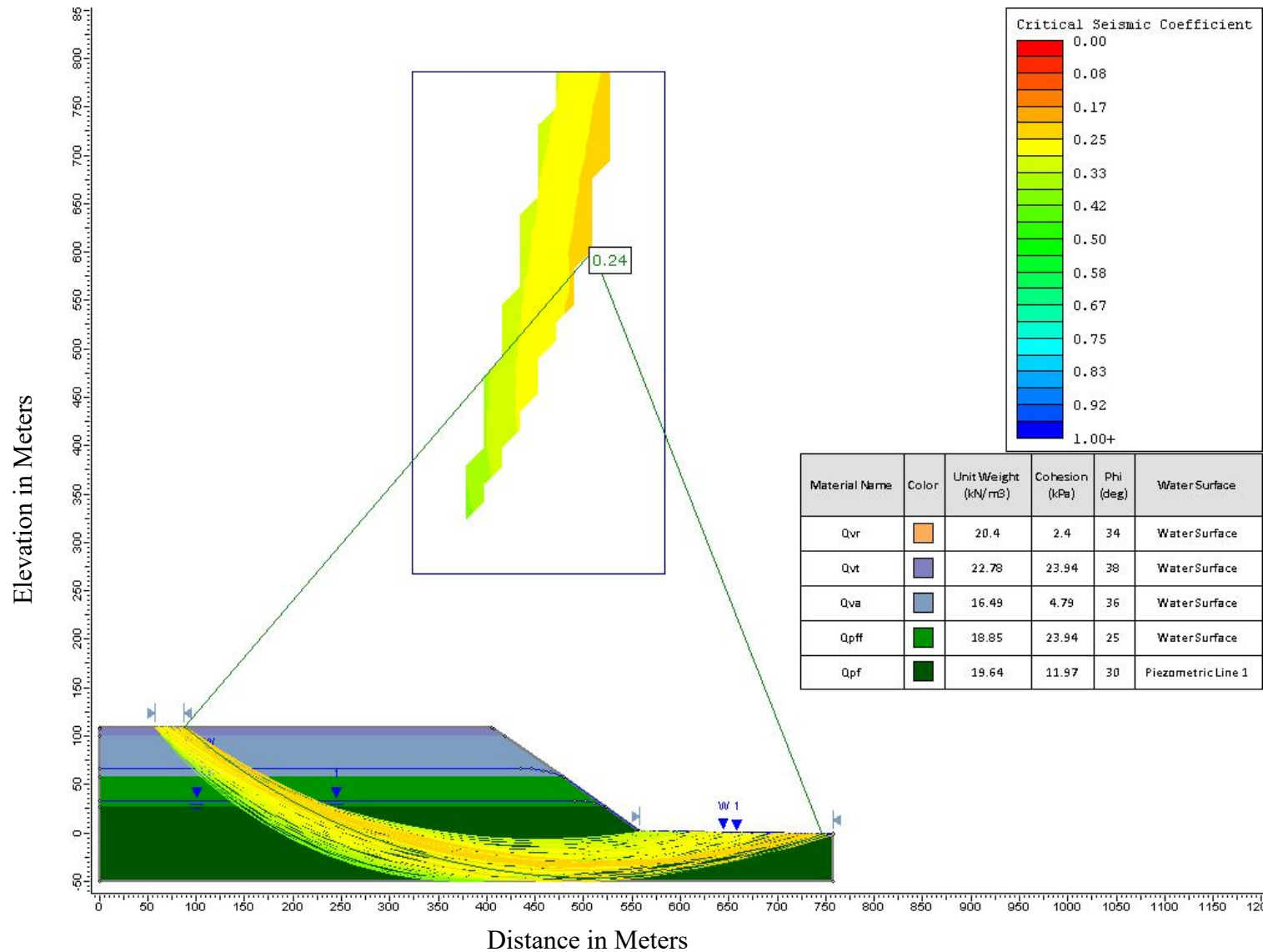


Figure 22: Scenario 1 dry season model results for critical acceleration. The average of all slip surfaces was used to assign a general critical acceleration to this scenario. The critical acceleration value shown in green is the global minimum slip surface.

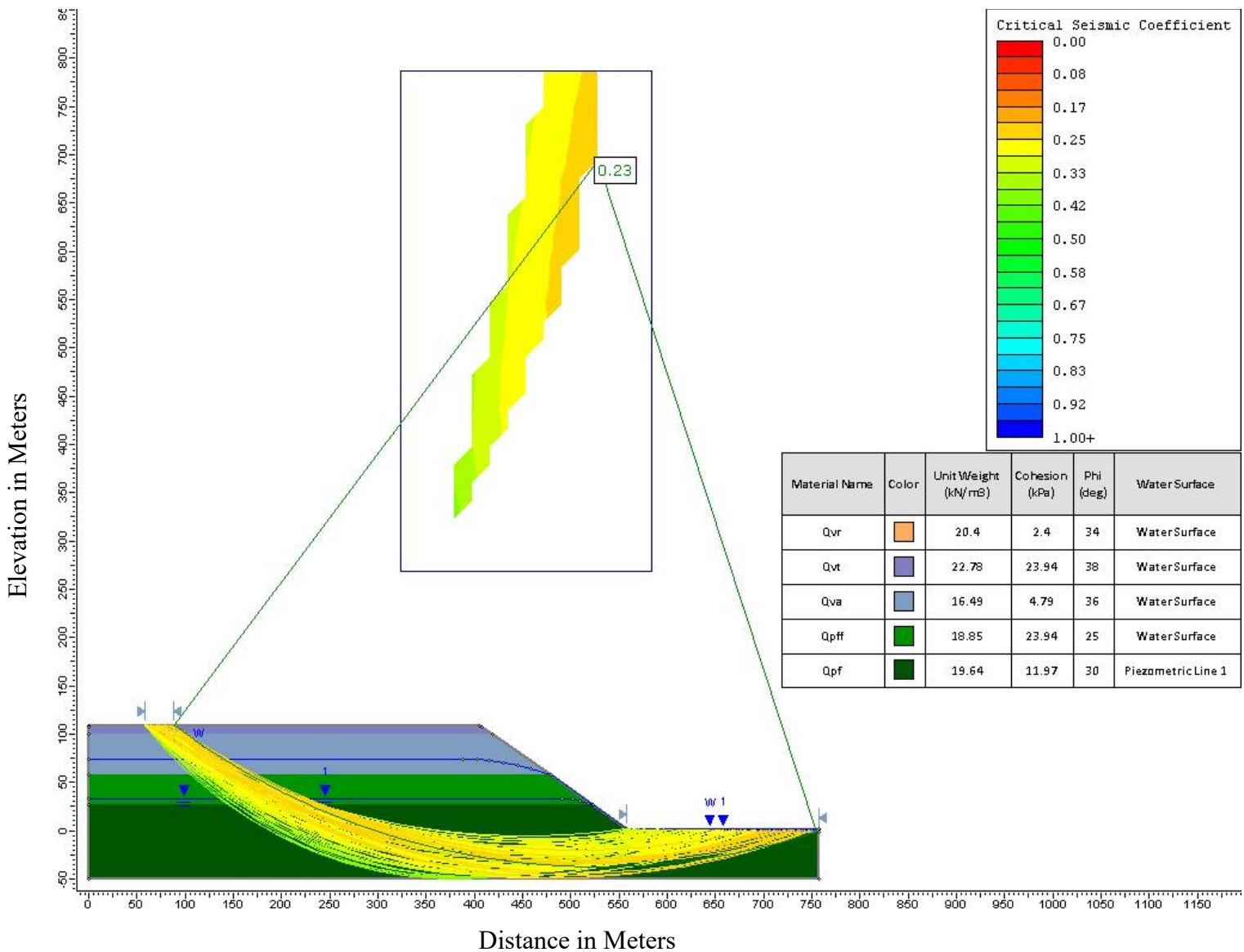


Figure 23: Scenario 1 wet season model results for critical acceleration. The average of all slip surfaces was used to assign a general critical acceleration to this scenario. The critical acceleration value shown in green is the global minimum slip surface.

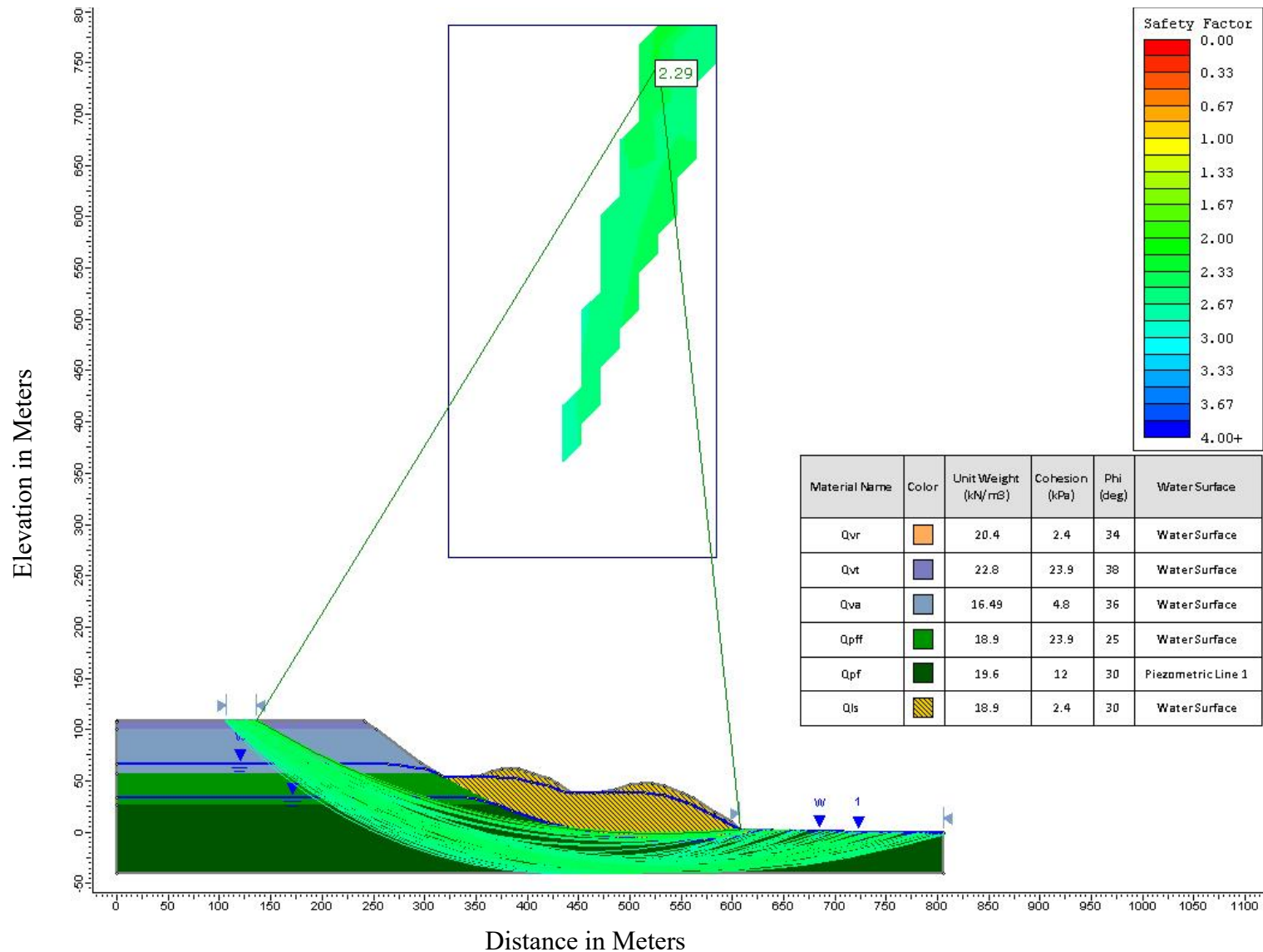


Figure 24: Scenario 2 dry season model results for factor of safety. The average of all slip surfaces was used to assign a general factor of safety to this scenario. The factor of safety value shown in green is the global minimum slip surface.

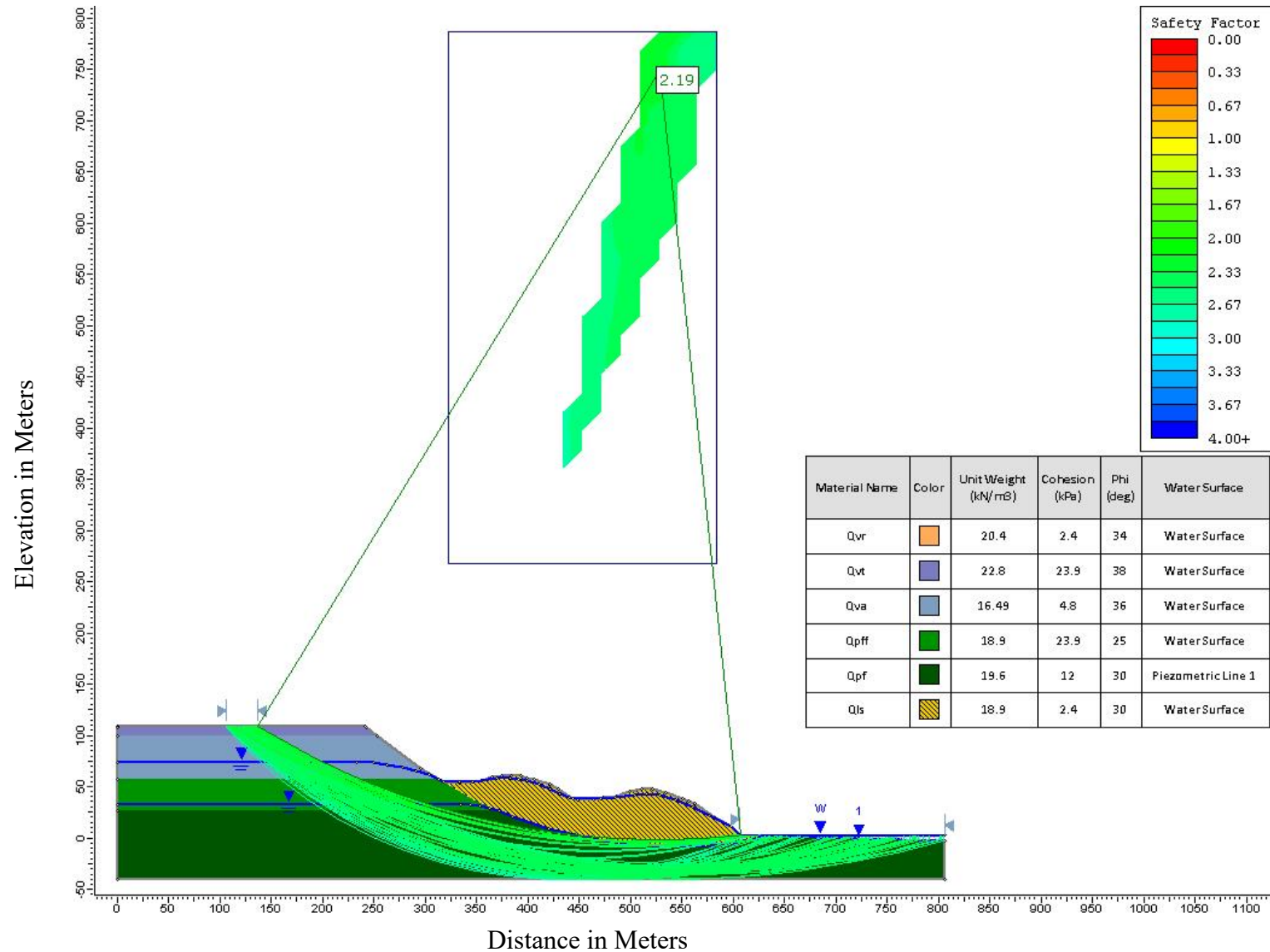


Figure 25: Scenario 2 wet season model results for factor of safety. The average of all slip surfaces was used to assign a general factor of safety to this scenario. The factor of safety value shown in green is the global minimum slip surface.

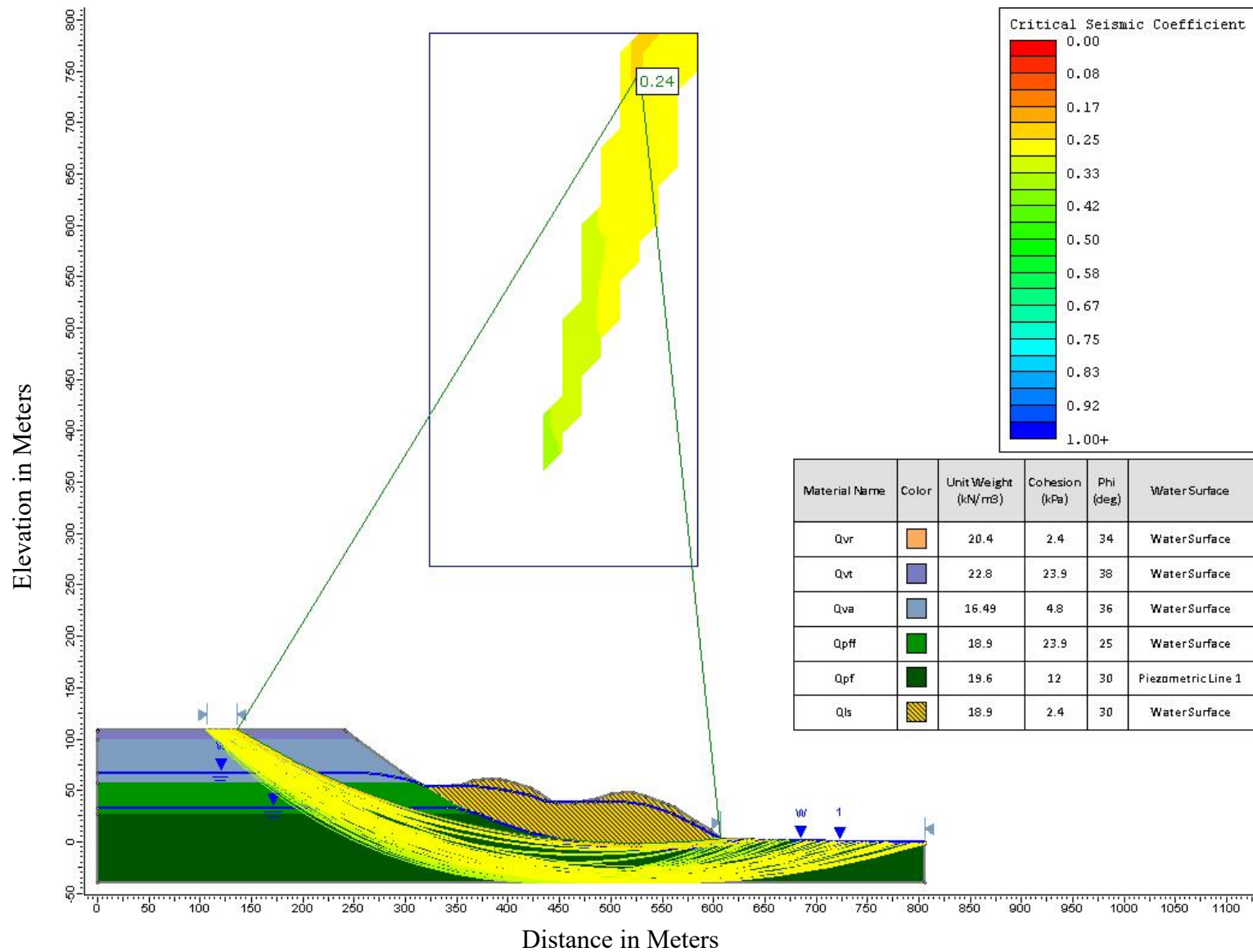


Figure 26: Scenario 2 dry season model results for critical acceleration. The average of all slip surfaces was used to assign a general critical acceleration to this scenario. The critical acceleration value shown in green is the global minimum slip surface.

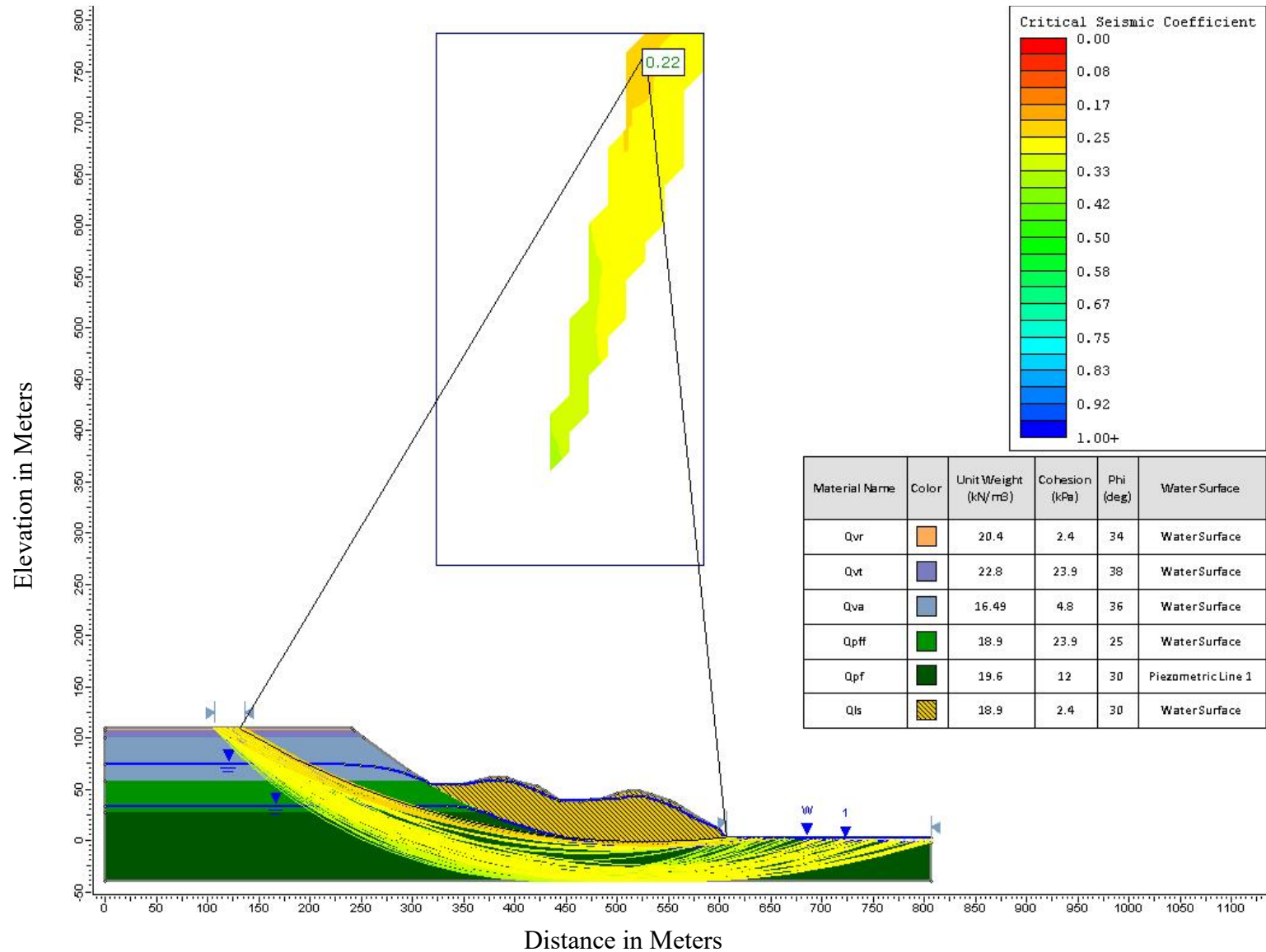


Figure 27: Scenario 2 wet season model results for critical acceleration. The average of all slip surfaces was used to assign a general critical acceleration to this scenario. The critical acceleration value shown in green is the global minimum slip surface.

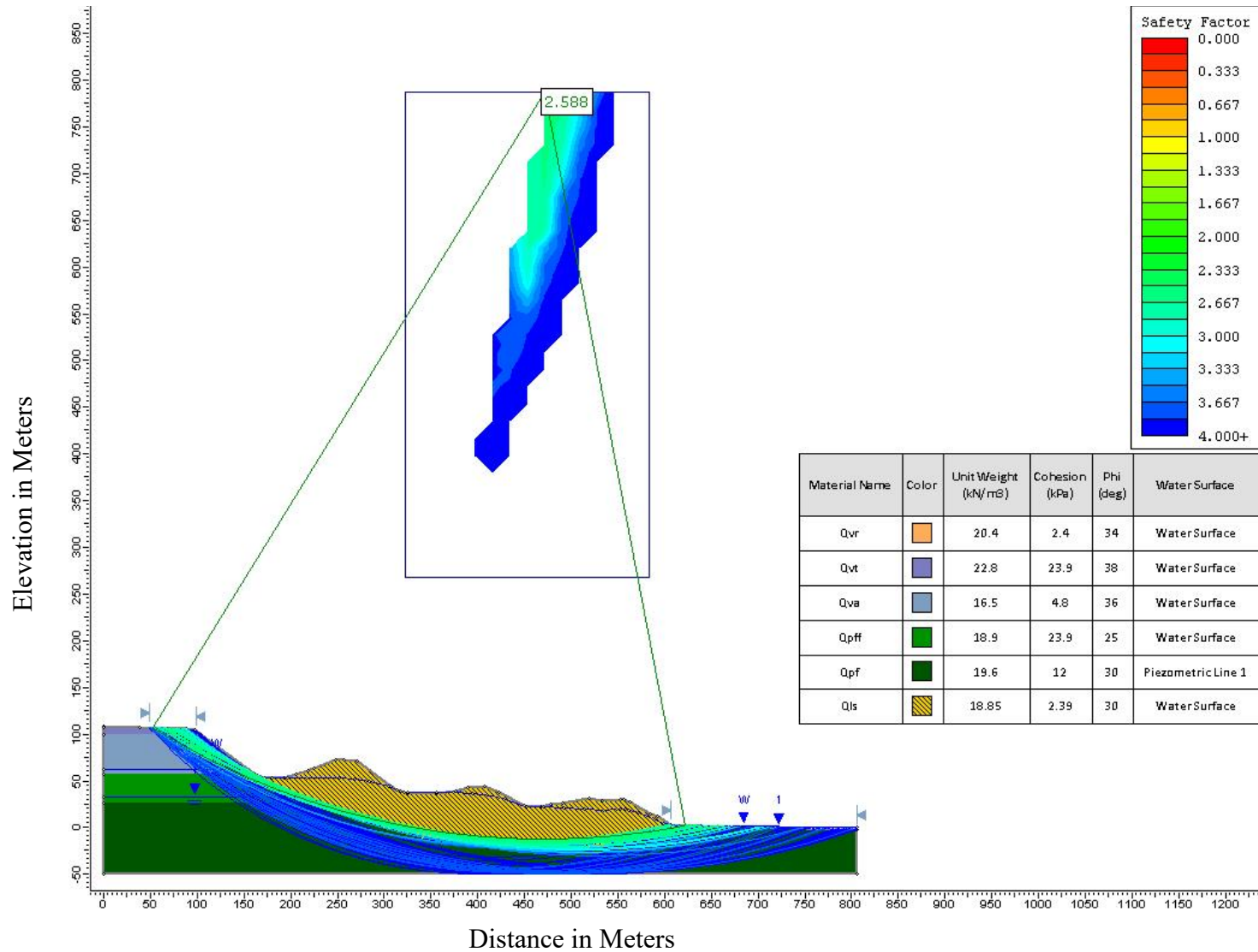


Figure 28: Scenario 3 dry season model results for factor of safety. The average of all slip surfaces was used to assign a general factor of safety to this scenario. The factor of safety value shown in green is the global minimum slip surface. Note the Factor of safety scale is from zero to four rather than zero to three on Scenarios 1 & 2.

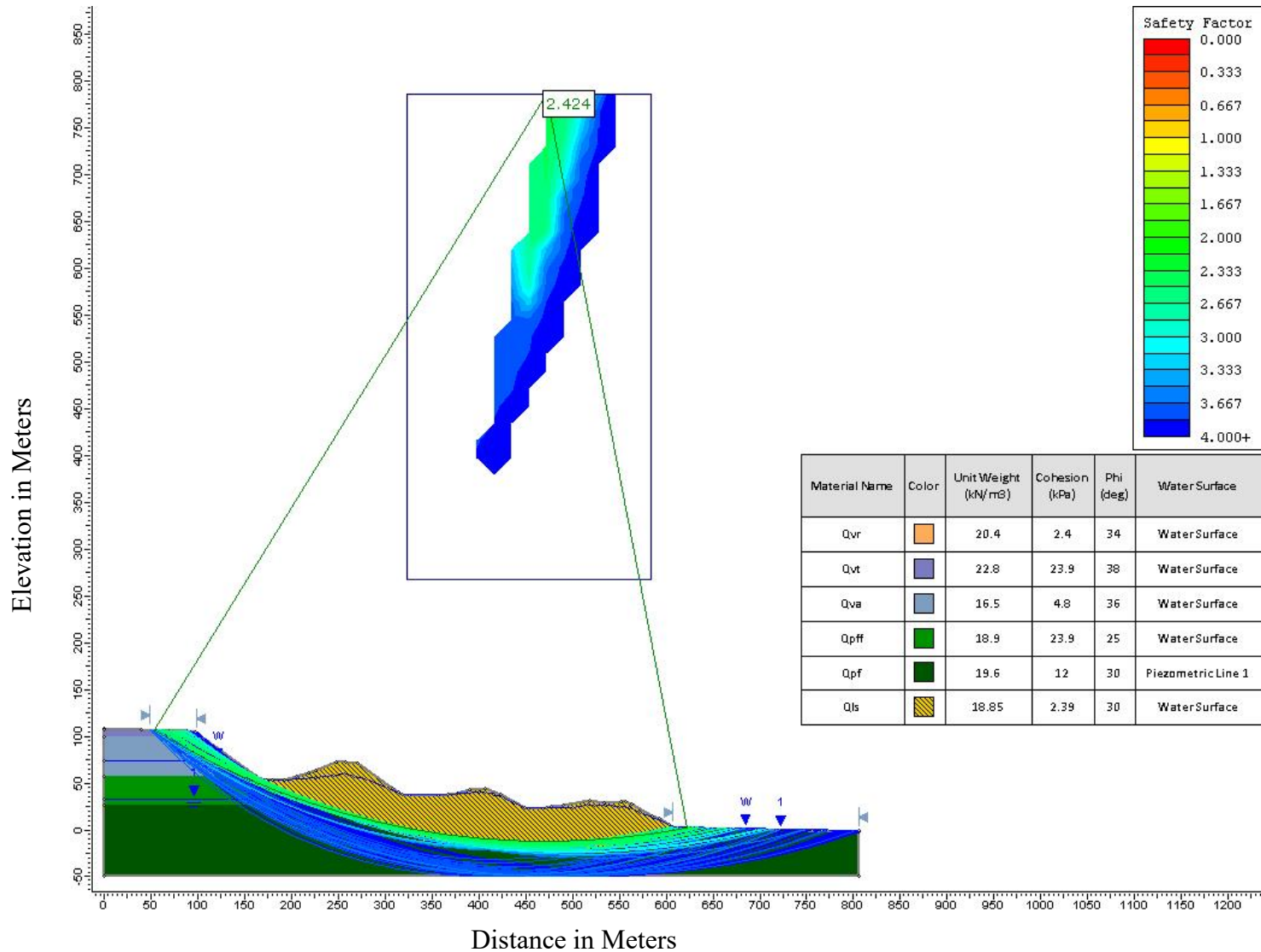


Figure 29: Scenario 3 wet season model results for factor of safety. The average of all slip surfaces was used to assign a general factor of safety to this scenario. The factor of safety value shown in green is the global minimum slip surface. Note the Factor of safety scale is from zero to four rather than zero to three on Scenarios 1 & 2.

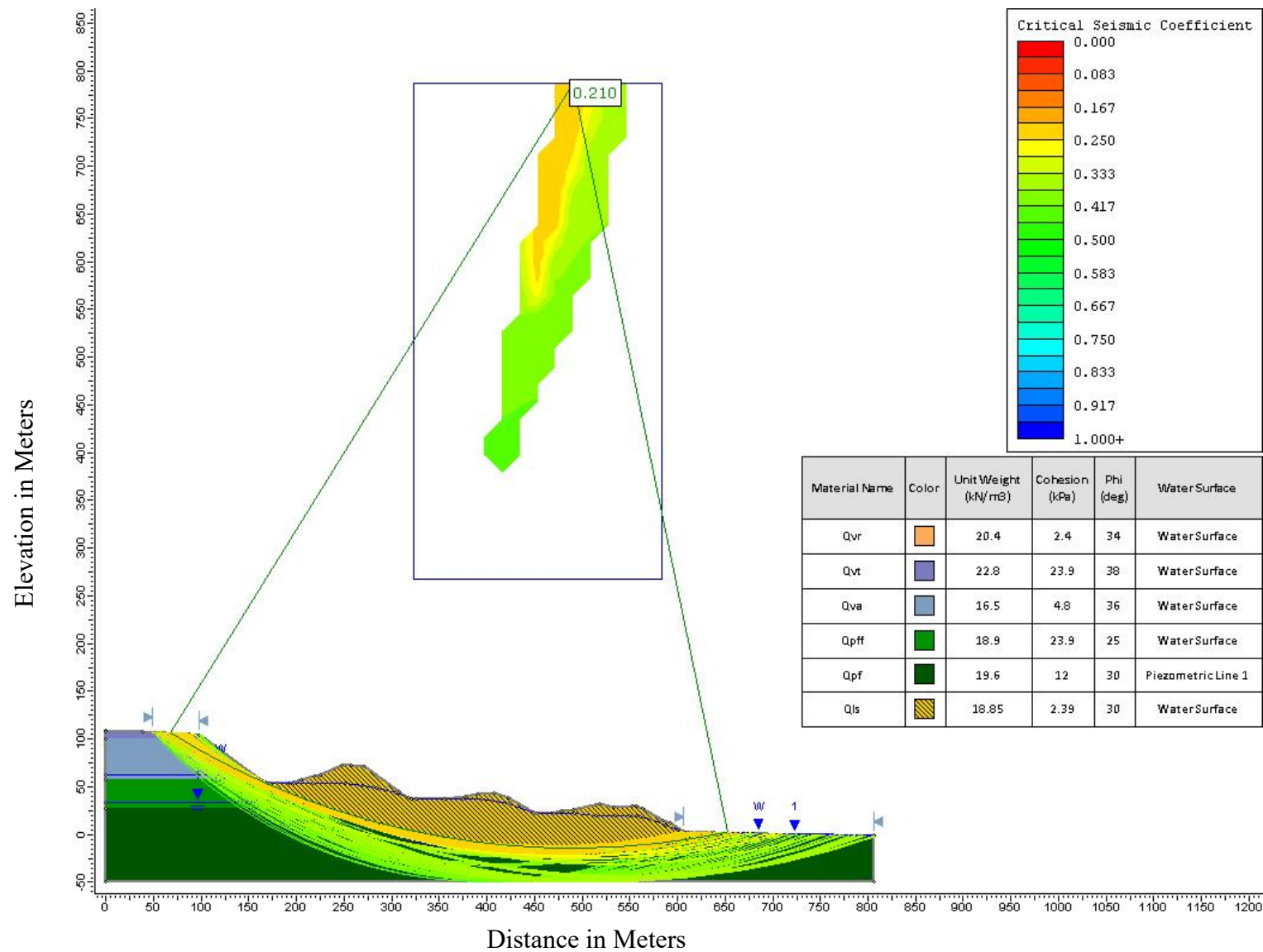


Figure 30: Scenario 3 dry season model results for critical acceleration. The average of all slip surfaces was used to assign a general critical acceleration to this scenario. The critical acceleration value shown in green is the global minimum slip surface.

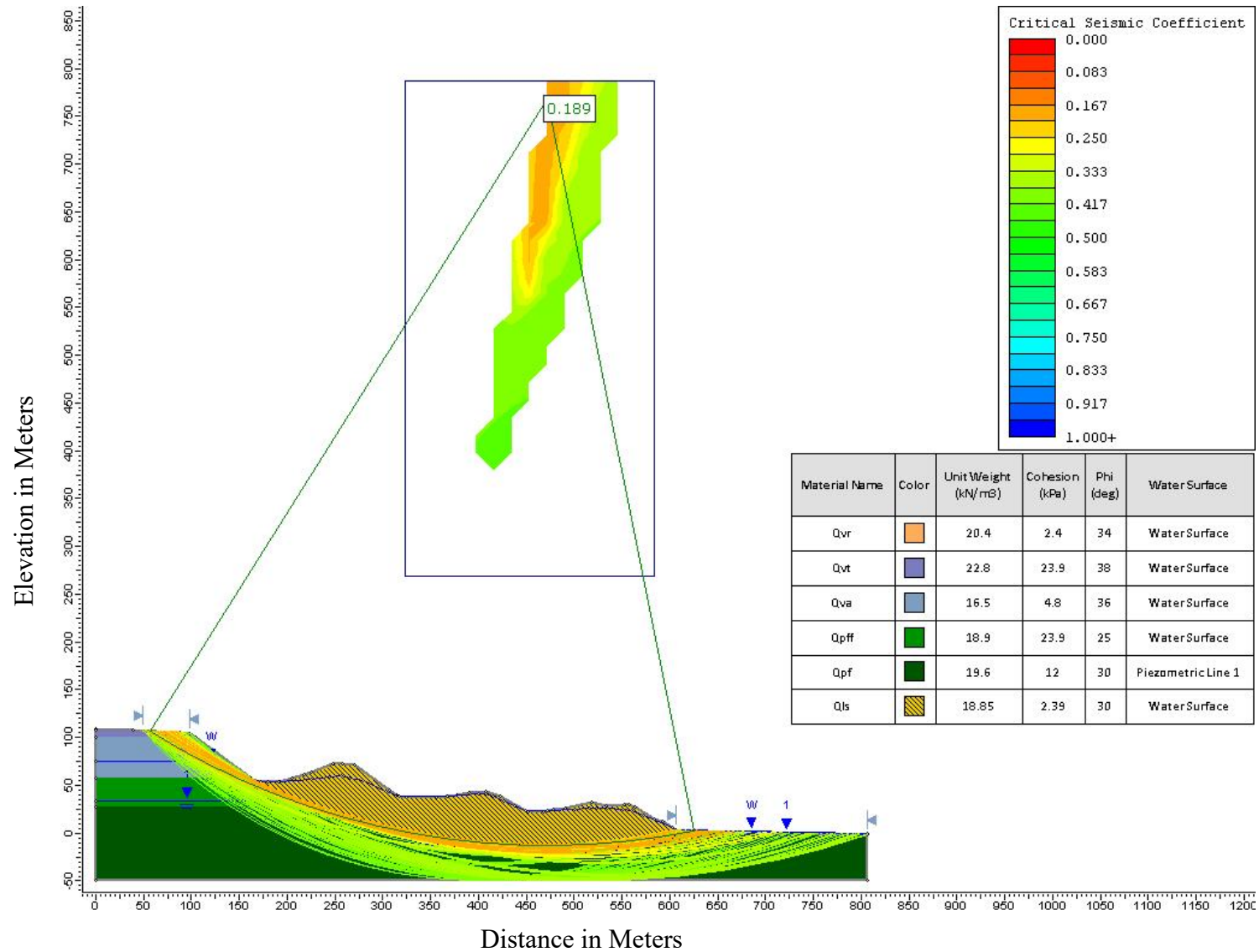


Figure 31: Scenario 3 wet season model results for critical acceleration. The average of all slip surfaces was used to assign a general critical acceleration to this scenario. The critical acceleration value shown in green is the global minimum slip surface.

## ***APPENDIX***

File Original with  
Department of Ecology  
Second Copy - Owner's Copy  
Third Copy - Driller's Copy

96342 22-2E-25L  
**WATER WELL REPORT**  
STATE OF WASHINGTON

Notice of Intent W117738  
UNIQUE WELL ID # AAW 895

12156

Water Right Permit No \_\_\_\_\_

(1) OWNER: Name BRUCE STERLING Address 811 T STREET VANCOUVER WA 98661  
(2) LOCATION OF WELL: County KING NE 1/4 SW 1/4 Sec 25 T 22 N.R. 2E WM  
(2a) STREET ADDRESS OF WELL (or nearest address) \_\_\_\_\_  
TAX PARCEL NO 2522 02 9099

(3) PROPOSED USE  
 Domestic  Industrial  Municipal  
 Irrigation  Test Well  Other  
 DeWater

(4) TYPE OF WORK: Owner's number of well (if more than one) \_\_\_\_\_  
 New Well Method \_\_\_\_\_  
 Deepened  Dug  Bored  
 Reconditioned  Cable  Driven  
 Decommission  Rotary  Jetted

(5) DIMENSIONS: Diameter of well 6 inches  
Drilled 342 feet Depth of completed well 342 ft

(6) CONSTRUCTION DETAILS  
Casing installed  
 Welded 6 : Diam from 0 ft to 337 ft  
 Liner Installed \_\_\_\_\_ : Diam from \_\_\_\_\_ ft to \_\_\_\_\_ ft  
 Threaded \_\_\_\_\_ : Diam from \_\_\_\_\_ ft to \_\_\_\_\_ ft

Perforations:  Yes  No  
Type of perforator used \_\_\_\_\_  
SIZE of perforations \_\_\_\_\_ in by \_\_\_\_\_ in  
\_\_\_\_\_ perforations from \_\_\_\_\_ ft to \_\_\_\_\_ ft

Screens  Yes  No  K-Pec Location 332  
Manufacturer's Name COOK  
Type STAINLESS Model No \_\_\_\_\_  
Diam 6 Slot Size 012 from 337 ft to 342 ft  
Diam \_\_\_\_\_ Slot Size \_\_\_\_\_ from \_\_\_\_\_ ft to \_\_\_\_\_ ft

Gravel/Filter packed:  Yes  No  Size of gravel/sand \_\_\_\_\_  
Material placed from \_\_\_\_\_ ft to \_\_\_\_\_ ft

Surface seal:  Yes  No To what depth? 18 ft  
Material used in seal BENTONITE  
Did any strata contain unusable water?  Yes  No  
Type of water? \_\_\_\_\_ Depth of strata \_\_\_\_\_  
Method of sealing strata off \_\_\_\_\_

(7) PUMP: Manufacturer's Name \_\_\_\_\_  
Type \_\_\_\_\_ H P \_\_\_\_\_

(8) WATER LEVEL: Land-surface elevation above mean sea level \_\_\_\_\_ ft  
Static level 232 ft below top of well Date 6/17/01  
Artesian pressure \_\_\_\_\_ lbs per square inch Date \_\_\_\_\_  
Artesian water is controlled by \_\_\_\_\_ (Cap, valve, etc)

(9) WELL TESTS: Drawdown is amount water level is lowered below static level  
Was a pump test made?  Yes  No If yes by whom? \_\_\_\_\_  
Yield \_\_\_\_\_ gal/min with \_\_\_\_\_ ft drawdown after \_\_\_\_\_ hrs  
Yield \_\_\_\_\_ gal/min with \_\_\_\_\_ ft drawdown after \_\_\_\_\_ hrs  
Yield \_\_\_\_\_ gal/min with \_\_\_\_\_ ft drawdown after \_\_\_\_\_ hrs  
Recovery data (time taken as zero when pump turned off) (water level measured from well top to water level)  
Time Water Level Time Water Level Time Water Level  
\_\_\_\_\_  
Date of test \_\_\_\_\_  
Bailer test 12 gal/min with 10 ft drawdown after 1 hrs  
Artesian \_\_\_\_\_ gal/min with \_\_\_\_\_ ft drawdown after \_\_\_\_\_ hrs  
Artesian flow \_\_\_\_\_ g.p.m. Date \_\_\_\_\_  
Temperature of water \_\_\_\_\_ Was a chemical analysis made?  Yes  No

(10) WELL LOG or DECOMMISSIONING PROCEDURE DESCRIPTION  
Formation Describe by color, character size of material and structure, and the kind and nature of the material in each stratum penetrated, with at least one entry for each change of information indicate at water encountered

MATERIAL	FROM	TO
DOWN GRAVELLY H.P.	0	65
BROWN SAND	65	180
CLAY CLAY	180	210
GREENISH SAND	210	330
CLAY SAND	330	342

Work Started 6/3/01 Completed 6/13/01

RECEIVED  
JUN 19 2001  
DEPT OF ECOLOGY

WELL CONSTRUCTION CERTIFICATION  
I constructed and/or accept responsibility for construction of this well and its compliance with all Washington well construction standards. Materials used and the information reported above are true to my best knowledge and belief  
Type or Print Name JOHNSON License No 0220  
(Licensed Driller/Engineer)  
Trainee Name \_\_\_\_\_ License No \_\_\_\_\_  
Drilling Company STATEWIDE  
(Signed JOHNSON License No 0220)  
(Licensed Driller/Engineer)  
Address 1333 PETERSON WAY S. Renton  
Contractor's Registration No STATEDC12006 Date 6/15/01  
(USE ADDITIONAL SHEETS IF NECESSARY)  
Ecology is an Equal Opportunity and Affirmative Action employer. For special accommodation needs contact the Water Resources Program at (360) 407-8600. The TDD number is (360) 407-8006

ECY 060-1-20 (11/98)

96342

100068

12155  
Notice of intent W117738  
UNIQUE WELL ID # AAW 898

File Original with  
Department of Ecology  
Second Copy - Owner's Copy  
Third Copy - Driller's Copy

# WATER WELL REPORT

STATE OF WASHINGTON

Water Right Permit No. \_\_\_\_\_

(1) OWNER: Name ANDERSON, DELAMIN Address 1557 WEATHER VALE CT FROST W.N.  
(2) LOCATION OF WELL: County KLING AW 1/4 SE 1/4 Sec 25 T 22 N.R. 2E WM  
(2a) STREET ADDRESS OF WELL: (or nearest address) \_\_\_\_\_  
TAX PARCEL NO. 252202-9048 22-2E-25K

(3) PROPOSED USE:  Domestic  Industrial  Municipal  
 Irrigation  Test Well  Other  
 DeWater

(4) TYPE OF WORK: Owner's number of well (if more than one) \_\_\_\_\_  
 New Well Method \_\_\_\_\_  
 Deepened  Dug  Bored  
 Reconditioned  Cable  Driven  
 Decommission  Rotary  Jetted

(10) WELL LOG or DECOMMISSIONING PROCEDURE DESCRIPTION  
Formation. Describe by color, character, size of material and structure, and the kind and nature of the material in each stratum penetrated, with at least one entry for each change of information indicate all water encounters.

MATERIAL	FROM	TO
BROWN CLAY	0	12
GRAY CLAY	12	280
FINE GRAY SILTY CLAY	280	290
FINE SAND GRAY	290	302

(5) DIMENSIONS: Diameter of well 6 inches  
Orled 302 feet. Depth of completed well 302 ft.

(6) CONSTRUCTION DETAILS  
Casing installed:  
 Welded 6 Diam from 0 ft to 290 ft  
 Liner installed \_\_\_\_\_ Diam from \_\_\_\_\_ ft to \_\_\_\_\_ ft  
 Threaded \_\_\_\_\_ Diam from \_\_\_\_\_ ft to \_\_\_\_\_ ft

Perforations:  Yes  No  
Type of perforator used \_\_\_\_\_  
SIZE of perforations \_\_\_\_\_ in by \_\_\_\_\_ in  
\_\_\_\_\_ perforations from \_\_\_\_\_ ft to \_\_\_\_\_ ft

Screens:  Yes  No  K-Pac Location 290  
Manufacturer's Name JOHNSON  
Type SPAINLESS Model No \_\_\_\_\_  
Diam 6 Slot Size 006 from 290 ft to 302 ft  
Diam \_\_\_\_\_ Slot Size \_\_\_\_\_ from \_\_\_\_\_ ft to \_\_\_\_\_ ft

Gravel/Filter packed:  Yes  No  Size of gravel/sand \_\_\_\_\_  
Material placed from \_\_\_\_\_ ft to \_\_\_\_\_ ft

Surface seal:  Yes  No To what depth? perforator ft.  
Material used in seal \_\_\_\_\_  
Did any strata contain unusable water?  Yes  No  
Type of water? \_\_\_\_\_ Depth of strata \_\_\_\_\_  
Method of sealing strata off \_\_\_\_\_

(7) PUMP: Manufacturer's Name \_\_\_\_\_  
Type \_\_\_\_\_ H P \_\_\_\_\_

(8) WATER LEVELS: Land surface elevation above mean sea level \_\_\_\_\_  
Static level 80 ft below top of well Date 6/30/01  
Artesian pressure \_\_\_\_\_ lbs per square inch Date \_\_\_\_\_  
Artesian water is controlled by \_\_\_\_\_ (Cap, valve, etc.)

(9) WELL TESTS: Drawdown is amount water level is lowered below static level  
Was a pump test made?  Yes  No If yes, by whom? \_\_\_\_\_  
Yield \_\_\_\_\_ gal./min. with \_\_\_\_\_ ft. drawdown after \_\_\_\_\_ hrs  
Yield \_\_\_\_\_ gal./min. with \_\_\_\_\_ ft. drawdown after \_\_\_\_\_ hrs  
Yield \_\_\_\_\_ gal./min. with \_\_\_\_\_ ft. drawdown after \_\_\_\_\_ hrs  
Recovery data (time taken as zero when pump turned off) (water level measured from well top to water level)  
Time Water Level Time Water Level Time Water Level  
\_\_\_\_\_  
Date of test 1/2 gal./min. with 160 ft. drawdown after 2 hrs  
Artesian test \_\_\_\_\_ gal./min. with \_\_\_\_\_ ft. drawdown after \_\_\_\_\_ hrs  
Artesian flow \_\_\_\_\_ g p m Date \_\_\_\_\_  
Temperature of water \_\_\_\_\_ Was a chemical analysis made?  Yes  No

RECEIVED  
JUL 31 2001  
DEPT OF ECOLOGY

Work Started 6/25/01 Completed 6/30/01

### WELL CONSTRUCTION CERTIFICATION:

I constructed and/or accept responsibility for construction of this well, and its compliance with all Washington well construction standards. Materials used and the information reported above are true to my best knowledge and belief.  
Type or Print Name JOHNSON License No. 0220  
(Licensed Driller/Engineer)  
Trainer Name \_\_\_\_\_ License No. \_\_\_\_\_  
Drilling Company STARWIDE  
(Signed) A. Johnson License No. 0220  
(Licensed Driller/Engineer)  
Address 1333 BEACON WAY S. NEWTON  
Contractor's Registration No. STARDC1306 Date 6/30/01  
(USE ADDITIONAL SHEETS IF NECESSARY)

Ecology is an Equal Opportunity and Affirmative Action employer. For special accommodation needs, contact the Water Resources Program at (360) 407-6600. The TDD number is (360) 407-6006.

ECY 050-1-20 (11/98)

100068







File Original and First Copy with Department of Ecology  
 Second Copy — Owner's Copy  
 Third Copy — Driller's Copy

# ENTERED WATER WELL REPORT

22-2-36F 2057  
 Start Card No. 098553

UNIQUE WELL I.D. # \_\_\_\_\_

STATE OF WASHINGTON

Water Right Permit No. \_\_\_\_\_

(1) OWNER: Name Ruth Williams Address 13118 Vermont with Red Vashon

(2) LOCATION OF WELL: County King SE 1/4 NW 1/4 Sec 36 T. 22 N. R. 25 W.M.

(2a) STREET ADDRESS OF WELL (or nearest address) \_\_\_\_\_

(3) PROPOSED USE:  Domestic  Industrial  Municipal   
 Irrigation  Test Well  Other   
 DeWater

(4) TYPE OF WORK: Owner's number of well (if more than one) \_\_\_\_\_  
 Abandoned  New well  Method: Dug  Bored   
 Deepened  Cable  Driven   
 Reconditioned  Rotary  Jetted

(5) DIMENSIONS: Diameter of well 6 inches.  
 Drilled 420 feet. Depth of completed well 420 feet.

(6) CONSTRUCTION DETAILS:  
 Casing installed: 6 - Diam. from 0 ft. to 410 ft.  
 Welded  Liner installed  Diam. from \_\_\_\_\_ ft. to \_\_\_\_\_ ft.  
 Threaded  Diam. from \_\_\_\_\_ ft. to \_\_\_\_\_ ft.

Perforations: Yes  No   
 Type of perforator used \_\_\_\_\_  
 SIZE of perforations \_\_\_\_\_ in. by \_\_\_\_\_ in.  
 \_\_\_\_\_ perforations from \_\_\_\_\_ ft. to \_\_\_\_\_ ft.  
 \_\_\_\_\_ perforations from \_\_\_\_\_ ft. to \_\_\_\_\_ ft.  
 \_\_\_\_\_ perforations from \_\_\_\_\_ ft. to \_\_\_\_\_ ft.

Screens: Yes  No   
 Manufacturer's Name JOHANSON  
 Type Stainless Model No. \_\_\_\_\_  
 Diam. 6 Slot size 012 from 410 ft. to 415 ft.  
 Diam. 6 Slot size 020 from 415 ft. to 420 ft.

Gravel packed: Yes  No  Size of gravel \_\_\_\_\_  
 Gravel placed from \_\_\_\_\_ ft. to \_\_\_\_\_ ft.

Surface seal: Yes  No  To what depth? 70 ft.  
 Material used in seal PORTLAND CEMENT  
 Did any strata contain unusable water? Yes  No   
 Type of water? \_\_\_\_\_ Depth of strata \_\_\_\_\_  
 Method of sealing strata of \_\_\_\_\_

(7) PUMP: Manufacturer's Name \_\_\_\_\_  
 Type: \_\_\_\_\_ H.P.

(8) WATER LEVELS: Land surface elevation above mean sea level \_\_\_\_\_  
 Static level 265 ft. below top of well Date 2/5/98  
 Artesian pressure \_\_\_\_\_ lbs. per square inch Date \_\_\_\_\_  
 Artesian water is controlled by \_\_\_\_\_ (Cap, valve, etc.)

(9) WELL TESTS: Drawdown is amount water level is lowered below static level  
 Was a pump test made? Yes  No  If yes, by whom? \_\_\_\_\_  
 Yield: \_\_\_\_\_ gal./min. with \_\_\_\_\_ ft. drawdown after \_\_\_\_\_ hrs.

Recovery data (time taken as zero when pump turned off) (water level measured from well top to water level)  
 Time Water Level Time Water Level Time Water Level

Date of test \_\_\_\_\_  
 Boiler test 15 gal./min. with 10 ft. drawdown after 1 hrs.  
 Artesian \_\_\_\_\_ gal./min. with stem set at \_\_\_\_\_ ft. for \_\_\_\_\_ hrs.  
 Artesian flow \_\_\_\_\_ g.p.m. Date \_\_\_\_\_  
 Temperature of water \_\_\_\_\_ Was a chemical analysis made? Yes  No

(10) WELL LOG or ABANDONMENT PROCEDURE DESCRIPTION  
 Formation: Describe by color, character, size of material and structure, and show thickness of aquifers and the kind and nature of the material in each stratum penetrated, with at least one entry for each change of information.

MATERIAL	FROM	TO
<u>BROWN H.P.</u>	<u>0</u>	<u>40</u>
<u>BROWN SAND</u>	<u>40</u>	<u>180</u>
<u>BROWN SAND &amp; GRAVEL</u>	<u>180</u>	<u>183</u>
<u>GRAY CLAY</u>	<u>183</u>	<u>200</u>
<u>BROWN SANDY H.P.</u>	<u>200</u>	<u>240</u>
<u>GREENISH SAND (w.b.)</u>	<u>240</u>	<u>380</u>
<u>" SAND &amp; SMALL GRAVEL (WATER BEARING)</u>	<u>380</u>	<u>412</u>
<u>MED. TO LARGE GRAVEL (WATER BEARING)</u>	<u>412</u>	<u>420</u>

RECEIVED  
 APR 7 1998  
 NWRO - WR  
 DEPT OF ECOLOGY

Work Started 1/31/98 19. Completed 2/5 98

**WELL CONSTRUCTOR CERTIFICATION:**

I constructed and/or accept responsibility for construction of this well, and its compliance with all Washington well construction standards. Materials used and the information reported above are true to my best knowledge and belief.

**STATEWIDE DRILLING CO.**

NAME STATEWIDE DRILLING CO.  
(PERSONAL FIRM OR CORPORATION) (TYPE OR PRINT)  
1333 Cedar View S  
Renton, WA 98055  
 Address 772-6777  
 (Signature) [Signature] License No. 0220  
(WELL DRILLER)

Contractor's Registration No. STATEWIDE 12426 Date 2/5 19 98

(USE ADDITIONAL SHEETS IF NECESSARY)

Ecology is an Equal Opportunity and Affirmative Action employer. For special accommodation needs, contact the Water Resources Program at (206) 407-6800. The TDD number is (206) 407-5006.

12056

File Original with Department of Ecology  
Second Copy - Owner's Copy  
Third Copy - Driller's Copy

# WATER WELL REPORT

STATE OF WASHINGTON

ENTERED  
Project No. W119266  
Single Well ID # APA-527  
Water Right Permit No. \_\_\_\_\_

(1) OWNER: Name BOB CASWELL Address 12633 S.W. 276 WASHWON W  
(2) LOCATION OF WELL: County King NE 1/4 NW 1/4 Sec 36 T 22 N.R. 25 W4  
(3a) STREET ADDRESS OF WELL: (or nearest address) SAME  
TAX PARCEL NO.: 22-20-361

(3) PROPOSED USE:  Domestic  Industrial  Municipal  
 Irrigation  Test Well  Other  
 DeWater

(4) TYPE OF WORK: Owner's number of well (if more than one) \_\_\_\_\_  
 New Well Method: \_\_\_\_\_  
 Deepened  Dug  Bored  
 Reconditioned  Cased  Driven  
 Decommissioned  Rotary  Jetted

(10) WELL LOG or DECOMMISSIONING PROCEDURE DESCRIPTION  
Formation: Describe by color, character, size of material and structure, and the kind and nature of the material in each stratum penetrated, with at least one entry for each change of information. Indicate all water encountered.

MATERIAL	FROM	TO
ADDED GARBAGE H.P.	0	65
GRAVEL SAND H.P.	65	120
CLAY H.P.	120	145
CLAY H.P.	145	160
GARBAGE GARBAGE H.P.	160	165
CLAY CLAY	165	172
GARBAGE GARBAGE	172	179
CLAY CLAY	179	180

(5) DIMENSIONS: Diameter of well 6 inches  
Orded 180 feet. Depth of completed well 179 ft.

(6) CONSTRUCTION DETAILS  
Casing installed:  Welded 6 Diam. from 0 ft. to 179 ft.  
 Liner installed \_\_\_\_\_ Diam. from \_\_\_\_\_ ft. to \_\_\_\_\_ ft.  
 Threaded \_\_\_\_\_ Diam. from \_\_\_\_\_ ft. to \_\_\_\_\_ ft.

Perforations:  Yes  No  
Type of perforator used \_\_\_\_\_  
SIZE of perforations \_\_\_\_\_ in. by \_\_\_\_\_ in.  
\_\_\_\_\_ perforations from \_\_\_\_\_ ft. to \_\_\_\_\_ ft.

Screens:  Yes  No  K-Pac Location \_\_\_\_\_  
Manufacturer's Name \_\_\_\_\_ Model No. \_\_\_\_\_  
Diam. \_\_\_\_\_ Slot Size \_\_\_\_\_ from \_\_\_\_\_ ft. to \_\_\_\_\_ ft.  
Diam. \_\_\_\_\_ Slot Size \_\_\_\_\_ from \_\_\_\_\_ ft. to \_\_\_\_\_ ft.

Gravel/Pitir passes:  Yes  No  Size of gravel/sand \_\_\_\_\_  
Material placed from \_\_\_\_\_ ft. to \_\_\_\_\_ ft.  
Surface seal:  Yes  No To what depth? 30 ft.  
Material used in seal PORTLAND CEMENT  
Did any strata contain unusable water?  Yes  No  
Type of water? \_\_\_\_\_ Depth of strata \_\_\_\_\_  
Method of sealing strata off \_\_\_\_\_

(7) PUMP: Manufacturer's Name \_\_\_\_\_  
Type: \_\_\_\_\_ H.P. \_\_\_\_\_

(8) WATER LEVELS: Land-surface elevation above mean sea level \_\_\_\_\_ ft.  
Static level 150 ft. below top of well Date 11/7/99  
Artesian pressure \_\_\_\_\_ lbs. per square inch Date \_\_\_\_\_  
Artesian water is controlled by \_\_\_\_\_ (Cap. veins, etc.)

NOV 15 1999  
Work Started \_\_\_\_\_ Completed 11/7/99

(9) WELL TESTS: Drawdown is amount water level is lowered below static level  
Was a pump test made?  Yes  No If yes, by whom? \_\_\_\_\_  
Yield: \_\_\_\_\_ gal./min. with \_\_\_\_\_ ft. drawdown after \_\_\_\_\_ hrs.  
Yield: \_\_\_\_\_ gal./min. with \_\_\_\_\_ ft. drawdown after \_\_\_\_\_ hrs.  
Yield: \_\_\_\_\_ gal./min. with \_\_\_\_\_ ft. drawdown after \_\_\_\_\_ hrs.  
Recovery data (time taken to zero when pump turned off (water level measured from well top to water level))  
Time \_\_\_\_\_ Water Level \_\_\_\_\_ Time \_\_\_\_\_ Water Level \_\_\_\_\_ Time \_\_\_\_\_ Water Level \_\_\_\_\_  
Type of test 3  
Baker test 3 gal./min. with 3 ft. drawdown after 2 hrs.  
Artesian 3 gal./min. with \_\_\_\_\_ ft. drawdown after \_\_\_\_\_ hrs.  
Artesian flow \_\_\_\_\_ g.p.m. Date \_\_\_\_\_  
Temperature of water \_\_\_\_\_ Was a chemical analysis made?  Yes  No

WELL CONSTRUCTION CERTIFICATION:  
I constructed and/or accept responsibility for construction of this well, and compliance with all Washington well construction standards. Material use and the information reported above are true to my best knowledge and belief.  
Type or Print Name JOHNSON License No. 0220  
(Licensed Driller/Engineer)  
Trainee Name \_\_\_\_\_ License No. \_\_\_\_\_  
Drilling Company Statewide  
(Signed) McPherson License No. 0222  
(Licensed Driller/Engineer)  
Address 1333 PETHON WAY S  
Contractor's Registration No. W119266 Date 11/7/99  
(USE ADDITIONAL SHEETS IF NECESSARY)




Date(s) Drilled	10/24/03	Logged By	GRL	Checked By	DSP
Drilling Contractor	R&R Drilling	Drilling Method	Hollow Stem Auger	Sampling Methods	1.5 inch I.D. SPT
Auger Data	4 1/4 inch ID Continuous Flight Auger	Hammer Data	140 (lb) hammer/ 30 (in) drop	Drilling Equipment	Mobile B-61
Total Depth (ft)	59	Surface Elevation (ft)	68	Groundwater Level (ft. bgs)	27
Datum/ System	MLLW				

Elevation feet	Depth feet	SAMPLES			Water Level	Graphic Log	Group Symbol	MATERIAL DESCRIPTION	Water Content, %	Dry Unit Weight, lbs/ft <sup>3</sup>	OTHER TESTS AND NOTES
		Interval Number	Recovered (ft)	Blows/foot							
0						TS	Brown silty fine to medium sand with occasional gravel and organics (medium dense, moist) (topsoil)				
5	1	7	15			SP	Brown fine to medium sand with occasional gravel (medium dense, moist)				
10	2	16	14					11			
15	3	18	28			SP	Gray fine sand (medium dense, moist)				
20	4	16	42			ML	Gray silt (hard, moist)				
25	5	18	66			SP	Gray fine sand (very dense, moist)				
30	6	15	51			SP-SM	Gray fine sand with silt (dense, moist)	29			
35	7	18	33			ML	Gray silt (hard, moist)				
40	8	18	48					34		%F=99.5	
45	9	18	60								
50	10	18	39								
55	11	18	85					29			
60	12	18	65								

Completed at 59 feet on 10/24/03

Note: See Figure 3 for explanation of symbols

11043-001-00 DE OTB-CORING 2.1.0 P1111104300100FINAL1104301008.DWG: gdriv2.dwg 11/19/03

<b>LOG OF BORING B-1</b>	
	Project: Landslide/Erosion/Siesmic Hazard Eval. - Porter Res.
	Project Location: Vashon Island, Washington
	Project Number: 11043-001-00
Figure: 5 Sheet 1 of 1	

ENTERED

1823

WATER WELL REPORT

Start Card No. W055899  
Unique Well I.D. # ABW370  
Water Right Permit No.

STATE OF WASHINGTON

(1) OWNER: Name LEWIS, ED Address 28828 125TH PLACE SW VASRON, WA 98070-2126/1

(2) LOCATION OF WELL: County KING 1/4 NE 1/4 Sec 1 T 21 N., R 2E W

(2a) STREET ADDRESS OF WELL (or nearest address) 28828 125TH PL. SW, VASRON

(3) PROPOSED USE: DOMESTIC (10) WELL LOG

(4) TYPE OF WORK: NEW WELL  
Owner's Number of well (if more than one)  
Method: ROTARY  
Formation: Describe by color, character, size of material and structure, and show thickness of aquifers and the kind and nature of the material in each stratum penetrated, with at least one entry for each change in formation.

(5) DIMENSIONS: Diameter of well 8 inches  
Drilled 127 ft. Depth of completed well 127 ft.

(6) CONSTRUCTION DETAILS:  
Casing installed: 6 " Dia. from +6 ft. to 123 ft.  
WBLOED " Dia. from ft. to ft.  
" Dia. from ft. to ft.

Perforations: NO  
Type of perforator used  
SIZE of perforations in. by in.  
perforations from ft. to ft.  
perforations from ft. to ft.  
perforations from ft. to ft.

Screens: YES  
Manufacturer's Name HOUSTON  
Type STAINLESS STEEL  
Diam. 6 slot size .006 from 123 ft. to 127 ft.  
Diam. slot size from ft. to ft.

Gravel packed: NO  
Gravel placed from ft. to ft. Size of gravel ft.

Surface seal: YES To what depth? 18 ft.  
Material used in seal BENTONITE CLAY  
Did any strata contain unusable water? NO  
Type of water? Depth of strata ft.  
Method of sealing strata off N/A

(7) PUMP: Manufacturer's Name GRUNDFOSS805-13 H.P. 1/2  
Type SUBMERSIBLE

(8) WATER LEVELS: Land-surface elevation  
Static level 75 ft. below top of well Date 12/14/94  
Artesian Pressure lbs. per square inch Date  
Artesian water controlled by N/A

(9) WELL TESTS: Drawdown is amount water level is lowered below static level.  
Was a pump test made? NO If yes, by whom? hrs.  
Yield: gal./min with ft. drawdown after hrs.

Recovery data  
Time Water Level Time Water Level Time Water Level

Date of test 1/1  
Bailer test gal./min. ft. drawdown after hrs.  
Air test 2-3 gal./min. w/ stem set at 126 ft. for 1 hrs.  
Artesian flow g.p.s. Date  
Temperature of water Was a chemical analysis made? YES

MATERIAL FROM TO  
BROWN SAND 0 14  
SAME, BUT W/ LENSES OF SILTY 14 28  
GRAVEL 14 28  
BROWN SAND 28 78  
SAME, BUT DAMP TO 78 127  
NET 78 127  
BLUE CLAY 127 127

RECEIVED  
JAN 12 1995  
DEPT. OF GEOLOGY

Work started 12/13/94 Completed 12/14/94

WELL CONSTRUCTOR CERTIFICATION:  
I constructed and/or accept responsibility for construction of this well, and its compliance with all Washington well construction standards. Materials used and the information reported above are true to my best knowledge and belief.

NAME OELKE DRILLING, INC.  
(Person, firm, or corporation) (Type or print)

ADDRESS 4312-166 AVE E. SUMNER, WA

(SIGNED) License No. 837 E. NCEBWA

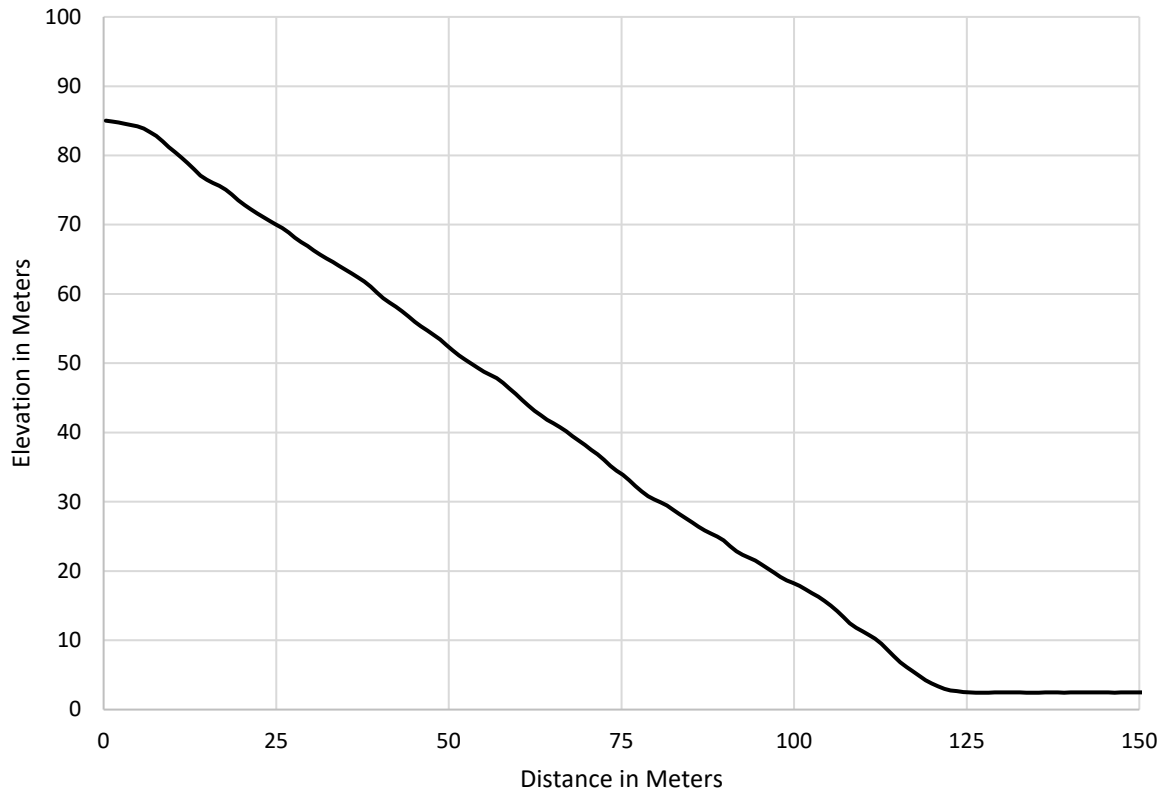
Contractor's Registration No. OELKEDI 136QC Date 01/09/95



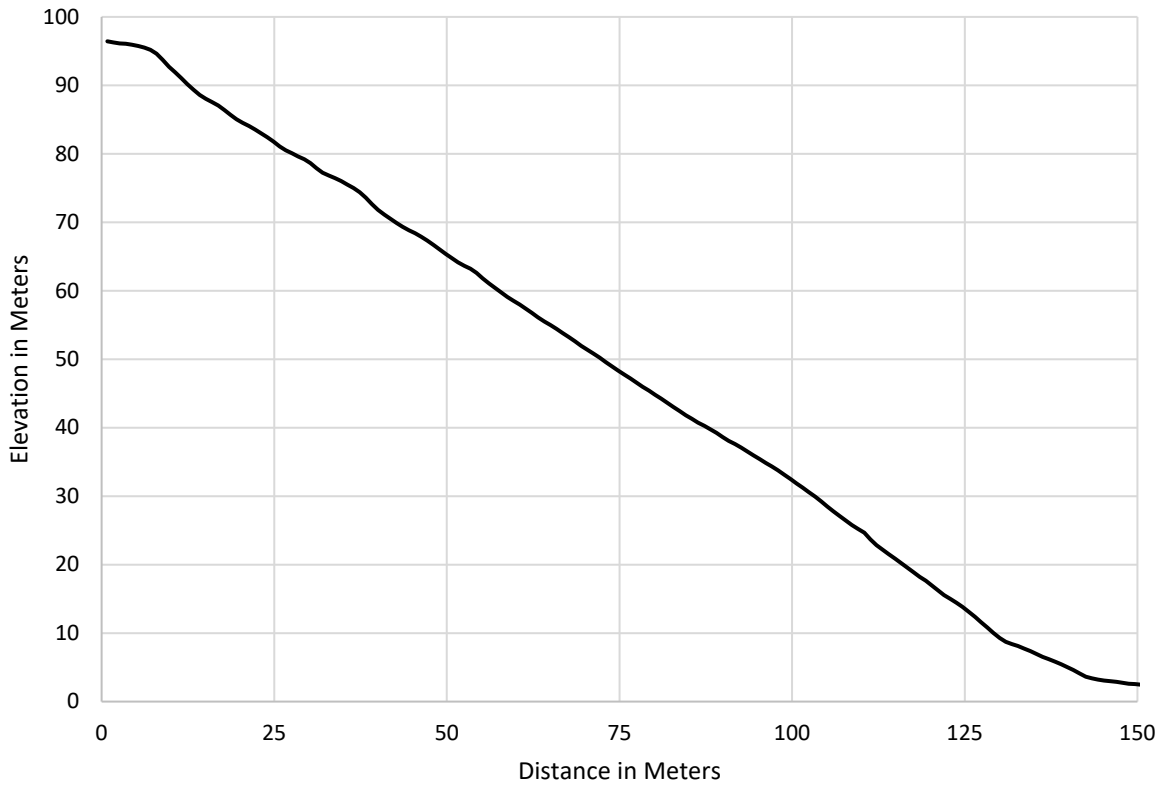




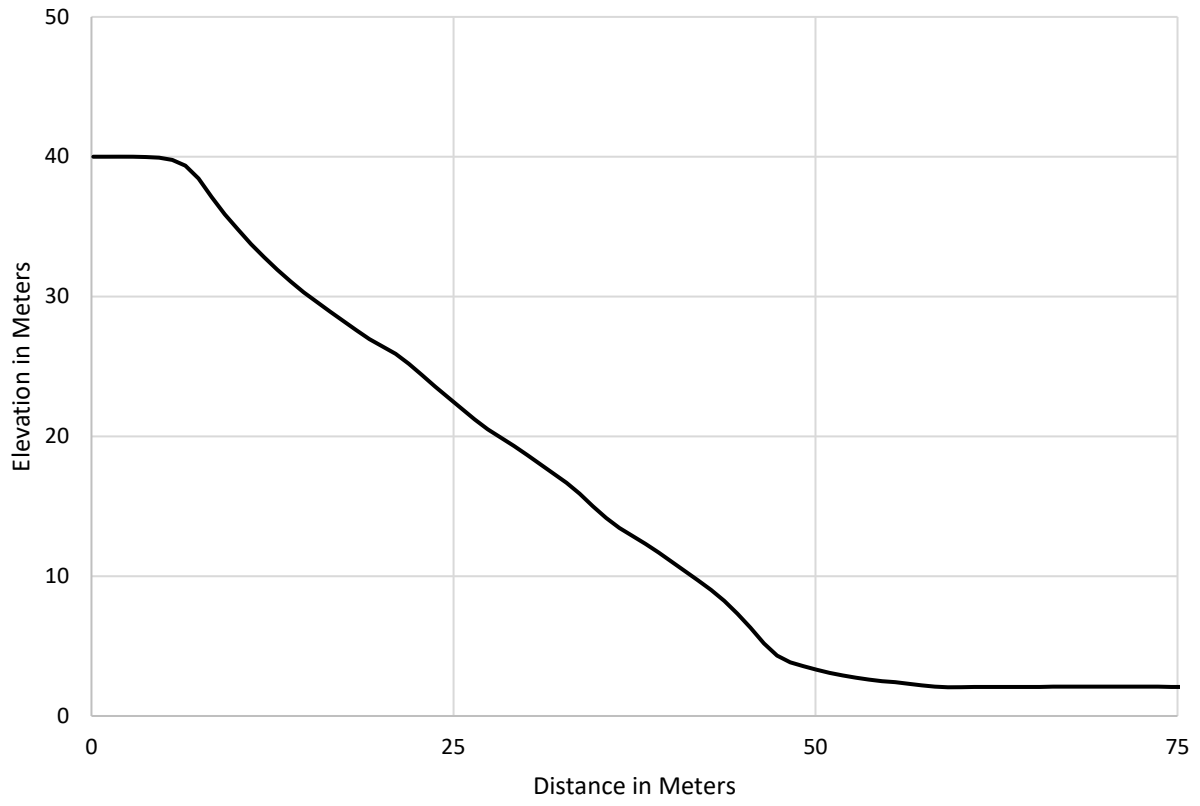
Intact Bluff Profile 1



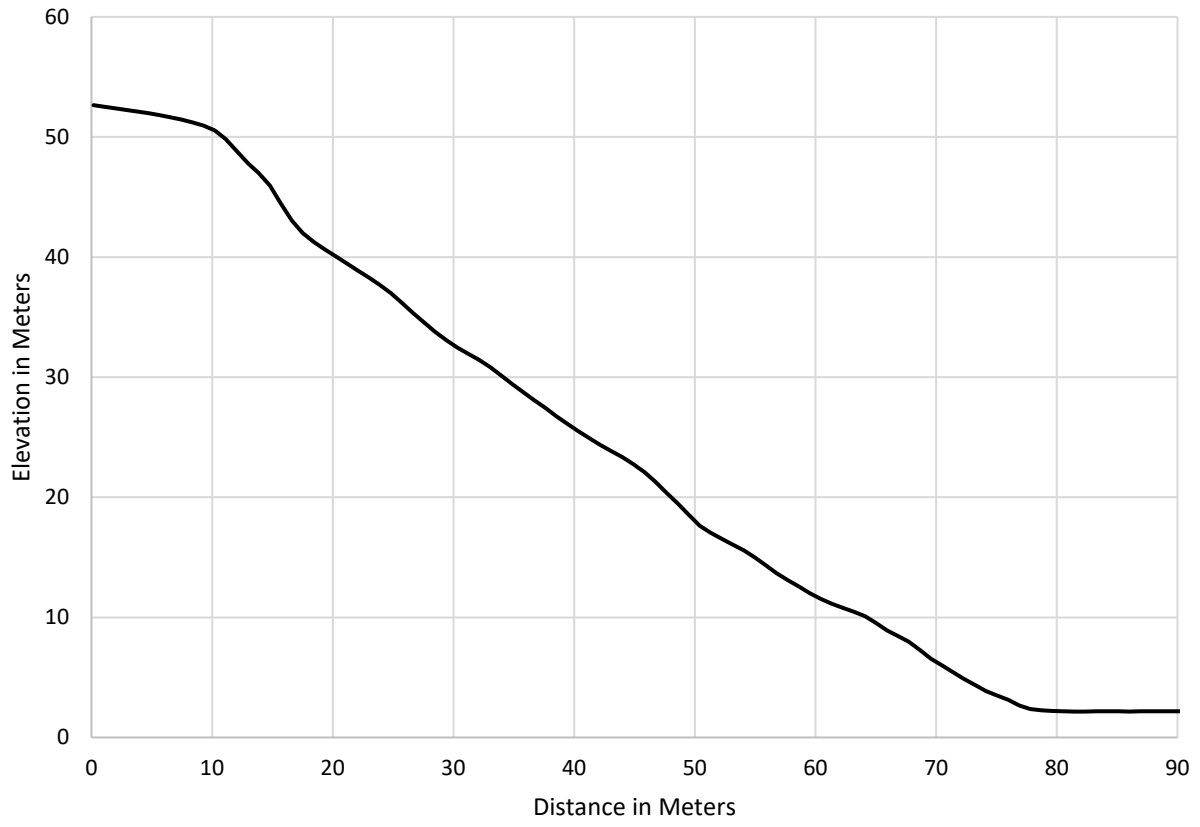
Intact Bluff Profile 2



Intact Bluff Profile 3



Intact Bluff Profile 4



## LIST OF TABLES

Page 20.	Table 1	Paleo-bluff Reconstruction Average Slope
Page 20.	Table 2	Factor of Safety and Critical Acceleration Results
Page 20.	Table 3	Critical Acceleration Exceedance Results

## LIST OF FIGURES

Page 21	Figure 1	Location Map
Page 22	Figure 2	LiDAR and Bathymetry Map
Page 23	Figure 3	Lost Lake Landslide Fault Zones
Page 24	Figure 4	Lost Lake Landslide Slope Profile
Page 25	Figure 5	Ledgewood Landslide Map
Page 26	Figure 6	Southeastern Mercer Island Landslide Map
Page 27	Figure 7	Conceptual Geologic Model
Page 28	Figure 8	Geologic Map Vashon Island, Washington
Page 29	Figure 9	Draft Geologic Cross Section Vashon Island, Washington
Page 30	Figure 10	Vashon Island VAS-W-64 Groundwater Monitoring
Page 31	Figure 11	Vashon and Maury Island Intact Bluff Locations
Page 32	Figure 12	Slope Stability Model Discretization of Slices and Forces
Page 33	Figure 13	Seattle Fault Zone Peak Ground Acceleration
Page 34	Figure 14	Tacoma Fault Zone Peak Ground Acceleration
Page 35	Figure 15a	Scenario 1 Dry Season Model
Page 36	Figure 15b	Scenario 1 Wet Season Model
Page 37	Figure 16	Scenario 2 Model Geometry Set-up
Page 38	Figure 17a	Scenario 2 Dry Season Model
Page 39	Figure 17b	Scenario 2 Wet Season Model
Page 40	Figure 18a	Scenario 3 Dry Season Model
Page 41	Figure 18b	Scenario 3 Wet Season Model
Page 42	Figure 19	Paleo-bluff Reconstruction
Page 43	Figure 20	Scenario 1 Factor of Safety Results Dry Season
Page 44	Figure 21	Scenario 1 Factor of Safety Results Wet Season
Page 45	Figure 22	Scenario 1 Critical Acceleration Results Dry Season
Page 46	Figure 23	Scenario 1 Critical Acceleration Results Wet Season
Page 47	Figure 24	Scenario 2 Factor of Safety Results Dry Season
Page 48	Figure 25	Scenario 2 Factor of Safety Results Wet Season
Page 49	Figure 26	Scenario 2 Critical Acceleration Results Dry Season
Page 50	Figure 27	Scenario 2 Critical Acceleration Results Wet Season
Page 51	Figure 28	Scenario 3 Factor of Safety Results Dry Season
Page 52	Figure 29	Scenario 3 Factor of Safety Results Wet Season
Page 53	Figure 30	Scenario 3 Critical Acceleration Results Dry Season
Page 54	Figure 31	Scenario 3 Critical Acceleration Results Wet Season

## *Acknowledgements*

I want to thank my readers Kathy Troost, Alison Duval, and Mike Brown for providing a useful perspective on how to approach the project and for their insight at critical points throughout the project. Their invaluable guidance during the report writing process made this project more meaningful. I also want to thank my peers in MESSAGE Cohort 7 for being a set of ears when I needed to talk through problems related to my project.